CHEMICAL REVIEWS

Review

pubs.acs.org/CR

Photoinduced Chemistry in Fluorescent Proteins: Curse or Blessing?

Atanu Acharya,[†] Alexey M. Bogdanov,[‡,§] Bella L. Grigorenko,[∥,⊥] Ksenia B. Bravaya,[#] Alexander V. Nemukhin,[∥,⊥] Konstantin A. Lukyanov,[*,‡,§] and Anna I. Krylov[*,†]

[†]Department of Chemistry, University of Southern California, Los Angeles, California 90089-0482, United States

[‡]Shemyakin-Ovchinnikov Institute of Bioorganic Chemistry, Moscow, Russia

[§]Nizhny Novgorod State Medical Academy, Nizhny Novgorod, Russia

[∥]Department of Chemistry, Lomonosov Moscow State University, Moscow, Russia

[⊥]Emanuel Institute of Biochemical Physics, Russian Academy of Sciences, Moscow, Russia

[#]Department of Chemistry, Boston University, Boston, Massachusetts United States

ABSTRACT: Photoinduced reactions play an important role in the photocycle of fluorescent proteins from the green fluorescent protein (GFP) family. Among such processes are photoisomerization, photooxidation/photoreduction, breaking and making of covalent bonds, and excited-state proton transfer (ESPT). Many of these transformations are initiated by electron transfer (ET). The quantum yields of these processes vary significantly, from nearly 1 for ESPT to 10^{-4}–10^{-6} for ET. Importantly, even when quantum yields are relatively small, at the conditions of repeated illumination the overall effect is significant. Depending on the task at hand, fluorescent protein photochemistry is regarded either as an asset facilitating new applications or as a nuisance leading to the loss of optical output. The phenomena arising due to phototransformations include (i) large Stokes shifts, (ii) photoconversions, photoactivation, and photoswitching, (iii) phototoxicity, (iv) blinking, (v) permanent bleaching, and (vi) formation of long-lived intermediates. The focus of this review is on the most recent experimental and theoretical work on photoinduced transformations in fluorescent proteins. We also provide an overview of the photophysics of fluorescent proteins, highlighting the interplay between photochemistry and other channels (fluorescence, radiationless relaxation, and intersystem crossing). The similarities and differences with photochemical processes in other biological systems and in dyes are also discussed.

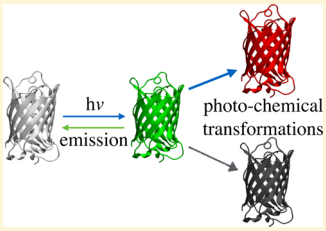

CONTENTS

Special Issue: Light Harvesting

Received: April 19, 2016
Published: October 18, 2016

DOI: 10.1021/acs.chemrev.6b00238
Chem. Rev. 2017, 117, 758–795

1. INTRODUCTION

The unique properties of green fluorescent protein (GFP) have revolutionized many areas in the life sciences[1−5] by enabling in vivo observations of protein localization and interactions, intracellular measurements of concentrations of physiologically important ions (Ca^{2+}, Cl^-, H^+), mapping gene expressions, etc. The significance of fluorescent proteins and related technologies was recognized with the 2008 Nobel Prize in Chemistry. The 2014 Nobel Prize, conferred "for the development of super-resolved fluorescence microscopy", is also directly relevant to fluorescent proteins and, particularly, to their photophysical properties discussed in this review.

GFP was first characterized[6] at the protein level in extracts from the jellyfish *Aequorea victoria* in 1962. It then took more than 30 years to clone the GFP gene and demonstrate that functional GFP can be expressed in various model organisms.[7,8] This discovery opened the era of GFP applications as a fluorescent label fully encoded by a single gene. In addition to their role in practical applications, fluorescent proteins are interesting for their own sake. In particular, natural diversity and functioning of fluorescent proteins represent intriguing fundamental problems. Thus far, GFP-like proteins have been found only in multicellular animal species (Metazoa kingdom), specifically in hydroid jellyfishes and coral polyps (phylum Cnidaria), combjellies (Ctenophora), crustaceans (Arthropoda), and lancelets (Chordata).[4] Together with the observation that most sequenced animal genomes contain no GFP-related sequences, this suggests that the GFP gene originated very early in animal evolution but then was lost in many species. Natural GFP-like proteins demonstrate a broad spectral diversity including cyan, green, yellow, orange, and red fluorescent proteins as well as a colorful palette of nonfluorescent chromoproteins.[4] Phylogenetic analysis and reconstruction of ancestral genes have shown that the green fluorescent phenotype (eGFP-like excitation and emission spectra) was likely characteristic of evolutionary ancient proteins, whereas other colors appeared later in evolution, independently in different taxa.[9]

The biological functions of GFP-like proteins have been studied only sparcely and for many species remain unclear or, at least, not experimentally proven. One well-studied example is the participation of GFPs in bioluminescent systems, where they act as secondary emitters.[10] Yet, most bioluminescent species contain no fluorescent protein, and conversely, most fluorescent protein-containing animals are nonbioluminescent. Thus, fluorescent proteins appear to have other functions. For example, it has been proposed that fluorescent proteins play a photoprotective role in corals.[11] A recent elegant study demonstrated that green fluorescent spots on jellyfish tentacles efficiently attract a prey.[12] This observation explains the predominant distribution of fluorescent proteins at the tentacles and around the mouth of jellyfishes and coral polyps. An association of fluorescent proteins with a physiological state of coral larvae has been demonstrated,[13] but possible molecular mechanisms of this phenomenon are unclear. It is reasonable to hypothesize that, at the time of their early evolution, fluorescent proteins had some basic functions not related to their visual appearance (bioluminescence, camouflage, attraction, recognition, etc.) as no organisms had eyes at that time. Such primary biochemical functions could be photoprotection, production or scavenging of reactive oxygen species (ROS), or light-induced electron or proton transfer. While direct observation of evolutionary ancient fluorescent protein functions is impossible, detailed studies of photophysics and photochemistry of GFP-like proteins might provide clues to the biological functioning of this protein family.

Not surprisingly, the photophysics of fluorescent proteins has motivated numerous experimental and theoretical studies.[14−24] Owing to the complexity of the system, many aspects of the

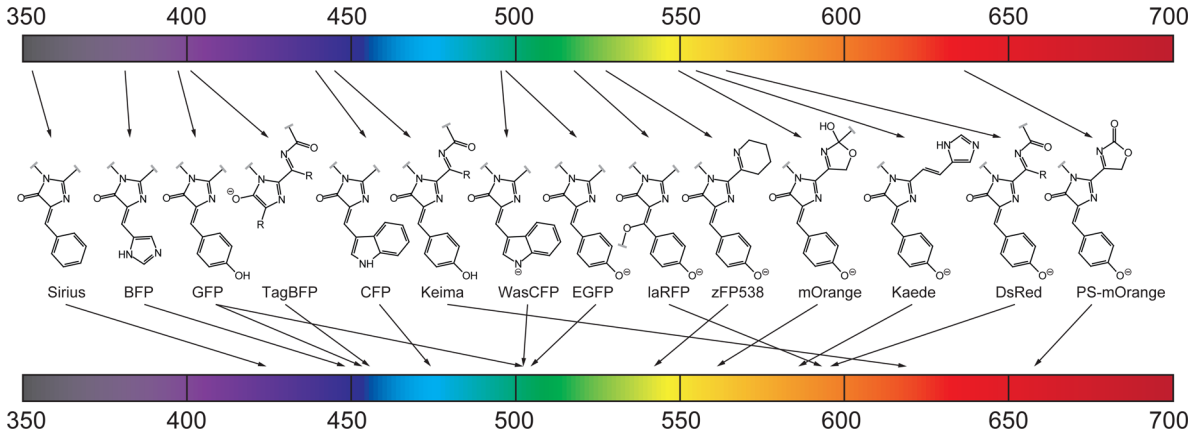

Figure 1. Color tuning in fluorescent proteins: Different chemical structures of the chromophore lead to different colors. Main types of chromophore structures are shown together with corresponding excitation (upper bar) and emission (bottom bar) wavelengths designated by arrows. The size of π-conjugated system is particularly important for determining the color: more extensive conjugation leads to red-shifted absorption (compare, for example, blue, green, and red chromophores). Changes in protonation states of the chromophore also affect the energy gap between the ground and the excited states. Excited-state deprotonation of the chromophore is one of the mechanisms of achieving large Stokes shifts. Absorption/emission can be red shifted by π-stacking of the chromophore with other aromatic groups (e.g., tyrosine), as in YFP (not shown). Specific interactions with nearby residues also affect the hue (for example, additional red shift in mPlum fluorescence is attributed to a hydrogen bond formed by acylimine's oxygen).

DOI: 10.1021/acs.chemrev.6b00238
Chem. Rev. 2017, 117, 758−795

fluorescent protein photocycle and chromophore formation are still largely unexplored. Yet, molecular-level understanding of these processes provides a crucial advantage in the design of new fluorescent proteins with properties to fit particular applications. While the significance of some properties (colors, Stokes shifts, brightness) is quite straightforward, the role of others (photostability, phototoxicity) and their optimal parameter space are more subtle.

Obviously, absorption and fluorescence wavelengths are among the key parameters. Fluorescent proteins of different colors can be used to mark different proteins (multicolor imaging) and to construct FRET (fluorescence resonance energy transfer) pairs. Variations in Stokes shifts enable single-laser dual-emission type of measurements. Red fluorescent proteins are of a particular importance as suitable markers for deep-tissue imaging.[25] Nonfluorescent chromoproteins can be used as efficient FRET acceptors, e.g., in FqRET (fluorescence quenching resonance energy transfer) imaging,[26,27] and for photoacoustic imaging in tissues.[28] Today, fluorescent proteins span the entire range of visible light including the far-red end of the spectrum.[2,14,21,25,29−32] As illustrated in Figure 1, color tuning in fluorescent proteins can be achieved by several distinct mechanisms, including varying the extent of the π-system, changing the protonation state of the chromophore, π-stacking, and electrostatic and other specific interactions with nearby residues. Brightness is another obviously important factor: brighter fluorescent proteins, i.e., those with larger extinction coefficients and fluorescence quantum yields, make better fluorescent labels. Other properties, such as photostability, phototoxicity, sensitivity to the presence of small molecules, ions, and reducing or oxidizing agents, are very important, yet their optimal values depend on the task at hand, that is, what is optimal for one application can be undesirable in others.

Consider, for example, photostability. In many applications, bleaching, a gradual loss of optical output upon repeated irradiation, is undesirable. Consequently, protein engineering often aims at more photostable fluorescent proteins. On the other hand, bleaching is exploited in super-resolution imaging.[4,33−37] Methods based on fluorescence loss and recovery are used to trace protein dynamics; photoconversions and photoswitching enable optical highlighting and timing of biochemical processes.[23,25,32] In a similar vein, phototoxicity, which is undesirable for in vivo imaging applications, can be exploited in photodynamic therapies and targeted protein/cell inactivation.[38] Likewise, the sensitivity of fluorescence to other chemical species may be regarded as a nuisance interfering with imaging or as an asset enabling new types of measurements and biosensing applications. For example, sensitivity of YFPs' fluorescence to halides limits their use as general-purpose yellow fluorescent tags but can be exploited in ratiometric measurements of halide concentrations. The same duality is engendered by photoconversion and photoswitching, phenomena entailing changes in fluorescence properties upon irradiation. For example, photooxidative redding,[39] photoconversion leading to a red-shifted absorption/emission, may be exploited in applications[4,25,40] such as timing biochemical processes, optical highlighting, or intracellular redox measurements; yet, it interferes with standard imaging measurements in live cells, which always contain copious amounts of oxidizing and reducing agents. In single-molecule visualization applications, properties such as blinking frequency and photon budget need to be considered.[36,41−44]

Owing to their rich photophysics and photochemistry, the fluorescent proteins feature a wide array of tunable properties. Our ability to manipulate these properties is critical for designing fluorescent proteins optimal for specific applications. Knowledge of the structure−function relationship and detailed molecular-level mechanistic understanding of the fluorescent proteins' photocycle are essential prerequisites for controlling these properties.

On a fundamental level, the same molecular-level processes that operate in fluorescent proteins are encountered in other systems of technological and biological significance. For example, natural and artificial light harvesting involves photoexcitation, energy transfer (either coherent or via FRET) between multiple chromophores, and generation and transport of photoelectrons. Photocatalysis and production of solar fuels is based on photochemical transformations. Light sensing in many biological systems is initiated by photoinduced cis−trans isomerization coupled with excited-state proton transfer (ESPT). Thus, understanding fundamental aspects of fluorescent proteins' photophysics will aid our progress in other areas. These similarities in the underlying physical processes have already inspired several ideas for exploiting fluorescent proteins in entirely new areas. For example, a model light-harvesting unit based on a fusion of eGFP with cytochrome b_{562} has been designed; in this chimera, eGFP's chromophore serves as an antenna transferring the absorbed energy to the b_{562} unit with 65% efficiency.[45] Using chromophores of fluorescent proteins as sensitizers in solar cells has also been considered.[46] Possible uses of fluorescent proteins in nanobiophotonic devices[47,48] and for optical data storage[49,50] have been described. To illustrate the latter capability, rsEGFP was used to repeatedly write and read the text of Grimm's Fairy Tales with a DVD storage density; it was shown that the same rsEGFP layer can be used for ∼15 000 read/write cycles.[50] We believe that this is just the beginning of a new exciting era of emerging biotechnology applications of fluorescent proteins.

Various aspects of FPs have been extensively reviewed.[1,2,4,14−24,31,32,36] Studies prior to 2009 have been comprehensively reviewed in a topical issue of *Chemical Society Reviews*.[3,15−17,20] Transient dark states, their possible structure and connection to protonation equilibria, and the implication for single-molecule studies have been discussed in ref 20. Mechanistic details of ESPT have received considerable attention.[15,17] Photoconvertible and photoswitchable fluorescent proteins and their applications have been discussed in refs 22−24 and 32. The uses of fluorescent proteins in super-resolution imaging have been reviewed in refs 51 and 52.

The focus of this review is on photoinduced transformations in fluorescent proteins, such as photoisomerization, photooxidation, or photoreduction of the chromophore, chemical modifications of the chromophore and/or the protein environment, and ESPT. Some of these processes are initiated by (or coupled with) photoinduced electron transfer (ET). The suitability of a particular fluorescent protein in a particular imaging technique is determined by the interplay between these processes and their competition with the fluorescence and radiationless relaxation channels. Despite their importance, our mechanistic understanding of photoinduced transformations in fluorescent proteins is quite limited. We highlight the most recent studies that have not been covered in earlier reviews and photoinduced processes that have not received considerable attention yet. Thus, we will provide only a cursory overview of ESPT and focus primarily on ET and chemical transformations

DOI: 10.1021/acs.chemrev.6b00238
Chem. Rev. 2017, 117, 758−795

of the chromophore and the protein environment. The quantum yields of these photochemical transformation are relatively small (i.e., quantum yield for bleaching is $\sim 10^{-5}$, refs 41, 42, and 53−56); however, at the conditions of repeated illumination the overall cumulative effect is significant. For example, in the photooxidation of eGFP,[39] the estimated yield of oxidized eGFP is 0.5−0.7.

The structure of the review is as follows. We begin with a brief overview of photoinduced transformations in fluorescent proteins (section 2). We then review the main aspects of the fluorescent protein photocycle (section 3), with emphasis on relevant time scale and yields. The similarities and differences with photochemical processes in synthetic dyes and in other biological systems are also highlighted. We then proceed to discuss specific photoinduced processes (ET, section 4; ESPT, section 5; photoisomerization and photochemical transformations, section 6), focusing on mechanistic details and highlighting connections with applications. We then discuss mechanistic aspects of blinking and formation of transient dark states (section 7), photobleaching and phototoxicity (section 8), and photoconversions (section 9).

2. PHOTOINDUCED TRANSFORMATIONS IN FLUORESCENT PROTEINS

Figure 2 summarizes various types of light-induced changes in optical properties, which are exploited in applications. When fluorescent proteins are used as simple fluorescent tags, light is used to excite them and then fluorescence is recorded. The difference between the absorption and the emission wavelength is called Stokes shift. Combining fluorescent proteins with large and small Stokes shifts enables multicolor applications in which only one laser is required (single-excitation/dual-emission mode). These practical considerations motivated the development of fluorescent proteins with large Stokes shifts.[57−60] Large Stokes shifts are also desirable in FRET applications: in FRET acceptors, they improve the spectral gap between the donor's and the acceptor's emission, whereas large Stokes shifts in FRET donors reduce the direct excitation of the acceptor.

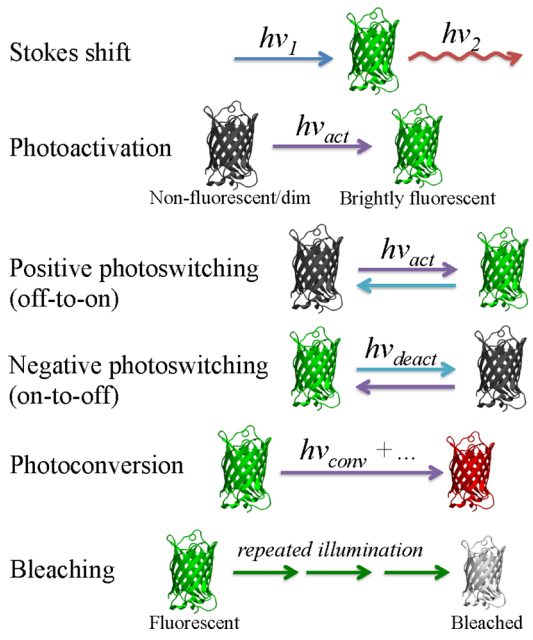

Figure 2. Various light-induced phenomena in fluorescent proteins.

The ability to use light to modify optical properties of fluorescent proteins has greatly expanded their usage.[22−24,31,32] Light can be used to selectively activate or deactivate fluorescent proteins. In some fluorescent proteins this can be done in a reversible fashion. Photoactivation (PA) entails the conversion of a dark, nonfluorescent form of the protein into a bright one. Using light to switch between dark and bright forms is called photoswitching (proteins that are dark in their most stable state are called positive photoswitchers, in contrast to negative photoswitchers, which are naturally bright and can be switched into a long-lived dark state). Some fluorescent proteins permit photoconversion (PC) rather than just photoactivation or photoswitching. These fluorescent proteins switch between two colors (e.g., from green to red), both of which can be visualized. Photoswitchable and photoconvertible fluorescent proteins provide a basis for many super-resolution techniques.[36,37]

There is a growing number of photoconvertible and photoswitchable fluorescent proteins (PC-FPs and PS-FPs).[22−24,31,32] The palette of currently useful PC-FPs includes PS-CFP,[61] Dendra,[62] mEosFP,[63] Kaede,[64] KikGR,[65] mIrisFP,[66] and PSmOrange,[30] all of which exhibit red-shifted absorption and fluorescence maxima upon irradiation with near-UV or deep blue light. Some phototransformations can be reversible, giving rise to the reversibly switchable fluorescent proteins (RS-FPs); in these, the fluorescent and nonfluorescent states are interconvertible by photoexcitation of each form using light of a specific wavelength. RS-FPs may be used in monochromatic multilabel imaging and dual-color fluorescence nanoscopy[67] as well as in optical memory and optical switches.[68]

Our state of knowledge on phototransformations in fluorescent proteins is rapidly evolving. For a long time, photoconversions were perceived as an unusual property of a few outliers from the large fluorescent protein family. The ability to undergo photoconversions was attributed to a specific amino-acid environment conductive of intramolecular reactions involving the chromophore and leading to its chemical modification. This paradigm substantially shifted in 2009, when several new photoconversions were described. One of them is the so-called photooxidative redding (green to red photoconversion in the presence of oxidants, section 9.4), which occurs in many fluorescent proteins with tyrosine-based chromophores and appears to be relatively insensitive to the chromophore's environment.[39] Subsequent studies provided additional examples of the ubiquity of photoconversion phenomena. Screening of the photobehavior of 12 different orange and red fluorescent proteins led to the discovery of novel red to green and orange to far-red conversions.[69] In cellulo red to green photoconversion of Katushka, mKate, and HcRed1 was observed both in one- and in two-photon excitation regimes; it can be induced by irradiation ranging from 3.06 to 2.21 eV (from 405 to 561 nm). Orange fluorescent proteins, mOrange1 and mOrange2, photoconvert to far-red forms emitting at 1.94 eV (640 nm) upon excitation by blue lasers; it was shown that these photoconversions proceed via multiphoton processes (more on this in section 9.1). Thus, the above examples of oxidative redding in GFPs and orange fluorescent proteins as well as greening of red fluorescent proteins illustrate that photoconversions are rather common among spectrally diverse fluorescent proteins.

The mechanisms and structural motifs of photoactivation, photoconversions, and photoswitching include cis−trans isomerization (often coupled with changes in protonation

DOI: 10.1021/acs.chemrev.6b00238
Chem. Rev. 2017, 117, 758−795

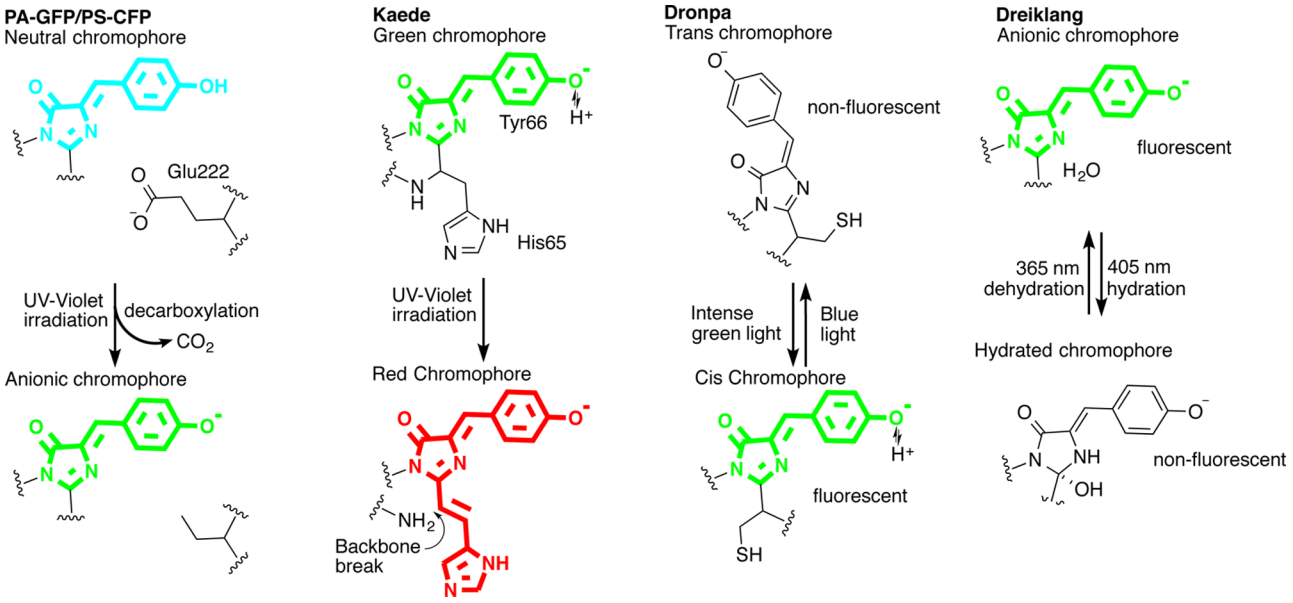

Figure 3. Different mechanisms of photoconversion, photoswitching, and photoactivation.

state), oxidation/reduction of the chromophore, and chemical changes involving the breaking of covalent bonds. Figure 3 shows several established mechanisms of photoconversion and photoswitching.[22,70] In PA-GFP,[71] photoactivation is achieved by changing the chromophore's environment (by decarboxylation of the nearby glutamine residue), which shifts the equilibrium between the two different protonation states of the chromophore. In Kaede,[72] Dendra,[62] and EosFP,[63] the change in color results from the photoinduced chemical modification of the chromophore (extension of the π-system and breaking the backbone of the protein). In Dronpa,[73] the switching between the dark and the bright states involves cis−trans isomerization coupled with changes in protonation states (a similar mechanism likely operates in Padron[67] and KFP[74]). In Dreiklang,[75] the switching is based on reversible photoinduced hydration/dehydration of the imidazolinone ring of the chromophore.

Cumulative tables with properties of currently used PA and PS fluorescent proteins can be found in refs 2, 4, 32, 36, 76, and 77. Reference 36 also provides a compilation of optical properties of monomeric not photoactivatable fluorescent proteins. In addition to monomeric fluorescent proteins ref 4 also provides a compilation of optical properties of dimeric and tetrameric fluorescent proteins. References 51 and 52 focus on fluorescent proteins used in super-resolution applications.

What can be said about photoconversions whose structural basis is not yet known? Oxidative redding in GFPs (section 9.4) entails one-photon two-electron oxidation of the chromophore by the external electron acceptors,[39] whereas the proposed mechanism of orange to far-red conversion[30] involves a two-photon photooxidation (discussed in section 9.4). The mechanism of greening of red fluorescent proteins remains unknown. Considering that green fluorescence was earlier described in DsRed-derived tetrameric proteins as emission from immature chromophores[78] and that greening occurs in cellulo and had not been observed in vitro, one can suppose an intermolecular mechanism, such as photoreduction by the external electron donors. Below, we review specific examples of phototransformations with emphasis on the underlying molecular-level mechanisms. We begin with an overview of the photocycle of fluorescent proteins (section 3) and then discuss various photoinduced processes such as ET, ESPT, and cis−trans photoisomerization. We illustrate by specific examples how these fundamental phenomena give rise to PA-FPs, PC-FPs, and PS-FPs.

3. FLUORESCENT PROTEIN PHOTOCYCLE

The photophysics and photochemistry of fluorescent proteins bear considerable resemblance to those of synthetic dyes.[34,79] From the chemical point of view, typical fluorescent protein chromophores (Figure 1) are similar to cyanine dyes, owing to their common structural feature: a methyne bridge connecting conjugated aromatic moieties. However, the presence of the protein barrel (Figure 4) leads to significant differences. The rigid protein environment restricts the chromophore's range of motion and limits its accessibility to the solvent and other species present in solution (ambient oxygen, salt ions, oxidating and reducing agents, etc.). Indeed, photophysical properties of

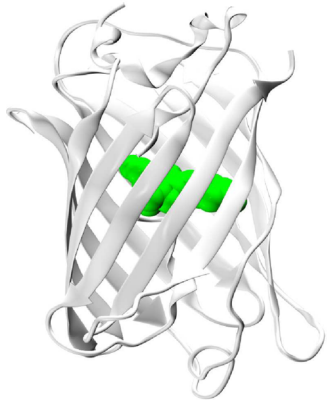

Figure 4. Typical structure of a fluorescent protein represented by eGFP. In all fluorescent proteins, the chromophore, which is formed autocatalytically upon protein folding, is buried inside a tight 11-stranded β-barrel comprising 220−240 amino acids. Approximate molar weight is 25−30 kDa. The diameter of the barrel is ~24 Å, and its height is ~42 Å.

DOI: 10.1021/acs.chemrev.6b00238
Chem. Rev. 2017, 117, 758−795

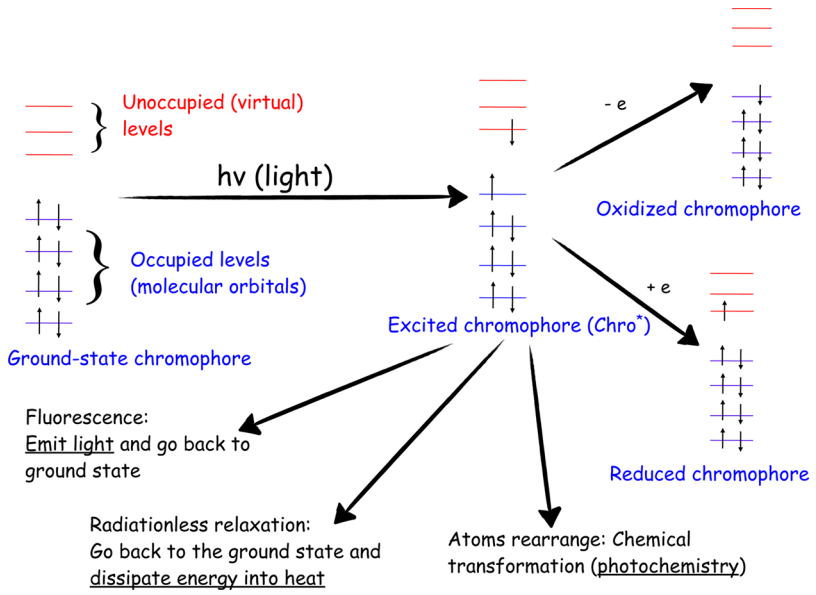

Figure 5. Excited-state processes in fluorescent proteins. The main relaxation channel is fluorescence. Radiationless relaxation, a process in which the chromophore relaxes to the ground state by dissipating electronic energy into heat, reduces the quantum yield of fluorescence. Other competing processes, such as transition to a triplet state via intersystem crossing (not shown), excited-state chemistry, and electron transfer, alter the chemical identity of the chromophore, thus leading to temporary or permanent loss of fluorescence (blinking and bleaching) or changing its color (photoconversion).

the model chromophores in solutions differ strikingly from those of the respective parent fluorescent proteins:[1,15] the solvated chromophores do not fluoresce, they often have different colors, and they are more efficient photosensitizers.

The ability of the wt-GFP to fluoresce is rather fragile and can be easily impeded even by a single mutation: a recent high-throughput systematic investigation of the local fitness landscape of av-GFP, in which 51 715 protein structures were assessed, has shown that the landscape is narrow, with 75% of the derivatives with a single mutation showing reduced fluorescence and 50% of the derivatives with four mutations being completely nonfluorescent.[80]

Figure 5 outlines various excited-state processes in fluorescent proteins. The photocycle is initiated by light absorption, producing an initial electronically excited state of the chromophore. The main relaxation channel restoring the ground-state chromophore is fluorescence. The color of the emitted light may differ from the absorbed light due to a structural relaxation of the chromophore, its hydrogen-bond network, or ESPT. Alternatively, the chromophore may return to the ground state by dissipating the electronic energy into nuclear motions via radiationless relaxation. Such thermal relaxation fully dominates in GFP-like chromoproteins, which have extremely low fluorescence quantum yield (10^{-4}–10^{-5}). Since the bonding pattern in the excited states is different, electronic excitation can initiate various chemical transformations of the chromophore, such as isomerization, making or breaking covalent bonds, photooxidation/photoreduction, or reactions with nearby residues or small molecules (e.g., ambient oxygen). Changes in bonding pattern upon excitation also affect the acidity of the chromophore, which is a driving force for ESPT. These processes alter optical properties, leading to the formation of transient dark or permanently bleached states as well as changing the color of the absorption/fluorescence. Thus, the yields of bleaching and blinking, photostability, phototoxicity, photoswitching, and photoconversion phenomena are determined by the competition between the main relaxation channels (fluorescence and radiationless relaxation) and various photoinduced transformations. The time scales of different channels are crucially important for understanding the branching ratios and yields. A finite excited-state lifetime limits the scope of excited-state processes. Typical for fluorescent systems, the excited-state lifetimes in fluorescent proteins are 1–10 ns. Thus, in order to have a noticeable effect on the photocycle, an excited-state process should be initiated on a time scale comparable with that of the excited-state lifetime. Below we briefly review typical lifetimes and yields of these excited-state processes.

3.1. Fluorescence and Radiationless Relaxation

Not surprisingly, the dominant excited-state process in fluorescent proteins is fluorescence; its quantum yield (Y_f) is high, e.g., 0.6 in eGFP and eYFP.[81] Among the fluorescent proteins with the highest Y_f are Citrine (Y_f = 0.76, ref 53), Ypet (Y_f = 0.77, ref 82), Dronpa (Y_f = 0.85, ref 73), mEOS2 (Y_f = 0.84, ref 83), and mTurquoise2 (Y_f = 0.93, ref 84). However, many fluorescent proteins have relatively low Y_f, despite significant efforts to improve it. For example, mFruit series have Y_f as low as 0.22 (in mCherry).[85] The fluorescent proteins with large Stokes shift (so-called LSS-FPs) have rather low Y_f, e.g., 0.08 and 0.17 in LSS-mKate1 and LSS-mKate2, respectively.[57] Two years after LSS-mKates, LSS-mOrange with Y_f of 0.45 was developed.[86] In 2016, the LSS-FP with the highest Y_f of 0.76, CyOFP1, was reported.[60]

Interestingly, Y_f of model fluorescent protein chromophores in solutions are 3–4 orders of magnitude lower than in the protein environment; this phenomenon has been attributed to the increased flexibility of the bare chromophore and its interactions with solvent molecules.[15,87–89]

The dominant process leading to the loss of fluorescence is radiationless relaxation. In contrast to bleaching, this is a relatively benign process since it simply restores the ground-state chromophore (although long-lived dark states can also be formed via radiationless relaxation). The upper limit for this

DOI: 10.1021/acs.chemrev.6b00238
Chem. Rev. 2017, 117, 758–795

channel is given by $1 - Y_f$. For dyes in solutions, the rate of radiationless relaxation can be controlled by solvent viscosity and temperature: it slows down in viscous solvents and at low T. Excited-state lifetime τ can be written as follows[79]

$$\tau = \frac{1}{k_f + \frac{k_b T}{4\pi r^3 \eta}} \quad (1)$$

where η is solvent viscosity in N s m^{-2}, r is the radius of the chromophore (in meters), T is the temperature, and k_f is the fluorescence rate constant. Overall, typical increases in τ at low T are moderate, usually a factor of 2−3 in the same solvent (changing the viscosity of the solvent may have a more significant effect, up to several orders of magnitude).[79] The effect of the tight protein barrel on the excited-state chromophore appears to be somewhat similar to high-viscosity solvent: both lead to an increase in excited-state lifetime. The correlation between the rigidity of the chromophore and its ability to fluoresce has been illustrated experimentally: model GFP chromophores become fluorescent when confined in nonprotein rigid scaffolds[90,91] or encapsulated in other, non-native proteins, such as human serum albumin.[92]

By restricting the protein/solvent range of motion, Y_f in fluorescent proteins can also be controlled by hydrostatic pressure. Such experiments have been carried out for the green,[93−97] blue,[96,98−100] yellow,[101,102] and several red[96,103] FPs. In many systems (e.g., TagRFP-S, TagRFP-T, mOrange2, and mStrawberry), Y_f increases upon a pressure increase of up to 250−530 MPa; however, in some cases (mCherry and mKO) the fluorescence only decreases. At pressures above 250−530 MPa, the fluorescence intensity decreases dramatically for all proteins,[103] probably due to denaturation. Simulations, which investigated the effect of pressure on structural fluctuations of the chromophore and the protein barrel,[104] have shown that hydrostatic pressure has almost no effect on the chromophore's structure (e.g., planarity), whereas the hydrogen-bond network around the chromophore and backbone fluctuations are strongly affected. On the basis of the calculations, it was concluded[104] that pressure increase causes initial increase of Y_f only for relatively floppy fluorescent proteins, whereas for fluorescent proteins with more rigid structures Y_f is already close to its maximum. This study suggested that low Y_f in some fluorescent proteins is dynamic in nature and depends on the range of thermal motion of the chromophore and fluctuations in the hydrogen-bonding network rather than on their average structure (this issue is discussed in detail in section 6.1). Brighter blue and red fluorescent proteins were developed by following a rational design idea, restricting the chromophore's range of motion by sandwiching it between bulky groups.[105,106] A similar motif, a GFP-like chromophore immobilized by bulky guanine residues, is exploited in Spinach, an RNA mimic of GFP developed for in vivo real-time imaging of biological RNAs.[107]

Typical fluorescence lifetimes are in the 1−10 ns range. In green and cyan fluorescent proteins, lifetimes are within 1.5−3 ns;[108−110] the longest reported lifetime value for green fluorescent proteins is 5.1 ns.[110] In some fluorescent proteins (such as mFruit[85]), lifetimes can be relatively short, on a subnanosecond scale. Often shorter lifetimes lead to the decline in optical output (i.e., amount of fluorescence) but result in higher photostability because rapid relaxation reduces the yield of the competing excited-state processes. Interestingly, larger Stokes shifts, which are related to the increased flexibility of the chromophore and its hydrogen-bonding network, correlate with decline in lifetime. Fluorescence lifetime depends on the structure of a particular fluorescent protein; yet, it is also highly sensitive to the viscosity, temperature, pH, and interactions with other species. In in cellulo imaging, these conditions depend on cell physiology. This provides a foundation for the class of techniques known as fluorescence lifetime imaging microscopy (FLIM). In contrast to the gross optical output (fluorescence intensity), the fluorescence lifetime does not depend on the concentration of the fluorescent protein. Thus, by measuring the changes in fluorescence lifetime one can monitor the changes in local environment.[111] Some variants of FLIM exploit environment-dependent lifetime changes for measuring intracellular physiological parameters (e.g., ion strength and pH) and for measuring protein−protein interactions visualized by FRET.[44] Distinct fluorescence lifetimes represent an additional spectral parameter, which allows one to distinguish, spatially and temporally, fluorescent proteins with similar emission maxima, giving rise to the lifetime unmixing technique.[108]

3.2. Stokes Shifts: Large and Small

A Stokes shift arises due to structural changes of the electronically excited system that occurs prior to emission. In the gas phase, the Stokes shift is determined by the structural relaxation of the chromophore alone. In solutions and in protein-bound chromophores, the environment also contributes to the Stokes shift, either increasing or decreasing it. Typical Stokes shifts in fluorescent proteins are 0.1 eV or less. They can be as small as a few wave numbers or as large as 0.7 eV (e.g., in LSS-mKate[112]). In wt-GFP, the Stokes shift of 0.75 eV is responsible for its ability to convert blue absorbed light into green fluorescence. Stokes shifts around 0.2 eV or larger are considered to be enhanced or extended. A large Stokes shift (LSS) is defined[57] as a Stokes shift exceeding 100 nm.

In fluorescent proteins, at least three mechanisms are responsible for Stokes shifts: (i) relaxation of the chromophore, (ii) ESPT, and (iii) rearrangement of the hydrogen-bond network around the chromophore. These rather diverse excited-state structural changes are driven by changes in the bonding pattern upon electronic excitation. Changes in bonding are often accompanied by charge redistribution, which drives the rearrangement of the solvent molecules around the chromophore.

ESPT is arguably the most important mechanism because it can lead to very large Stokes shifts[57,58,60,86] due to strongly red-shifted excited states in deprotonated anionic chromophores relative to their neutral forms (see the discussion on color tuning in section 3.5). The mechanism of ESPT in fluorescent proteins is discussed in detail in section 5.

Because ESPT occurs only in fluorescent proteins with photoacidic chromophores, such as neutral GFP-like ones, the Stokes shifts in anionic chromophores arise due to structural relaxation of the chromophore and the rearrangement of its hydrogen-bond network. The structural relaxation of isolated electronically excited GFP chromophores can lead to Stokes shifts of ∼0.5 eV, as observed computationally in anionic DsRed-like chromophores,[113] but the protein environment restricts the relaxation, reducing the overall shift by more than half. Extended Stokes shifts in several red fluorescent proteins with anionic chromophores,[24] such as TagRFP675[114] and mPlum,[29] have been attributed to specific features of the hydrogen-bond network around the chromophore (as observed

DOI: 10.1021/acs.chemrev.6b00238
Chem. Rev. 2017, 117, 758−795

in crystal structures)[24,60,85] and its flexibility.[114] While the importance of specific residues (such as Glu16 in mPlum) for producing the extended Stokes shift had been tested by mutagenesis,[114−116] the detailed mechanistic picture has begun to emerge only recently, as a result of several experimental and theoretical studies.[58,113,116−118] Ground-state molecular dynamics simulations of mPlum and its mutants have shown that in mPlum and mutants with large Stokes shifts there are two interconverting populations in the ground state (that differ by hydrogen-bond pattern), whereas mutants with small Stokes shifts have only one dominant structure.[116] The authors conjectured that the flexibility of the hydrogen-bond network is responsible for the enhanced Stokes shift.[116] The flexibility of the hydrogen-bond network was also assumed to be responsible for the large Stokes shift (0.24 eV) in TagRFP675, the most red-shifted of all red fluorescent proteins.[114] Later, QM/MM calculations[113] of the excited-state structures of mPlum showed that both populations—one with the direct (Chro-Ile65···Glu16) and one with the water-mediated (Chro-Ile65···Wat321···Glu16) hydrogen bonds—collapse into a single emitting state with the water-mediated (Chro-Ile65···Wat321···Glu16) pattern. The Stokes shift of 0.20 eV arises due to a large energy change in the first (dominant) population. This picture has been confirmed by a time-resolved experiment[118] showing that the emission spectra of mPlum feature a clear isoemissive point, which is a signature of the two emitting states relaxing to a single emitting state within the lifetime of the excited state.[118] Figure 6 illustrates this mechanism. The fast (160 fs) and slow (37 ps) excited-state relaxation time scales[58,118] were assigned to the relaxation of the chromophore and the hydrogen-bond reorganization around the chromophore, respectively.

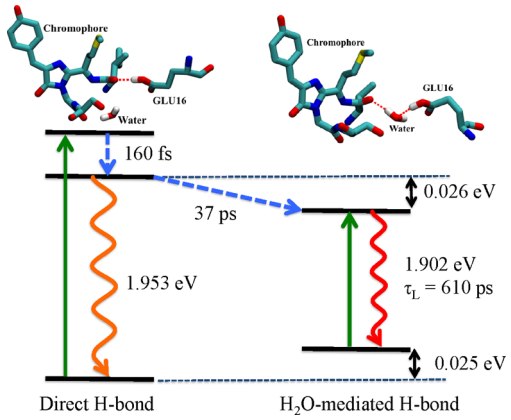

Figure 6. Energy-level diagram explaining the mechanism of the Stokes shift in mPlum. Extended Stokes shift in mPlum arises due to the interconversion of the two ground-state populations, which differ by hydrogen bonds formed by the chromophore, into a single emitting state. The slow relaxation component of 37 ps corresponds to the reorganization of the hydrogen-bond network. Energies and time constants are from ref 118.

Such excited-state hydrogen-bond interconversion might be operational in other fluorescent proteins. As noted in ref 118, in TagRFP675,[114] *N*-acylimine carbonyl also forms two hydrogen bonds: a water-mediated bond with Gln106 and a direct bond with Gln41. Thus, rearrangement of this pattern might be responsible for its large Stokes shift. This motif might become an effective modality for extending Stokes shifts in fluorescent proteins.

A more recent study of TagRFP675 and several of its mutants designed to interrupt the hydrogen-bond network has revealed interesting differences between mPlum and TagRFP675.[119] By using spectrally resolved transient grating and time-resolved fluorescence spectroscopies and molecular dynamics simulations,[119] the authors observed several ground-state populations corresponding to different hydorgen-bond networks. In contrast to mPlum, the distinct emitting states in TagRFP675 do not relax to a single emitting state within the lifetime of the S_1 state. The authors attributed[119] the large Stokes shift in TagRFP675 to a subpicosecond relaxation of the chromophore itself and to the changes in the hydrogen-bond network in the vicinity of Gln41, which does not directly involve the chromophore. By revealing an interesting feature of this protein (and also mKate-M41Q), this study[119] highlights the complexity of excited-state relaxation mechanisms in fluorescent proteins.

3.3. Transient Dark States

Blinking, a temporary loss of fluorescence, is a common phenomenon in many fluorescent systems, from dyes to nanoparticles.[34,121] Figure 7 shows typical blinking behavior illustrated by a fluorescence signal recorded from a single immobilized fluorescent protein molecule. In this example[120] individual molecules blink several times per second. Figure 8 shows a simplified diagram illustrating photoinduced interconversion between bright ("on") and dark ("off") states. In fluorescent proteins, blinking is attributed to the formation of transient dark states of various nature such as different protonation forms or cis−trans isomerization (or both), formation of triplet states, or transient reduced or oxidized species.[122] In applications such as single-molecule studies,[121] blinking is a nuisance. However, when induced in a controlled manner, temporary fluorescence switching on and off offers new opportunities exploited in, for example, PS-FPs.[22] A well-

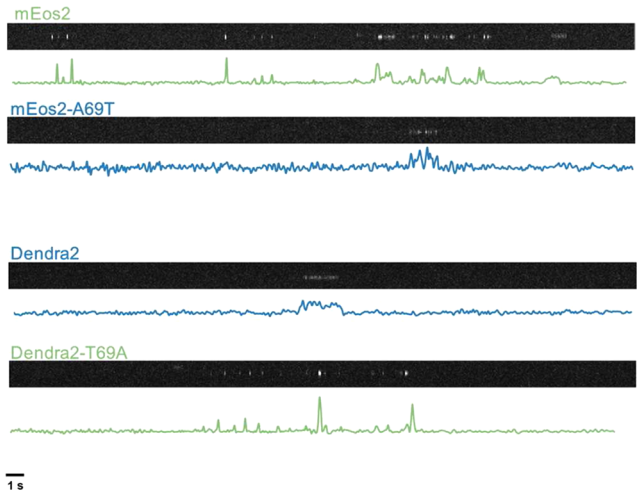

Figure 7. Blinking in fluorescent proteins. Plots show fluorescence signals as a function of time from a single immobilized molecule of mEos2, Dendra2, and their single-point mutants. Blinking in these systems occurs 6−9 times per second. mEos2 and Dendra2-T69A exhibit high-blinking behavior (the fraction of blinking molecules is ~40%), whereas Dendra2 and mEos2-A69T show low blinking (the fraction of blinking molecules is about 20−26%). Reproduced with permission from ref 120. Copyright 2015 American Chemical Society.

DOI: 10.1021/acs.chemrev.6b00238
Chem. Rev. 2017, 117, 758−795

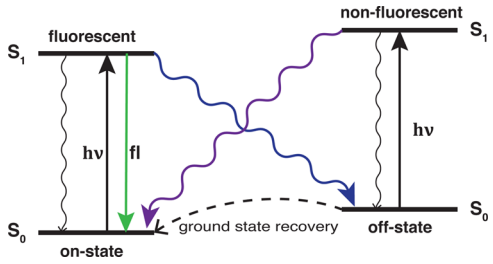

Figure 8. Energy diagram illustrating interconversion between bright and dark states. Short-living dark forms give rise to blinking. Long-living dark states are exploited in photoswitching. Fluorescent and nonfluorescent forms of a photoswitchable fluorescent protein can be interconverted via excited-state processes.

known example of a system where temporary dark states can be formed in a controlled fashion by photoinduced cis−trans isomerization coupled with changes in protonation state is Dronpa[123] and its counterpart, Padron[67] (in Dronpa, the native bright state can be photoconverted into a dark state, whereas in Padron, the native state is dark and can be turned on by irradiation). Such dark states are formed via excited states and can be relatively long lived (up to hours). Blinking kinetics was investigated[124] in YFP, in which the quantum yield of forming transient dark states was measured as 3×10^{-4}, which is not too different from common dyes.[34]

Formation of triplet states, which can be populated via intersystem crossing (ISC), is also common in dyes.[34] The typical quantum yield of triplets in dyes[34] is 10^{-3}; they are quenched by oxygen. The lifetimes of triplets in anaerobic conditions are up to milliseconds; however, they are much shorter in the presence of oxygen. Triplet lifetimes of 10−40 μs have been reported for selected fluorescent proteins (KillerRed,[125] eGFP mutants[126,127]); such long triplet lifetimes in aerobic conditions provide yet another manifestation of the protective role of the β-barrel.

Formation of transient oxidized/reduced states (radicals) also contributes to temporary or permanent loss of fluorescence or changes of its color. For example, in RFPs a red-shifted transient species with a micro- to millisecond lifetime was observed and assigned to the dianion−radical produced by chromophore photoreduction.[128] One-electron oxidation of the anionic chromophores (as in eGFP and eYFP) leads to strongly blue-shifted absorption.[129]

Despite recent progress, the exact nature of transient dark states in fluorescent proteins remains unclear. Different types of dark states may be formed in the same fluorescent protein, and different fluorescent proteins are likely to feature different dark states.

3.4. Bleaching, Photoconversions, and Phototoxicity

Permanently bleached and/or photoconverted states can be produced by chemical modifications of the chromophore (as in oxidative redding[30,39] or in Kaede[72] green to red photoconversion) or of the protein (as in decarboxylation[130,131]). Typical quantum yields of bleaching (Y_{bl}) in fluorescent proteins without oxidants are 10^{-5} (refs 41, 42, and 53−56), which means that an individual fluorescent protein molecule can endure, on average, up to 100 000 excitation−deexcitation cycles. In the presence of an oxidant, Y_{bl} might be higher (up to an order of magnitude[39]). In GFP and some other fluorescent proteins (most prominently, KillerRed and other red fluorescent proteins derived from DsRed), Y_{bl} is strongly oxygen dependent. The mechanisms of bleaching in fluorescent proteins are not yet fully elucidated and are likely to be diverse and include multiple competing channels.

Y_{bl} determines photostability and photofatigue, key parameters in applications.[36] High photostability (i.e., low Y_{bl}) is mandatory for detection of weak fluorescence signals, long-term data acquisition, and quantitative measurements (such as those based on FRET).

Theoretical modeling has suggested that enhanced bleaching in mFruits is due to oxygen accessibility to the chromophore.[132] Another computational study has illustrated that the diffusion of oxygen inside the barrel is greatly facilitated in KillerRed, relative to eGFP.[133] Experimentally, the connection between photosensitization efficiency and oxygen accessibility to the chromophore has been established by considering eGFP mutants[126,127] derived by mutating His148 to less bulky amino acids.

The exact mechanism of bleaching is unclear. Bleached forms may be produced by chemical reactions of the chromophore or the protein that could be initiated by ET or by reactions with ROS such as superoxide or singlet oxygen (see Figure 9).

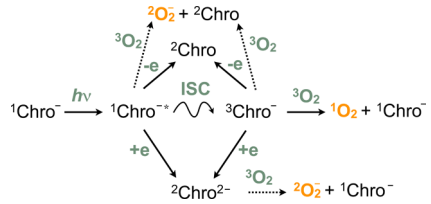

Figure 9. Photoinduced processes that can lead to the formation of reactive oxygen species (ROS), $^1O_2$ (singlet oxygen) and $^2O_2^-$ (superoxide). Reproduced with permission from ref 128. Copyright 2014 American Chemical Society.

3.5. Structural Variations in Fluorescent Proteins

Despite their diversity in origin and photophysical properties, fluorescent proteins are remarkably similar in structure. Figure 10 shows the alignment of 202 crystal structures, revealing striking similarity of the proteins' three-dimensional structures. All fluorescent proteins feature an 11-stranded β-barrel structure with a single distorted helix in the center of the barrel comprising the three amino acids that form the chromophore. These amino acids are located at positions 65−67 (av-GFP numbering); they always correspond to an *XZG* tripeptide, where *X* is variable, *Z* is an aromatic amino acid (tyrosine in naturally occurring proteins), and *G* denotes glycine. Yet, the chemical structures of the chromophores are rather diverse (Figure 1). Within the same structural motif of a chromophore, differences in its protonation state and conformation (cis versus trans) affect color and other photophysical properties. Interestingly, most of the chromophores in fluorescent proteins occur in the cis state, as clearly seen from the bottom panel of Figure 10.

Color tuning in fluorescent proteins involves several distinct mechanisms (see Figure 1). As can be rationalized by the particle-in-the-box model, more extensive electronic delocalization leads to red-shifted absorption/emission. The delocalization can be achieved by extended conjugation of the chromophore's π-system or by π-stacking with other aromatic residues, such as tyrosines. A red shift also arises upon deprotonation of the phenolic moiety, which can be explained

DOI: 10.1021/acs.chemrev.6b00238
Chem. Rev. 2017, 117, 758−795

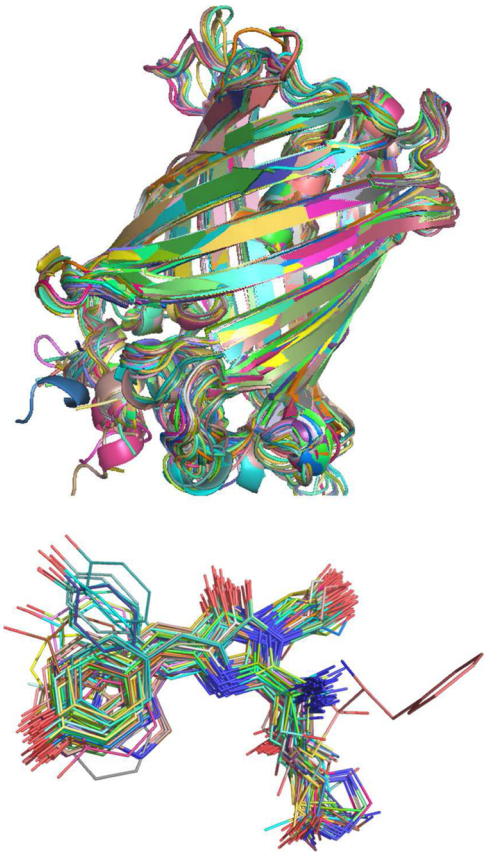

Figure 10. Alignment of 202 crystal structures of different fluorescent proteins. (Top) Three-dimensional structures of the β-barrel. (Bottom) Alignment of the chromophores. Note that the majority of the chromophores are in the cis state. Reproduced with permission from ref 31. Copyright 2013 American Chemical Society.

by the Hückel model.[21] The electrostatic and hydrogen-bonding interactions between the chromophore and the nearby residues also contribute to color tuning.[134,135] A recent QM/MM study,[134] which analyzed the contributions of π-stacking and electrostatic interactions to the YFP's red shift, concluded that the effect of electrostatic interactions with nearby polar side chains is of the same magnitude as the effect due to delocalization via π-stacking.

The analysis[136] of 266 entries of GFP-like proteins deposited in the protein data bank by 2011 has shown that the similarities in the amino-acid sequence relative to av-GFP vary from ~85% to 25%. Interestingly, among the 21 most conserved residues, the majority are located at the top and the bottom of the barrel; this observation has led to assigning a special significance of these lid residues.[136] A high-throughput study[80] of the local fitness landscape of avGFP (defined in terms of its native function, fluorescence) has shown that the fitness landscape is narrow, that is, the fluorescence is easily suppressed by even a single mutation (75% of single-residue mutations show reduced fluorescence). Most mutations that have a strong effect on fluorescence correspond to amino-acid residues oriented internally toward the chromophore (see Figure 11).

Different protonation states of GFP-like chromophores have distinctly different photophysical properties. For example, the neutral wt-GFP chromophore absorbs in blue, whereas its deprotonated form is green. Brightness also depends on the protonation state. Changes in protonation states can be

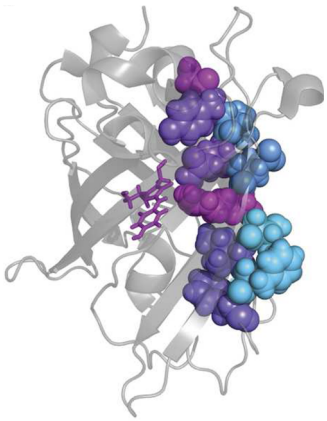

Figure 11. Selected β-strand of the GFP structure showing the location of single mutations strongly decreasing fluorescence (violet) versus neutral mutations (blue). Reproduced with permission from ref 80. Copyright 2016 Macmillan Publishers Limited.

controlled by pH and by changing the local chromophore's environment by point mutations[137] or via phototransformations,[130,131] which is exploited in some photoswitchable fluorescent proteins.[71]

Figure 12 shows different protonation states of the cis and trans conformations of a GFP-like chromophore. In most fluorescent proteins, the chromophore in its normal bright state has the cis conformation (see Figure 10), whereas trans conformers often correspond to transient dark forms;[138,139] however, there are also examples of fluorescent proteins with bright trans chromophores, e.g., eqFP611 and eqFP578.[139,140] The two most common protonation states of the tyrosine-based chromophores correspond to the neutral chromophore (denoted by N) and its deprotonated, phenolate-like, anionic form A. The interplay between these two forms controls many photophysical properties of fluorescent proteins.[1,2] In partic-

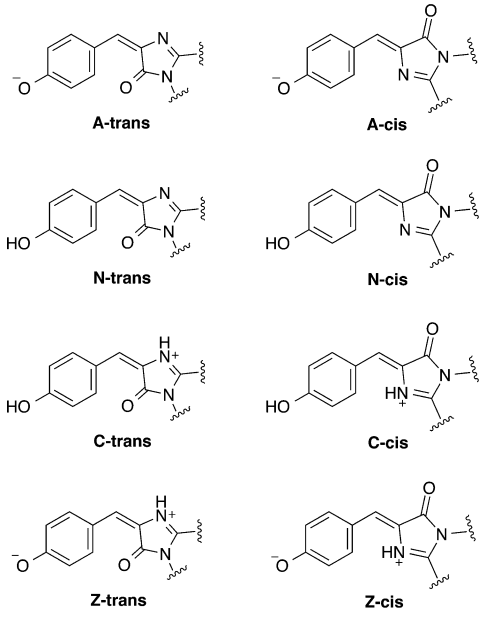

Figure 12. Possible states of the chromophore in GFP-like proteins. The chromophore can assume cis or trans conformations and be in the following protonation states: neutral (N), anionic (A), cationic (C), and zwitterionic (Z).

DOI: 10.1021/acs.chemrev.6b00238
Chem. Rev. 2017, 117, 758−795

ular, photoinduced proton transfer (ESPT, discussed in section 5) leads to a large Stokes shift in wt-GFP and in LSS-RFPs.

Determining protonation states requires a combination of techniques. Only indirect information about protonation states is provided by X-ray structures: the distances between heavy atoms may suggest the presence of a proton participating in a hydrogen bond. Kinetics studies (and, especially, isotope effects) and the pH dependence of optical properties are often used to elucidate protonation states. Protonation states can be unambiguously determined by vibrational spectroscopy. Computational methods, which include several complementary approaches, are also particularly useful for this task. The most rigorous approach is to compute Gibbs free energies of various protonation states in order to identify the most stable form.[141,142] Such calculations require high accuracy from an underlying electronic structure method and extensive thermodynamic averaging. This approach has been used, for example, to calculate pK_a shifts due to cis−trans photoisomerization in Dronpa and Padron.[143] As a shortcut, one can consider optimized structures of the protein in different protonation forms. Unfavorable protonation states might be found to be unstable or cause large deformation of the hydrogen-bonding network around the chromophore, allowing them to be ruled out.[144−146] Finally, one can compute spectroscopic properties of different forms and compare them with the experimental absorption maxima.[144] The combination of the latter two approaches has allowed the determination[144] of the protonation state of the so-called blue intermediate (a transient form in the red chromophore maturation process) for which several protonation states had been proposed.

The existence of other protonation states, Z and C forms, was hypothesized in the very first theoretical studies of fluorescent proteins.[147,148] Although Raman spectroscopy studies[149] of the isolated GFP chromophore showed no evidence of the C and Z forms, their formation in the protein matrix has not been ruled out, especially in the excited states. Possible involvement of the zwitterion form in the photocycle of other fluorescent proteins has been invoked to explain kindling phenomena[150] and photobleaching in IrisFP (more on this in section 6.2).

3.6. Spectroscopic Signatures of Transient Forms

Spectroscopy is commonly used for detection and monitoring of transient species. In particular, broad-band transient absorption (TA) spectroscopy spanning the time scale from picoseconds to seconds is a powerful tool for interrogating excited-state processes of fluorescent proteins and the nature of dark states.

In processes involving fluorescent proteins, intermediates usually are first identified spectroscopically. Being much more difficult, structure determination may lag behind for many years. Quantum-mechanical calculations can help to screen structures of possible candidates. For example, electronic structure calculations showed that one-electron oxidation of GFP-like anionic chromophores leads to strongly blue-shifted absorption,[129] whereas one-electron reduction results in the red shift.[128]

Even when crystallographic structures are available, calculations are needed to identify exact protonation and oxidation states. For example, six different structures are consistent with the X-ray structure[151,152] of the blue intermediate[153] in the red chromophore maturation processes in DsRed-like fluorescent proteins, the blue-emitting form of fluorescent timers,[154] and the dark form of PAmCherry.[155] Electronic structure calculations[144] have illustrated that only one form, the tagBFP structure shown in Figure 1, absorbs in blue and does not cause severe structural distortions of the surrounding protein. Similarly, on the basis of quantum-mechanical calculations possible structures of transient dark states in IrisFP have been proposed.[156] Thus, partnership between theory and experiment can be very productive in determining structures of the transient species and new chromophores.

4. PHOTOINDUCED ELECTRON TRANSFER: A GATEWAY STEP LEADING TO MULTIPLE OUTCOMES

Photoinduced ET to/from the chromophore can lead to a variety of outcomes. Well known in dyes, photoinduced redox properties of fluorescent proteins came into the spotlight in 2009, when it was discovered that fluorescent proteins can be efficient light-induced electron donors.[39] Bogdanov et al. observed that many fluorescent proteins with an anionic GFP chromophore (such as one in eGFP, see Figure 1) undergo photoconversion from green to red form upon irradiation in the presence of oxidants.[39] Chemical steps leading to the red chromophore formation (whose structure is still not known) are initiated by photooxidation, ET from the electronically excited chromophore to an external oxidant molecule.[39] Another type of photoconversion (based on the stabilization of the anionic form of the chromophore relative to the protonated neutral one) also involves a photoinitiated redox process: photoinduced ET from nearby Glu to the chromophore is believed to be a gateway step leading to decarboxylation.[130,157,158] Recently, photoreduction of the chromophore was invoked to explain the formation of long-lived red-shifted transient species in red fluorescent proteins.[128] Photoreduction may also play a role in anaerobic redding[159] or in greening of red fluorescent proteins.[69] Photoinduced ET from the anionic chromophores to O_2 may lead to superoxide formation, which might be responsible for phototoxicity.[125]

In short, there is a growing body of evidence of the importance of photoinduced ET in fluorescent proteins. Different types of ET may be operational, such as ET to and from the chromophore producing reduced or oxidized species. Furthermore, the redox partners of the chromophore may be different: ET may entail a nearby residue, such as glutamate as a donor or tyrosine as an acceptor, or an oxidant molecule (e.g., O_2).

ET can proceed by different mechanisms summarized in Figure 13. One possibility is ET from the electronically excited chromophore via the Marcus mechanism, which may involve the direct ET to an oxidant molecule, or a multistep hopping process via intermediate electron acceptors.[160−162] In the strong coupling regime, ET can proceed by adiabatic evolution of the initially excited state. Alternatively, the charge-transfer (CT) states can be populated directly by photoexcitation or via radiationless relaxation from higher excited states (especially at high-intensity conditions when multiphoton processes become operational).

4.1. Energetics of ET

The key thermodynamic quantity for ET is the Gibbs free energy of the chromophore's oxidation/reduction and, consequently, the standard oxidation/reduction potential. To date, these quantities have only been measured for model chromophores in solutions[163] and characterized computation-

DOI: 10.1021/acs.chemrev.6b00238
Chem. Rev. 2017, 117, 758−795

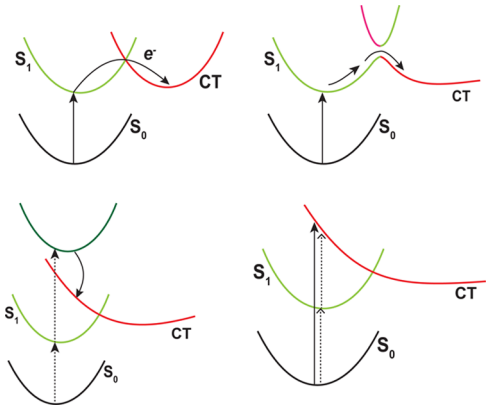

Figure 13. Different mechanisms for ET. Relevant states are the bright excited state (S_1) and the charge-transfer (CT) state. In photooxidation, the latter is of D^+A^- character (or $D{\cdot}A^-$, depending on the protonation state of the chromophore). (Top left) ET between the donor and the acceptor by the Marcus mechanism. (Top right) Adiabatic evolution of the initially excited state leading to CT via a barrier. (Bottom left) CT state accessed by radiationless relaxation from a higher excited state. (Bottom right) ET via direct one- or multiphoton excitation of the excited state of CT character.

ally, both for isolated and for protein-bound chromophores.[145,163−165] In the most recent study,[145] the Gibbs free energies of the chromophore oxidation were computed by the QM/MM calculations using high-level electronic structure methods and Warshel's linear response approximation[166] for thermodynamic averaging.

For the oxidation process to be thermodynamically possible, ΔG_{ox}(Chro) + ΔG_{red}(OX) should be negative. As one can see from the molecular orbital (MO) diagram in Figure 5, electronic excitation makes both the oxidation and the reduction processes more energetically favorable. For example, the energy required to remove an electron from the ground state is equal to minus the energy of the highest occupied MO (HOMO). However, an electronically excited chromophore can be oxidized by removing the electron from the lowest unoccupied MO (LUMO), which is higher in energy than the HOMO. By using energy balance

$$\Delta G_{ox}(\mathrm{ex}) \approx \Delta G_{ox}(\mathrm{gs}) - E_{ex} \quad (2)$$

$$\Delta G_{red}(\mathrm{ex}) \approx \Delta G_{red}(\mathrm{gs}) - E_{ex} \quad (3)$$

where E_{ex} is energy difference between the ground and the excited states (e.g., emission energy).

Table 1 shows the computed Gibbs free energies for oxidation of the chromophore in several fluorescent proteins that feature an anionic GFP-like chromophore.[145] The table shows ΔG_{ox} for eGFP, eYFP (in which the chromophore is π-stacked with tyrosine), eYFP with a bound halide anion, and an eGFP mutant (Tyr145Leu). For comparison, Table 2 shows Gibbs free energies for the reduction reactions for several oxidants.[145] As reported in the original GFP redding study,[39] GFP can be oxidized by various oxidizing agents with E^0 up to −0.114 V (relative to SHE), which corresponds to $\Delta G_{red} \leq$ −4.167 V at pH = 7 (using ΔG(SHE) = 4.281 eV, ref 167). The energetics from Tables 1 and 2 is consistent with estimated ΔG_{red}: oxidation of the ground-state chromophore is not thermodynamically favorable; however, it becomes possible upon electronic excitation.

Table 1. Redox Properties of the Chromophores of eGFP, YFP, and Halide-Bound YFP at T = 298 K in their Ground and Electronically Excited States[a]

system	ΔG_{ox}(gs)	λ_{ox}	E_{em}^{expt}	ΔG_{ox}(ex)	E_{red}^{0}(gs)
eGFP	4.551	1.599	2.44	2.111	0.27
YFP	4.697	1.400	2.35	2.347	0.42
YFP + Cl^-	4.274	1.686	2.35	1.924	−0.01
eGFP − Y145L	4.548	1.528	2.44	2.108	0.27

[a]Energies are in eV, and the reduction potential is in V with respect to SHE. From ref 145.

Table 2. Standard ΔG_{red} (eV) of Selected Oxidants with respect to SHE. From ref 145.

OX species	ΔG_{red}(OX)	source
O_2	−4.37	*a*
Cyt-c	−4.56	*a*
BQ	−4.30	*b*

[a]Estimated from E^0. [b]Calculated from gas-phase adiabatic attachment energy and solvation free energy.

Which factors control the redox energetics?[145,163−165,168] The structure of the chromophore is very important. The computational study[165] of model red, green, and blue chromophores revealed that the red chromophore is most difficult to oxidize (e.g., by ∼0.5 eV relative to the green chromophore, for the anionic form). As expected, anionic chromophores have lower ΔG_{ox} than their neutral (protonated) counterparts. All three anionic chromophores have lower ΔG_{ox} than phenolate. The extent of resonance delocalization plays an important role in determining the electron-donating ability of the chromophores.[163,165,168] The specific interactions with the protein affect the redox properties in several ways. First, the computed energetics[145,165] suggest that the protein-bound chromophores are slightly easier to oxidize (e.g., by about 0.2 eV) compared to the isolated aqueous ones, which can be rationalized by water strongly stabilizing anionic species, thus increasing ΔG_{ox}. Second, as illustrated by the data in Table 1, interactions with nearby residues can have a significant effect. For example, π-stacking interactions in eYFP increase ΔG_{ox} by 0.16 eV relative to eGFP. The chloride binding to YFP upsets π-stacking[145] and reduces ΔG_{ox}. The effect of mutations of nearby residues varies. For example, the mutation of Tyr145, a nearby residue forming a hydrogen bond with the chromophore, has no effect on ΔG_{ox} of the chromophore (but affects the overall rate of ET to outside oxidants).

4.1.1. Possible Electron Acceptors within the Protein.

In addition to solvated species, various protein residues can serve as reducing or oxidizing agents. The most likely electron acceptors are redox-active aromatic residues[162,169,170] such as tryptophan, tyrosine, phenylalanine, and histidine. The structures of these amino acids and their gas-phase electron-attachment (EA) energies are shown in Figure 14.

The trends in the relative electron-accepting ability of various amino acids can be understood on the basis of their gas-phase EAs. As one can see, the gas-phase EAs of tyrosine, tryptophan, phenylalanine, and histidine are positive, meaning that the respective anions would be unstable, in stark contrast to benzoquinone,[39] which is known to be an efficient oxidizing agent. In the protein (or solution), the anionic forms can be stabilized by electrostatic interactions. Still, relative gas-phase energetics provide a useful guideline for understanding their relative electron accepting ability, which is Trp > Tyr > Phe > His.

DOI: 10.1021/acs.chemrev.6b00238
Chem. Rev. 2017, 117, 758−795

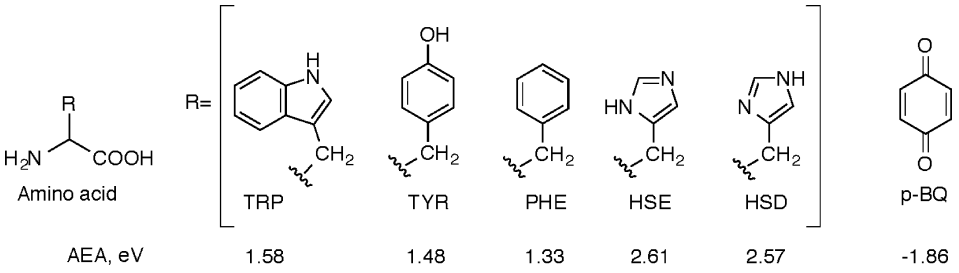

Figure 14. (Left) Structures of redox-active amino acids (tryptophan, tyrosine, phenylalanine, and histidine) and their adiabatic gas-phase electron-attachment energies (EA). (Right) Structure and adiabatic EA of benzoquinone. EA $\equiv E_{A^-} - E_A$; negative values mean that A^- is lower in energy than A. EAs are from ref 145.

4.2. Time Scales and Possible Mechanisms of ET

Whereas photoinduced chemical transformation can involve multiple steps and can be rather slow, the initial step (which occurs in the excited state) is limited by excited-state lifetime. For example, in the oxidative redding, the formation of the red form occurs on seconds to minutes time scale;[39] however, the rate of the initial step, photoinduced ET, must be very fast. Thus, redding can be described[145] as an effectively two-step process, as shown in Scheme 1, in which the rate-determining step is the second step involving slow chemical changes.

The first step is fast, but it is the gateway step, meaning that no redding can occur if there is no ET. A similar two-step framework can be applied to describe other transformations

Scheme 1. Two-Step Framework of the Oxidative Redding

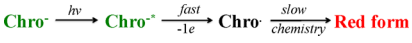

initiated by photoinduced ET, such as decarboxylation or bleaching via superoxide formation.

4.2.1. Bounds for the Excited-State ET Rates. Finite excited-state lifetimes set up a lower bound for photoinduced ET rates. The yield of bleaching, Y_{bl}, sets an upper bound for the total ET yield (assuming that all bleaching channels are initiated by ET). By considering two competing first-order processes

$$\mathrm{Chro}^{-*} \rightarrow \mathrm{Chro}^- \ (k_{fl}) \tag{4}$$

$$\mathrm{Chro}^{-*} \rightarrow \mathrm{Chro}^\bullet \ (k_{et}) \tag{5}$$

we obtain

$$Y_{bl} = \frac{k_{et}}{k_{et} + k_{fl}} \approx \frac{k_{et}}{k_{fl}} \tag{6}$$

assuming that $k_{et} \ll k_{fl}$. Thus, using Y_{bl} of 10^{-4}–10^{-5} and nanosecond lifetimes ($k_{fl} \approx 10^9\ s^{-1}$), the rates of ET should be $k_{et} = 10^4$–$10^5\ s^{-1}$. Larger Y_{bl} (as in the presence of oxidants) would increase this bound accordingly. ET from triplet states can be slower (10–100 s^{-1}). We note that in biological systems the ground-state ET rates between 10^2 and $10^8\ s^{-1}$ have been observed.[160]

4.2.2. ET from the Chromophore to an Outside Oxidant by Direct Tunneling or Hopping. Figure 15 shows two possible mechanisms[160,162] for photoinduced ET in fluorescent proteins: (i) direct ET from the chromophore to an oxidant molecule docked on the surface of the barrel and (ii) a two-step ET via an intermediate acceptor (hopping mechanism). One may also consider ET to an oxidant molecule inside

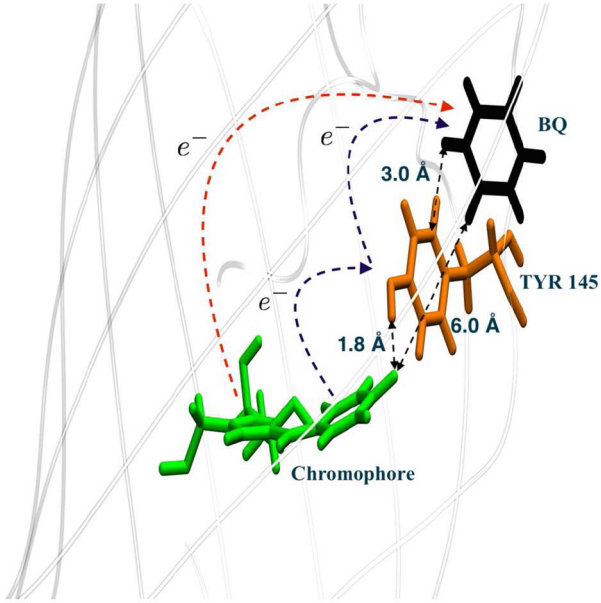

Figure 15. Possible mechanisms of photoinduced ET in fluorescent proteins. An oxidant molecule (represented by *p*-benzoquinone, BQ) docked to eGFP and the relevant distances. Direct tunneling and two-step hopping (via Tyr145) mechanisms for ET are shown by dashed arrows. Reproduced with permission from ref 145. Copyright 2016 American Chemical Society.

the barrel, since small oxidants can diffuse into the barrel. However, large oxidants such as cytochrome *c* (for which efficient redding was observed[39]) cannot penetrate the barrel. As one can see, the closest distance between docked BQ and the chromophore is about 6 Å, whereas the distance between the chromophore and Tyr145 is much shorter (~1.8 Å), suggesting that the hopping mechanism might outcompete direct tunneling. Section 9.4 discusses the feasibility of these two mechanisms in eGFP and eYFP.[145]

4.2.3. Electron Transfer via Charge-Transfer States. As summarized in Figure 13, ET can proceed by different mechanisms. In particular, CT states can be accessed by direct photoexcitation of the chromophore or by radiationless relaxation from higher excited states (this channel might be very important in multiphoton regime). The CT states of various nature have been implicated in decarboxylation[130,131,157,171] and in bleaching mechanisms.[172]

It was proposed[130] that decarboxylation, a photoconversion in which a CO_2 group is removed from a nearby glutamate residue (see Figure 2), proceeds via ET from Glu222 to the electronically excited chromophore (photoreduction) by a Kolbe-like mechanism. Subsequent electronic structure calcu-

DOI: 10.1021/acs.chemrev.6b00238
Chem. Rev. 2017, 117, 758–795

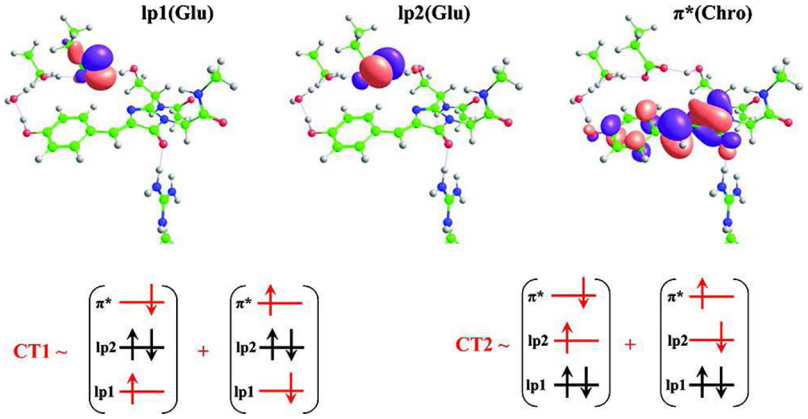

Figure 16. Relevant MOs and leading electronic configurations of the CT states in wt-GFP. Two CT states of Glu222 → Chro character are located around 4−6 eV above the ground state. Reproduced with permission from ref 157. Copyright 2012 American Chemical Society.

lations[157,171] identified such CT states for the neutral (protonated) GFP chromophore; these are located around 4−6 eV vertically (Figure 16). Grigorenko et al. proposed that these states are accessed either directly, by UV or multiphoton excitation of the chromophore, or via radiationless relaxation from a high-lying locally excited state.[157] Morokuma and co-workers put forward[171] an alternative mechanism via adiabatic evolution of the initially excited state (such as one in the top right panel of Figure 13), whereas van Thor and Sage considered[173] a Marcus-like process (in the top left panel of Figure 13).

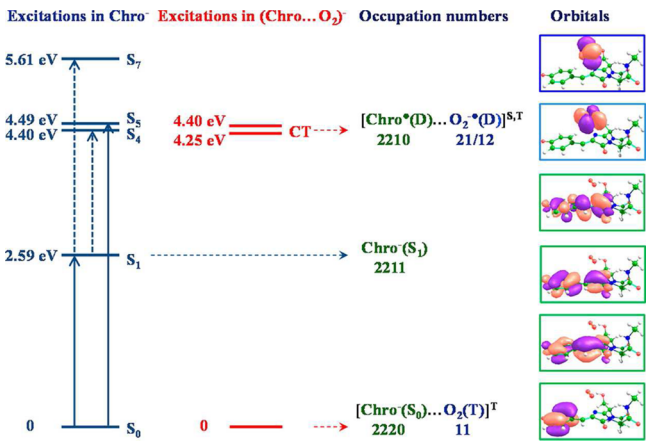

Figure 17. Relevant MOs and leading electronic configurations of the locally excited chromophore and the CT states of $Chro^- \rightarrow O_2$ character. Reproduced with permission from ref 172. Copyright 2015 American Chemical Society.

CT states of different character, $Chro^- \rightarrow O_2$, have been characterized computationally in ref 172. Figure 17 shows relevant MOs and energetics of the CT and locally excited states. A mechanism of irreversible bleaching via such states has been proposed.[172] The calculations showed[172] that (i) these CT states are accessible by photoexcitation and (ii) once reaching the CT state the system can undergo series of low-barrier transformations leading to the chromophore destruction.

5. EXCITED-STATE PROTON TRANSFER

ESPT plays an important part in the fluorescent protein photocycle;[17] its significance is on par with that of FRET and light-induced ET. The spectral properties of many fluorescent proteins are controlled by ESPT. The major fluorescence peak in fluorescent proteins with tyrosine-based chromophores is due to the emission of the anionic (i.e., deprotonated) chromophore; it more often results from the excitation of the neutral chromophore followed by ESPT than from the excitation of the anionic chromophore.

Mutations can affect the relative energetics of various protonation states and disrupt the PT route, a fact that has been exploited in fluorescent protein engineering and in mechanistic studies.[17,174,175]

Wt-GFP from *Aequorea victoria* jellyfish has become a classical model for ESPT not only within the GFP family but also in photobiology at large. The key residues involved in

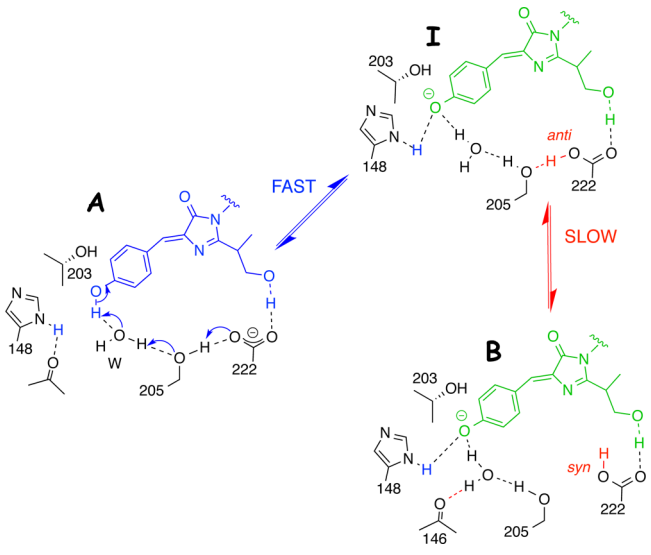

Figure 18. ESPT in wt-GFP. A 3.18 eV (390 nm) photon excites the neutral (protonated) chromophore (left center) and initiates proton transfer forming the electronically excited anion (I*), upper right, which subsequently emits a green photon (510 nm or 2.43 eV) and undergoes back PT restoring the neutral chromophore. A low-frequency event is transformation of the ground state (I) to a metastable ground state anion, B (lower right).

DOI: 10.1021/acs.chemrev.6b00238
Chem. Rev. 2017, 117, 758−795

ESPT in wt-GFP are shown in Figure 18. ESPT in wt-GFP proceeds as a sequential proton transfer from the excited neutral chromophore to the Glu222 carboxylate through a water molecule and the hydroxyl group of Ser205.[174,176−179] An attempt to block ESPT by a S205V substitution was foiled by opening an alternative proton-transfer pathway involving Thr203.[174] Only upon blocking this second route by the double T203V/S205V mutation was ESPT completely switched off.[175]

ESPT is driven by photoacidity,[180] a drop in pK_a of the chromophore upon electronic excitation. Photoacidity of the native fluorescent protein chromophores (which are similar to phenols) has been confirmed by calculations: QM/MM calculations[181] of the pK_a values of the GFP chromophore in solution have estimated the change in pK_a, $\Delta pK_a = pK_a^* - pK_a$, upon excitation to be ∼8 units. A recent study using more advanced calculations has reported $\Delta pK_a \approx 6$ (ref 182).

In wt-GFP, ESPT occurs on the picosecond time scale and leads to a substantial Stokes shift of 0.75 eV. A femtosecond stimulated Raman spectroscopy study[183] of wt-GFP provided detailed time-resolved vibrational spectra of the excited chromophore, revealing several skeletal motions defining multidimensional ESPT reaction coordinate and identifying early time ring-wagging motion of the chromophore as a principal component of the ESPT pathway.

Energy profiles along the PT route have been computed, aiming to validate the mechanism and to identify the underlying changes in electronic structure of the chromophore.[182,184−186] Recent calculations have accurately reproduced experimental absorption and emission maxima as well as ground-state protonation equilibria in wt-GFP and eGFP, providing further justification and refinement of the proposed structures along the PT chain.[179] This study has shown that the structural differences between the I and B forms are based not on the Thr203 orientation, but on the Glu222 position. In the I structures, the Glu222 side chain is in the anti conformation, and the proton wire Chr-Wat-Ser205-Glu222 facilitates efficient proton shuttling. In the B structures, the syn conformation of Glu222 disrupts the proton wire.

ESPT in the GFP family occurs in an extremely broad range of time scales (from ca. 100 fs to nanoseconds). For example, recently described cyan fluorescent protein, psamFP488, from reef building coral (genus Psammocora) demonstrated 170 fs proton shuttling from chromophore to Glu167,[187] whereas canonical biphasic av-GFP ESPT time constants are 3 and 15 ps. Compared to av-GFP, ESPT in the S205V and T203V/S205A mutants is 30 and 350 times slower.[174,175] On the basis of time-resolved infrared and visible pump−dump−probe spectroscopic measurements[188] in wt-GFP, the short time constant has been assigned to the partial shift of protons in the proton wire leading to partially protonated Glu222 and the long time constant has been assigned to complete deprotonation of the chromophore. In the calculations of potential energy profiles along the proton-transfer route, multiple I-like structures have been identified.[179]

ESPT has been utilized in developing RFPs with large Stokes shifts (ΔE), such as LSS-mKates (ΔE = 0.69 and 0.65 eV for LSS-mKate1 and LSS-mKate2 respectively),[57,112] its photoactivatable variant,[189] and bright cyan-excitable orange fluorescent protein, CyOFP1 (ΔE = 0.39 or 0.27 eV).[60]

The computational investigation of potential energy profiles in LSS-mKate revealed strongly exoergic ESPT, thus providing support to the proposed mechanism of its large Stokes shift.[190] A time-resolved spectroscopy study of the excited-state dynamics in LSS-mOrange reported that ESPT in this protein occurs on a subpicosecond time scale (0.8 ps).[191]

We note that ESPT in biologically relevant systems can be accompanied by photoinduced ET. For instance, fast subpicosecond ESPT in BLUF photoreceptor domains was shown to be coupled with electron transfer.[192] Likewise, photoinduced proton-coupled electron transfer is operational in phenols.[193] Thus, it is possible that similar processes occur in some fluorescent proteins.

6. CIS−TRANS PHOTOISOMERIZATION, CHANGES IN PROTONATION STATES, AND PHOTOSWITCHING

Since electronic excitation alters the bond-order pattern in conjugated systems, it often leads to cis−trans isomerization, one of the most common photoinduced transformations.[194] This reaction can also be coupled with other processes, such as changes in protonation state. Photoinduced cis−trans isomerization is the gateway step initiating photoresponse in biological systems (e.g., rhodopsin[195]); it is also exploited in molecular electronics and optogenetics.[196,197] In fluorescent proteins, cis−trans isomerization may lead to RS-FPs (reversibly switchable FPs).

The first efficient RS-FP discovered by Ando et al. is called Dronpa.[73] In this system, photoswitching can be achieved more than 100 times at a single-molecule level. Dronpa absorbs at 503 nm (2.46 eV) and emits at 518 nm (2.39 eV). It can be converted to the nonfluorescent form (which absorbs at 390 nm or 3.18 eV) by irradiating with an intense light of 488 nm (2.54 eV) wavelength, with a quantum yield of 3.2×10^{-4}. The reverse process, which is induced by weak illumination with a light of 405 nm (3.06 eV) wavelength,[198] is more efficient (quantum yield of 0.37).

The mechanism of photoswitching in Dronpa has been extensively debated. Habuchi et al. invoked ESPT to explain photoswitching; their proposed mechanism in which the on state (fluorescent) is deprotonated and the off state (dark) is protonated.[198,199] Andersen et al. solved the crystal structure of Dronpa in the off state (PDB id 2POX), showing that the off-state chromophore is a trans isomer of the on-state chromophore.[123] Their analysis proved that photoswitching in Dronpa results from cis−trans isomerization accompanied by proton transfer and structural changes around the chromophore, since the chromophore in the off state was shown to be protonated. This scheme is shown in Figure 19. This study also suggested that the local environment around the cis and trans chromophore is different, leading to different protonation states in the two conformations.

NMR studies of Dronpa in solution have shown that β-strands near the chromophore's phenolic ring become flexible in the dark state; this can contribute to the nonradiative relaxation.[200,201] Moreover, dark-state-specific conformational changes are sufficient to change the oligomeric state of Dronpa, which can be exploited for optogenetic control of target protein activities.[202]

In a more recent study, Warren et al. explained the photoswitching in Dronpa in terms of photoinduced cis−trans isomerization followed by ground-state proton transfer.[203] They showed that deprotonation of the chromophore's phenolic oxygen in the off state is a thermal ground-state process, which happens after an ultrafast (9 ps, quantum yield of ∼0.3) trans−cis photoisomerization, and that it does not involve ESPT. This study also considered possible involvement

DOI: 10.1021/acs.chemrev.6b00238
Chem. Rev. 2017, 117, 758−795

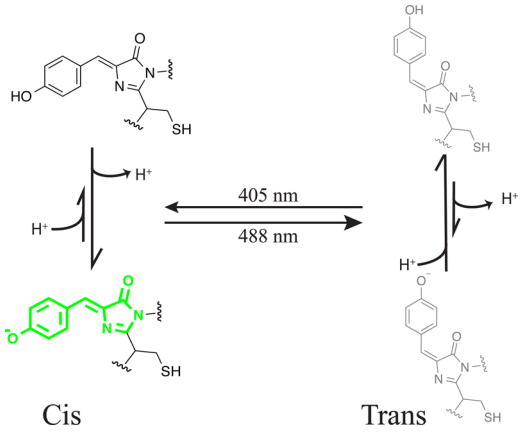

Figure 19. Proposed mechanism of reversible photoswitching in Dronpa and Padron via cis−trans isomerization of the chromophore. Bright and dark states correspond to the cis and trans forms of the chromophore, respectively. In both states, there is acid−base equilibrium between the two protonation forms. In Dronpa, the cis form is anionic and the trans form is neutral.

of other protonation states of the chromophore. On the basis of steady-state infrared difference measurements, the authors were able to rule out protonation of the imidazolinone nitrogen (structures C and Z in Figure 12) in both on and off states. A very recent Raman study[204] has provided additional details of the acid−base equilibria in the on and off states and has confirmed that the switching in Dronpa involves cis−trans isomerization and a protonation/deprotonation transition.

Another example of RS-FP is Padron, which was derived from and shares the same chromophore with Dronpa. It differs from Dronpa by several mutations: T59M, V60A, N94I, P141L, G155S, V157G, M159Y, F190S. The photoswitching of Padron is exactly opposite of Dronpa (hence, Pa···dron). Illumination with a blue light (503 nm or 2.46 eV) leads to off to on transition (503 nm light also induces fluorescence), and the on-state reverts back to the off-state when irradiated with UV light.[67]

On the basis of the capacity of its fluorescence to vanish and reappear, the protein developed by Ando et al. was named "Dronpa", after "dron", a ninja term for vanishing, and "pa", which stands for photoactivation.[73] The names of Dronpa and Padron thus reflect their different photoswitching behavior: Dronpa is a negative photoswitcher—it is fluorescent in its native, most stable form and can be turned off by light, whereas Padron is an example of a positive photoswitcher, i.e., it is dark in its most stable state and turned on by light (see Figure 2).

The photoswitching mechanism was investigated by Brakemann et al. using a related mutant, called Padron0.9 (it differs from Padron by the Y116C and K198I mutations).[143] They concluded that photoinduced cis−trans isomerization is the primary mechanism of photoswitching and that changes in protonation states of the on and off states are not mandatory for photoswitching, since Padron0.9 chromophore is deprotonated in both fluorescent and nonfluorescent states. Rather, the authors suggested the ability to fluoresce in a particular conformation depends on the flexibility of the chromophore. We discuss this point in detail below, in section 6.1.

In their study[205] of excited-state dynamics of Padron, Fron et al. determined that the cis (protonated) form of Padron decays in 1 ps to the excited cis (deprotonated) form, which then decays to the ground state of the trans (deprotonated) chromophore with a time constant of 14.5 ps. They also proposed that the trans-deprotonated chromophore then equilibrates with trans-protonated form, and when the trans-deprotonated form is excited with a 495 nm (2.50 eV) light cis−trans isomerization is followed by internal conversion, leading to the ground state of the cis chromophore (on).[205] The coupling of the isomerization with changes in protonation state was supported by free energy calculations,[143] which yielded free energy difference of 11.4 ± 3 kJ/mol between the trans and the cis chromophore in Padron. Thus, the free energy calculations predict that isomerization from cis to trans lowers the pK_a of the chromophore by 2.0 ± 0.5 pK_a. This trend is in good agreement with the experimentally determined pK_a shift of ∼1.5. A low-temperature study[206] of photoswitching in Padron has provided additional support for the above mechanism: the authors were able to isolate the intermediate anionic cis form of the chromophore, which can be reached at cryogenic temperatures, and showed that the final fluorescent state, a mixture of anionic and neutral chromophores in the cis configuration, can only be reached above the glass-transition temperature. These results suggest[206] that the chromophore's isomerization in Padron is nearly volume conserving, whereas the protonation step involves large structural reorganization of the solvent and the protein's scaffold.

A transient absorption spectroscopy study of the on to off transition in Dronpa has provided strong support for a fast (ps) trans to cis isomerization reaction, which occurs concomitantly with the excited-state decay and precedes the deprotonation of the chromophore, which occurs on the microsecond time scale.[207]

A recent femtosecond spectroscopy study of Padron by Walter et al. revealed additional complexity: it showed that the formation of cis chromophore (deprotonated) does not happen directly; rather, it proceeds through a hot ground state.[208] They also showed that the excitation of the protonated cis chromophore initiates ESPT, which is followed by relaxation to the deprotonated cis chromophore (on).

In summary, although the current understanding of the molecular-level basis of photoswitching in the GFP family is still incomplete in terms of the exact sequence and time scales of individual steps, it is evident that photoinduced cis−trans isomerization coupled to changes in protonation states play the central role in these processes.

6.1. Role of the Chromophore's Flexibility in Photoswitching

The chromophore's torsional degrees of freedom are directly related to its propensity to undergo cis−trans isomerization and radiationless relaxation to the ground state. This twisting motion is traditionally described in terms of the "tilt" (τ) and "twist" (ϕ) angles shown in Figure 20; in planar cis structures the values of τ and ϕ are zero. The cis−trans isomerization can be accomplished by rotation around one of the bridge bonds, via so-called one-bond flips, or via a concerted motion involving both angles. The analysis of different motions in terms of the displaced volume suggested that a hula-twist concerted motion provides the most efficient pathway for isomerization in a tight protein barrel.[209] This prediction, based on structural analysis, has been later confirmed by more sophisticated excited-state calculations.[210]

From the very outset of GFP studies, the fluorescent ability of the chromophore was linked to its flexibility. For example, the 3 orders of magnitude drop of fluorescence quantum yield

DOI: 10.1021/acs.chemrev.6b00238
Chem. Rev. 2017, 117, 758−795

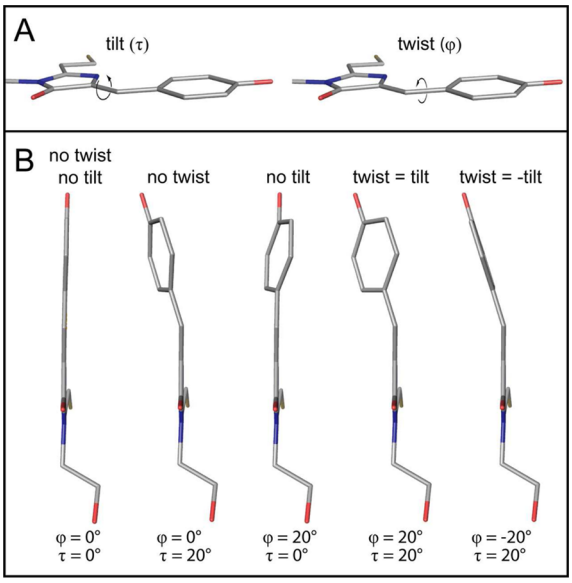

Figure 20. Two dihedral angles τ and ϕ quantifying the torsion between the two aromatic rings of the chromophore. (Top) Definition of the tilt (τ) and twist (ϕ) angle in the Padron0.9 chromophore. (Bottom) Structures of the Padron0.9 chromophore illustrating different values of τ and ϕ. In the planar cis chromophore (far left), $\tau = \phi = 0°$. Reproduced with permission from ref 143. Copyright 2010 The American Society for Biochemistry and Molecular Biology, Inc.

in solutions was attributed to the chromophore's increased range of motion, relative to the rigid protein matrix.[15,87,88] In analogy with other conjugated systems,[211] the twisting around the methyne bridge is expected to play a key role in facilitating radiationless relaxation. Several studies have illustrated that confinement of the fluorescent protein chromophores within rigid hosts results in an increase in fluorescence of several orders of magnitude.[90−92,107]

The electronic structure calculations[89,212−215] of isolated model GFP chromophores have located conical intersections between S_1 and S_0. These intersections occur at strongly twisted geometries; thus, the ability of the chromophore to twist in a flexible environment facilitates radiationless relaxation and reduces the quantum yield of fluorescence. Conversely, restricting the chromophore's range of motion by, for example, sandwiching it between two bulky tyrosine groups[106] in the triple-decker motif[216] leads to increased brightness. A similar design idea has led to brighter BFPs, Azurite and A5,[105] and to an RNA mimic of GFP, Spinach.[107]

Molecular dynamics simulations of selected proteins with hypothetic freely rotating chromophores have shown[217] that the dihedral freedom is inversely proportional to the fluorescence, e.g., the range of torsional motions decreases in the following series: BFP (Y_f = 0.2) > A5 (Y_f = 0.48) > YFP (Y_f = 0.59) > wt-GFP (Y_f = 0.8).

Several researchers have noticed the correlation between the apparent deviation from the planarity and the reduced quantum yield of fluorescence. For example, Remington and co-workers pointed out[85] that in highly fluorescent wt-GFP and DsRed the values of τ and ϕ do not exceed 4°, whereas in mCherry (Y_f = 0.22) ϕ = 11.3 and τ = 13.7. The effect is likely to be dynamic in nature, that is, the average structures with nonzero values of these angles indicate a large range of motions along these coordinates rather than increased rate of radiationless relaxation at a static Franck−Condon geometry. The simulations of mStrawberry and mCherry fluorescent proteins aiming to explain the increased yield of fluorescence under high pressure support this point: hydrostatic pressure has almost no effect on the chromophore's planarity, whereas the hydrogen-bond network around the chromophore and backbone fluctuations are strongly affected.

Brakemann et al. proposed that the primary factor determining the fluorescent ability of the chromophore in different conformations (i.e., in bright and dark forms of photoswitchable fluorescent proteins) is the chromophore's flexibility, which they quantified[143] in terms of the modulus of the sum of "tilt" and "twist" angles shown in Figure 20. By analyzing the structures of several fluorescent proteins (Padron, Dronpa, rsFastLime, asFP-A143S, mTFP0.7, and IrisFP), Brakemann et al. observed that for a particular chromophore $|\tau + \phi|$ is always lower in the fluorescent form than in the nonfluorescent form (see Table S5 in ref 143). For example, in the trans forms of Padron and Dronpa, $\|\tau + \phi\| \approx 21−22°$, whereas cis forms are more planar ($\|\tau + \phi\|$ is 11° and 4°, respectively). In the green state of IrisFP, $\|\tau + \phi\|$ in the trans and cis forms is 40° and 12°, respectively.

A recent theoretical study[210] of Dronpa has revealed the coexistence of several hydrogen-bonding networks in the on state of Dronpa and suggested that only one subpopulation, which is characterized by the fewest number of hydrogen bonds and, therefore, the most flexible chromophore, is responsible for off switching through photoisomerization, whereas other conformations (in which the chromophore is more rigid) inhibit the isomerization and promote the fluorescence instead. For example, the trajectories initiated from conformations with a single hydrogen bond undergo fast (subpicosecond) relaxation to S_0 via hula-twist motion (shown in Figure 21),

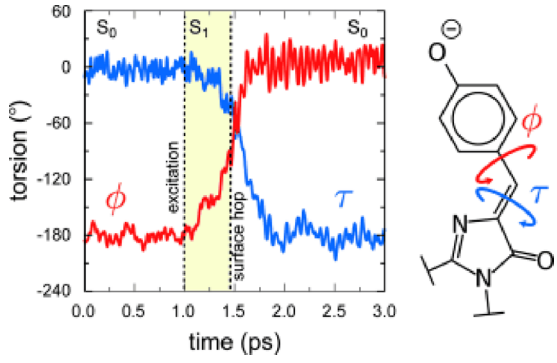

Figure 21. Time evolution of the τ and ϕ angles along a QM/MM surface-hopping trajectory for Dronpa. For this trajectory, which initiated from a configuration with a single hydrogen bond to the phenolate moiety, the radiationless transition to the ground state occurs in less than 0.5 ps after photoexcitation. Reproduced with permission from ref 210. Copyright 1999−2016 John Wiley & Sons, Inc.

whereas the trajectories initiated from the configurations with more hydrogen bonds feature a planar chromophore and remain on S_1 for about 50 ps.

A study[218] of photoswitching kinetics at cryo temperatures in Dronpa (moderately efficient photoswitcher), eYFP (low-efficiency photoswitcher), and IrisFP (high-efficiency photoswitcher) has shown that although all three proteins undergo photoswitching at 100 K, the quantum yield is reduced by several orders of magnitude. Interestingly, the efficiency of

DOI: 10.1021/acs.chemrev.6b00238
Chem. Rev. 2017, 117, 758−795

photoswitching at cryo temperature was anticorrelated with the efficiency of photoswitching at room temperature (i.e., IrisFP has shown the largest decrease in quantum yield at low temperature), which provides indirect support for the importance of structural heterogeneity due to thermal motions for photoswitching.

Molecular dynamics simulations of several fluorescent proteins (Dronpa, IrisFP, mEosFP, rsFastLime, rsKate) have shown that photoswitching behavior correlates with changes in structural flexibility of their on and off states,[219] that is, the dark forms of all fluorescent proteins were found to have more flexible protein barrels, as quantified by dynamical deviations from the X-ray structures.[219] In the photoswitchable proteins, the dark forms were found to be less flexible than in nonphotoswitchable ones. Thus, it was proposed that in nonphotoswitchable fluorescent proteins the dark states are short lived because they are too high in energy (relative to the bright states) and because their more flexible hydrogen-bond network results in faster relaxation of transient dark forms, thus precluding the photoswitching behavior.[219] The connection between the barrel's flexibility and photoswitching is supported by the dependence of the photoswitching kinetics in Dronpa on the viscosity of the surrounding medium,[220] e.g., the fluorescence trajectories of Dronpa in solution with 0 and 90% glycerol exhibit a single-exponential decay rate of 198 and 103 s^{-1}, respectively. This dependence was exploited to develop a genetically encoded fluorescent reporter of the viscosity in intracellular environments.[220]

To summarize, several diverse studies[104,210,219] highlight the importance of structural fluctuations on the photochemical properties of fluorescent proteins. In particular, the chromophore's flexibility along the twisting degrees of freedom is an important factor affecting brightness and blinking behavior. Structural heterogeneity and the coexistence of several hydrogen-bond networks, which play a role in determining the magnitude of Stokes shifts (section 3.2), are important factors in determining the yield of radiationless relaxation and photoswitching.

6.2. Kindling Phenomena

Kindling, the light-induced increase of fluorescence quantum yield of the initially nonfluorescent (dark) chromoproteins, is similar to positive photoswitching. It was observed in the asFP595 chromoprotein and its Ala143Gly mutated variant, called the kindling fluorescent protein (KFP).[74,221] Compared to GFP, the chromophore of asFP595 has an extended π-conjugated system,[138,222,223] as shown in Figure 22.

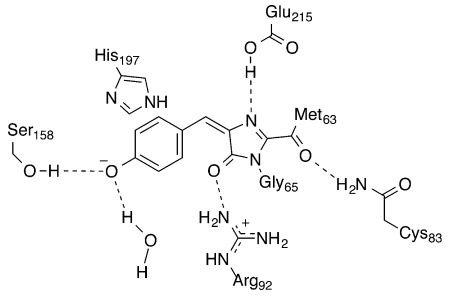

Figure 22. Chromophore of asFP595 and its environment. Reproduced with permission from ref 224. Copyright 2014 American Chemical Society.

As a mechanistic hypothesis behind kindling, photoinduced conformational cycling coupled with changes in protonation states has been proposed.[74,138,221−223] Schüttrigkeit et al. used femtosecond time-resolved spectroscopy to study the structural basis of kindling in asFP595;[150] this study proposed[150] that the kindling results from either chromophore trans−cis isomerization or proton transfer between an excited zwitterion and the protein cleft. Several computational studies[146,224−232] of asFP595 attempted to clarify the details of the photoswitching mechanism, in particular, a possible involvement of zwitterionic states (Figure 12). Such protonation states in Dronpa have been recently ruled out on the basis of vibrational spectroscopy of the on and off forms.[203] We note that formation of the zwitterionic chromophores (protonated at the imidazolinone ring) has also been hypothesized by Duan et al.[233] when considering the photobleaching mechanism in the reversibly switchable fluorescent protein, IrisFP.

Earlier QM/MM studies[225,226] suggested that the chromophore exists in the *Z* form (see Figure 12) both in the ground and in the excited states and that the source of the proton is the adjacent side chain of Glu215 (Figure 22). These studies suggested that photoswitching corresponds to the isomerization coupled with the proton transfer from the imidazolinone ring of the zwitterion to Glu215 leading to the anionic chromophore. However, other calculations[146,224,227−232] did not support the formation of zwitterions in the ground electronic state of asFP595; they showed that the *Z* forms correspond to shallow local minima on the ground-state potential surface lying higher in energy than the anionic states. Moreover, it was shown[146] that the chromophore's trans to cis isomerization in the ground state could be explained by considering the anionic forms alone; the corresponding free energy profiles computed using QM/MM were consistent with the experimental kinetics data. The computed energy barrier for thermal deactivation of the on-state (corresponding to the system with the cis chromophore) for KFP, 20.7 kcal/mol, is in fair agreement of and the experimentally determined[221] activation barrier of 17.0 kcal/mol derived from the Arrhenius plot of the fluorescence decay. In contrast to the ground-state case, the formation of zwitterions in the excited electronic state of asFP595 can be facilitated by a noticeable increase of basicity of the imidazolinone nitrogen upon excitation.[224] High-level quantum-chemistry calculations of the model asFP595 chromophore in the ground and excited states predicted that pK_a of the nitrogen changes upon electronic excitation by 3.5 ($\Delta pK_a = pK_a^* - pK_a = 3.5$), giving rise to $pK_a^* = 8.1$. This magnitude of change is consistent with a possible formation of the zwitterion in the excited state.

An increased basicity of the imidazolinone nitrogen in asFP595 upon excitation may also lead to the formation of the cation C form of the chromophore if the phenolic oxygen is protonated (see Figure 12). This possibility was explored in ref 234 by means of QM/MM calculations. As illustrated in Figure 23, upon excitation of the system with the neutral chromophore proton transfer between Glu215 and Chro may take place, leading to the C form.

To conclude, the calculations suggest that the C and Z forms of the GFP-like chromophore might be involved in photoswitching and kindling phenomena; however, more experimental studies are needed to fully elucidate their role in specific systems.

DOI: 10.1021/acs.chemrev.6b00238
Chem. Rev. 2017, 117, 758−795

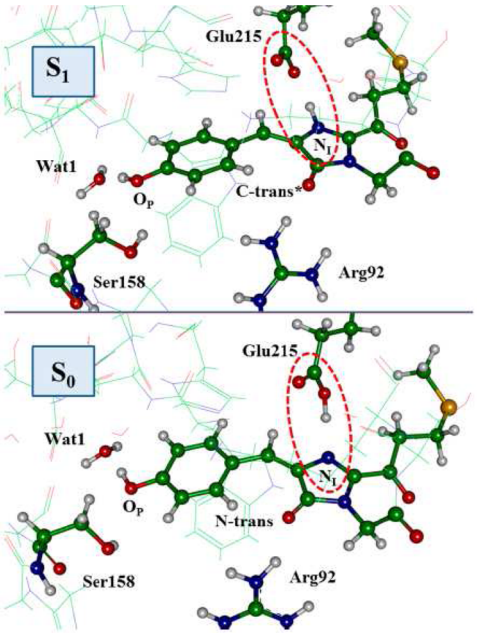

Figure 23. Minimum-energy structures of asFP595 with the neutral chromophore in the ground state (bottom) and with the cationic chromophore in the excited state (top). Reproduced with permission from ref 234. Copyright 2013 American Chemical Society.

6.3. Utilization of Photoswitchable and Photoactivatable Fluorescent Proteins in Super-Resolution Microscopy

The ability to switch the individual fluorophores between two spectroscopically distinct states (e.g., bright and dark or of two different colors) provides a basis for several super-resolution techniques affording spatial resolution of ~10 nm, about 20 times smaller than the diffraction limit.[36,44]

One class of approaches is based on patterned illumination in which one light source is used to excite the chromophores within a tightly focused spot (called the Airy disk), while a second (photoswitching) laser is used to create a toroidal (doughnut-shaped) intensity profile with zero intensity in its center superimposed with the Airy spot. If the second laser turns off all chromophores then only the fluorescence from the molecules in the center of the Airy disk (which is of a subwavelength size) is detected. This illumination pattern is used in STED (stimulated emission depletion) in which the second (depletion) laser de-excites the chromophores via stimulated emission. Thus, the depletion beam has to use high laser powers, which limits STED to highly photostable molecules. The RESOLFT (reversible saturable optical fluorescence transitions) technique[33] uses the same illumination pattern but instead of de-exciting the chromophores the second laser switches them off by converting them into the dark form. Thus, one can use orders of magnitude lower depletion laser intensities than when using STED.

Another class of techniques achieves super-resolution by repeatedly photoactivating individual molecules, while other surrounding molecules remain dark, such that the positions of the few activated molecules can be determined with high precision. The activated molecules are photobleached, and new emitters are activated. This cycle is repeated many times (1000−100 000) until all chromophores are bleached, producing a density map of all fluorophores that were detected. These techniques, developed independently by three groups, are called PALM[235] (photoactivated localization microscopy), FPALM[236] (fluorescence photoactivation localization microscopy), and STORM[237] (stochastic optical reconstruction microscopy).

Which properties of photoactivatable/photoswitchable fluorescent proteins are important for these techniques? RESOLFT relies on reversibly photoswitchable fluorophores. Although both negative and positive photoswitchers can be used, the former lead to a simpler experimental setup (only two beams are needed). Importantly, the resolution increases with the number of excitation-deexcitation cycles of individual molecules. Thus, RESOLFT calls for photoswitchers that can undergo many excitation-deexcitation cycles before permanently bleached, i.e., chromophores with a low switching fatigue. This property depends on the quantum yields of bleaching and photoswitching: for example, if the latter is high, the molecules, on average, spend a shorter time in the excited state, and therefore, they can survive many excitation cycles before becoming permanently bleached. Examples of fluorescent proteins with low switching fatigue are rsEGFP[50] and rsEGFP2[238]—they can be switched on and off more than 1000 times (compared, for example, with 10−100 cycles in Dronpa). Both are negative photoswitchers derived from eGFP with Thr-Tyr-Gly and Ala-Tyr-Gly chromophores, respectively (eGFP has Thr-Tyr-Gly). rsEGFP can endure ~2100 switching cycles and has faster switching kinetics than rsEGFP (about 6.5 times at light intensity of 5.5 kW/cm^2), which enables much faster image acquisition.[238]

PALM, FPALM, and STORM require fluorophores than can emit at least 100 photons from an individual molecule before becoming permanently bleached. In addition, brightness is very important, because these methods are single-molecule methods. Transient dark states can create problems, so chromophores with low blinking rates are desirable. Because these techniques require a high density of chromophores (about 1000 molecules per a spot with 200 nm diameter), high contrast between the fluorescence emission of the photoactivated and deactivated forms is critically important. This can be achieved with photoactivatable fluorescent proteins that have negligible fluorescence yield in their nonactivated state, or in photoconvertible fluorescent proteins that emit at different wavelengths in the initial and the converted state. In both cases, it is important that the quantum yield of activation or photoconversion with fluorescence excitation light is very small, which can be achieved if the absorption bands of the two forms are well separated. Thermally activated transitions between the two forms and the formation of short-lived dark states are undesirable. Depending on the exact flavor of the technique, additional considerations for the properties of fluorophores, such as quantum yields of photoconversions, time of photoactivation, etc., exist.[36] Better understanding of the mechanism of the complex photocycle will aid the development of fluorescent proteins that provide optimal fit for each technique.

7. BLINKING AND TRANSIENT DARK STATES

7.1. Kinetics and Structural Studies

Blinking (see Figure 7) is well known in dyes; it is an important factor in single-molecule experiments.[54] Various aspects of blinking in fluorescent proteins have been investigated, including kinetics, time scales, and pH dependence. Blinking spans a wide range of time scales, ranging from fast (10^3−10^5 times per seconds)[55,239−241] to slow (0.1−10 times per second).[242−244] Quantitatively, the kinetics of reversible

DOI: 10.1021/acs.chemrev.6b00238
Chem. Rev. 2017, 117, 758−795

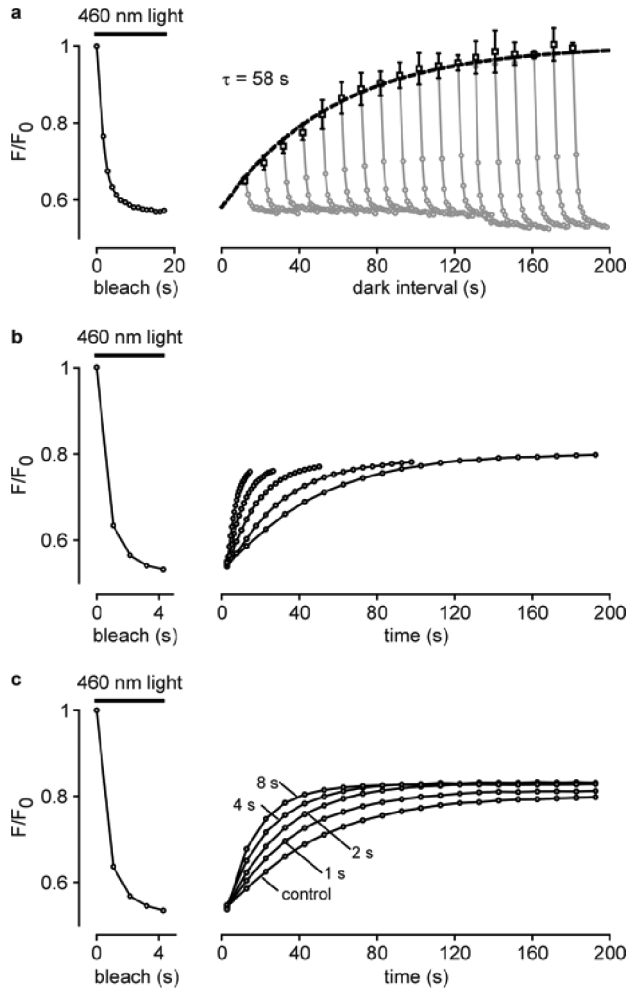

Figure 24. Spontaneous and light-induced recovery of reversibly bleached eCFP. Bleaching and fluorescence recovery are quantified by the ratio of fluorescence to the unbleached sample, F/F_0. Cells expressing eCFP were photobleached by 460 nm light. (a) After photobleaching, samples were kept in the dark for 10−180 s and then subjected to a second cycle of reversible photobleaching (gray symbols and lines). Extent of spontaneous recovery was plotted as a function of the dark interval duration and fitted to a monoexponential rise to maximum function (dashed line). (b) After reversible photobleaching, the recovery process was monitored by collecting fluorescence images at various acquisition frequencies (0.1−1.6 s^{-1}). (c) Images were acquired as in b at 10 s intervals. During each interval no illumination (control) or 500 nm light (1, 2, 4, or 8 s per cycle) was applied. Reproduced with permission from ref 124. Copyright 2005 American Chemical Society.

bleaching under low-intensity illumination in several variants of eGFP (i.e., eYFP, Citrine, eCFP) has been investigated.[124] Figure 24 shows an example of spontaneous and light-induced fluorescence recovery in a reversibly bleached eCFP.[124] It was found that these fluorescent proteins undergo reversible bleaching; the fluorescence recovers spontaneously with time constants of 25−58 s. The fit of the measurements to a simple 3-state kinetic model allowed the authors to estimate the ratio of the respective quantum yields of reversible and irreversible bleaching. They reported that, under their conditions, the reversible bleaching is about an order of magnitude more efficient than the irreversible process (the ratio of quantum yields were ∼67−168).[124] For eYFP, the quantum yield of reversible bleaching was reported to be 3×10^{-4}. Reversible

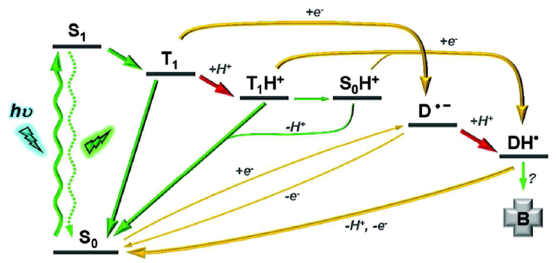

Figure 25. Proposed mechanisms for transient dark-state formation in IrisFP via photoreduction of the chromophore.[156] Thick orange and red arrows denote light-induced electron- and proton-transfer steps, respectively; green arrows mark other processes. Protonated species are denoted as T_1H^+, S_0H^+, and $DH^\bullet$. B marks the bleached state. Thinner orange arrows show processes that are induced by X-rays or, possibly, by strong reducing agents. Arrow with a question mark refers to a possible decarboxylation route. Reproduced with permission from ref 156. Copyright 2011 American Chemical Society.

bleaching was enhanced at low pH; thus, it was suggested that the dark species might be different protonation forms of the chromophore or the nearby residues, Tyr145 or His148.

Blinking kinetics in a YFP mutant has been also investigated by Boxer and co-workers.[245] They assigned the reversible bleached form to a protonated chromophore. Much slower rates (hours) of the spontaneous recovery have been observed.[245] Interestingly, in both studies,[124,245] it was found that the recovery can be accelerated by UV light.

The nature of transient dark states has been extensively investigated in IrisFP.[156,246] The crystallographic data suggested that the dark species feature a distorted chromophore with a bent methyne bridge.[246] The QM/MM calculations proposed two candidates for the dark species, both protonated at the C_α, which disrupts the conjugation of the π-system.[156] Figure 25 illustrates the suggested pathways leading to such distorted protonated structures (Figure 3 from ref 32 shows a more detailed picture of the transient dark and permanently bleached forms). It was proposed that the protonation may occur either in the radical anion (doublet) state or the T_1 state of the chromophore; thus, two intermediates may be involved in the process. Figure 26 shows the proposed mechanism of blinking in IrisFP, which involves photoinduced PT from Arg66 to the methyne bridge of the chromophore.

Roy et al. also posited that such transient species might be involved in green to red photoconvertible fluorescent proteins (EosFP, Dendra, and Kaede) in which the proposed proton donor, Arg66 (see Figure 26), is preserved.[156] A recent study[120] provided additional evidence supporting the role of Arg66 in the blinking behavior. The authors hypothesized that different orientations of Arg66 in mEos2 and Dendra2 are responsible for their different blinking behavior (mEos2 is highly blinking, whereas Dendra2 is low blinking). By designing the single-residue mutants (mEos2-A69T and Dendra2-T69A), in which the conformation of Arg66 was swapped, the blinking behaviors of mEos2 and Dendra2 were reversed,[120] as illustrated in Figure 7.

7.2. Utilization of the Long-Lived Dark States in Fluorescent Proteins

Can one utilize blinking phenomena in applications? In this section, we discuss three such examples. The first technique is based on the observation that blinking-associated submillisecond relaxation time in GFPs is highly temperature dependent. Thus, the members GFP family can potentially be

DOI: 10.1021/acs.chemrev.6b00238
Chem. Rev. 2017, 117, 758−795

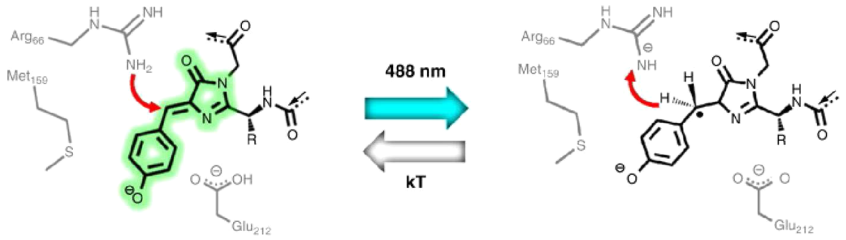

Figure 26. Proposed blinking mechanism in IrisFP involves a thermally reversible photoinduced proton exchange between Arg66 and the methyne bridge of the chromophore. Reproduced with permission from ref 32. Copyright 2014 Elsevier Ltd.

used as molecular thermometers, with signal being detected using fluorescence correlation spectroscopy (FCS).[247] The second example is super-resolution optical fluctuation imaging (SOFI), and the third example is given by modulatable fluorescent proteins.

In SOFI, subdiffraction optical resolution in three dimensions is attained from the statistical analysis of spatiotemporal fluctuations, i.e., the blinking, of fluorophores.[248,249] The key part of SOFI is a postprocessing algorithm based on the detailed analysis of the correlation between the blinking emitters.[250] Hence, SOFI allows multiple emitters to be present close to each other.

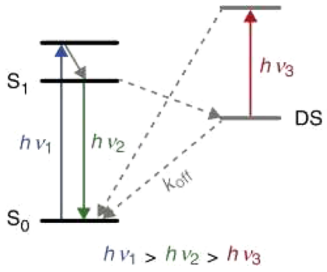

Figure 27. Jablonski diagram illustrating interconversion between bright and long-lived dark states (DS) of a fluorophore. $h\nu_3$ depopulates the dark state and repopulates S_0. Direct repopulation of S_1 may also be possible for some systems. Reproduced with permission from ref 5. Copyright 2015 Elsevier Ltd.

Modulated spectroscopy,[5] which was proposed by Dickson et al.,[251] is based on radiationless transitions between bright and dark states. A simplified Jablonski diagram of this technique is shown in Figure 27. The essence of this approach is that depopulation of a transient dark state leading to repopulation of the chromophore's emitting excited state (and, consequently, increased fluorescence output) may be induced by coillumination of the sample with a secondary laser.[251] The key requirement for such optically enhanced fluorescence is to have a relatively long-lived and red-shifted optically reversible dark state. One of the advantages of this method is that the photon energy of the secondary light source ($h\nu_3$) is less than that of the primarily $S_0 \rightarrow S_1$ excitation ($h\nu_1$) and the fluorescence ($h\nu_2$). Turning the coillumination on and off at a specific frequency dynamically modulates the collected fluorescence without generating additional background. This method, initially developed and utilized for metal nanodots and organic dyes, has recently been applied to fluorescent proteins. Some blue (modBFP, the variants of mKalama1), green (AcGFP), red, and other fluorescent proteins are susceptible to secondary pulsed excitation.[252,253]

Such photoinduction of dark states by a secondary laser can strongly enhance signal to background ratio, as shown in blue fluorescent proteins (BFPs) imaging.[253] In this technique, a continuous long-wave secondary laser depopulates dark states enriching the population of fluorophores that are able to emit. BFPs engineered to enable photoinducible dark-state depopulation are called modulatable BFPs (modBFPs); the secondary laser excitation represents a modulation.

Since the modulation changes the ratio between the dark and the fluorescent fluorophores, the fluorescence enhancement is determined by the rates of formation of dark states. In analogy with the well-characterized photoswitchable fluorescent proteins discussed above, the transitions between dark and bright states likely involve changes in protonation state and cis−trans conformational changes, which depend on the chromophore's environment. Thus, by changing the amino acids in the vicinity of the chromophore, one can differentially stabilize the relevant states. In this way, one can adjust the modulation depth and frequency. Optical modulation could be potentially applied to fluorescent proteins emitting in other than the blue parts of the spectrum.

Recently, a similar approach was applied to the green to red photoconvertible proteins Dendra2 and mEos to provide enhanced photoconversion levels in thick samples in vivo.[254] The authors used a pair of single-photon continuous-wave laser sources simultaneously illuminating the sample instead of a high-power 405 nm (3.06 eV) pulse laser beam. Such illumination regime was termed primed conversion, where 488 nm (2.54 eV) or another visible laser was referred to as the priming beam and the second near-infrared (700−780 nm) laser was called the converting beam. Taking into account data on comparison of photoconversion efficiency between the sequential and the simultaneous dual-laser scanning that showed a negligible difference up to 3.75 ms time delay, the authors supposed participation of a long-lived (millisecond scale) dark intermediate that is photoactivated directly by the converting laser.

8. PHOTOBLEACHING AND PHOTOTOXICITY

Photobleaching and phototoxicity of fluorescent labels are important parameters for applications. Most fluorescent proteins have relatively low phototoxicity, with the prominent exception of KillerRed and its monomeric variant SuperNova, which are strongly phototoxic when irradiated with green/orange light in the presence of oxygen.[255,256] KillerRed also exhibits very low photostability.[255] Recently, a new phototoxic fluorescent protein called KillerOrange was engineered; it was derived from KillerRed but has a tryptophan-based chromophore and is phototoxic when illuminated with blue/cyan light.[257,258] Figure 28 compares the tyrosine- and tryptophan-based chromophores. Based on the analogy with common synthetic dyes and a strong dependence of the bleaching and the phototoxicity on the presence of oxygen, the phototoxicity

DOI: 10.1021/acs.chemrev.6b00238
Chem. Rev. 2017, 117, 758−795

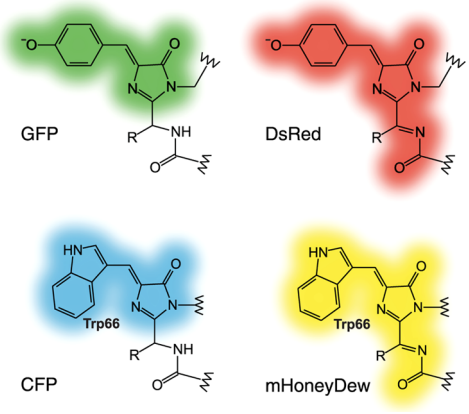

Figure 28. Tyrosine- and tryptophan-based chromophores. KillerRed has the same anionic chromophore as DsRed, whereas KillerOrange has a neutral tryptophan-based chromophore, as in HoneyDew. Reproduced with permission from ref 257. Copyright 2015 Sarkisyan et al. Publisher PlosOne.

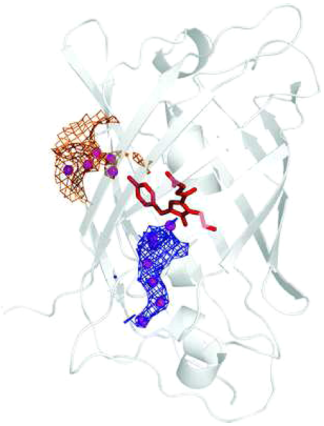

Figure 29. Cavities in KillerRed. Main water-filled channel is shown in blue, and the bifurcated pore is shown in orange. Water molecules and the chromophore are shown in pink and red, respectively. The pore, which is filled with water, is present in many nonphototoxic fluorescent proteins. The water channel containing a chain of seven water molecules is a distinct feature of GFP-based photosensitizers, KillerRed,[133] SuperNova,[256] and KillerOrange.[258] Reproduced with permission from ref 133. Copyright 2010 The Royal Society of Chemistry and Owner Societies.

of KillerRed was attributed to the formation of ROS,[38,125,255] e.g., $^1O_2$ (singlet oxygen) and $^2O_2^{-\bullet}$ (superoxide). Possible pathways of their formation are shown in Figure 9.

The dependence of bleaching on oxygen concentration has also been observed in other fluorescent proteins.[127,259] Direct observations of ROS in several fluorescent proteins have been reported (see, for example, refs 126, 127, and 259 and references therein). The focus of refs 126 and 127 was on eGFP and eGFP-derived mutants. The attempts to detect singlet oxygen in DsRed and KillerRed were not successful.[125,126] Interestingly, the documented cases of singlet oxygen production involve the anionic eGFP chromophore.[127] For HBDI (the model eGFP chromophore) in solution, the quantum yield of singlet oxygen production is 0.04, considerably higher than in eGFP.[126] The lifetime of $^1O_2$ photosensitized by eGFP is 4 μs, which is much shorter than that of $^1O_2$ produced by HBDI.[126] This suggests that $^1O_2$ is partially quenched by the amino acids surrounding the chromophore in eGFP. These observations again illustrate the protective role of the β-barrel.

On the basis of an unsuccessful attempt to detect singlet oxygen in KillerRed it was concluded that superoxide must be a primary phototoxic agent.[125] However, superoxide's relatively low toxicity is difficult to reconcile with the very strong phototoxicity of KillerRed. Moreover, computational modeling suggested that the diffusion of superoxide out of the protein barrel is strongly impeded due to its negative charge.[133]

The high phototoxicity and low photostability of KillerRed are often attributed to an interesting structural feature, a water channel connecting the chromophore's cavity with the exterior of the protein barrel (see Figure 29). A similar channel is present in KillerOrange.[258] It was suggested that this channel enables the diffusion of oxygen molecules to/from the chromophore. Computer simulations[133] have illustrated that the water channel indeed increases the chromophore's accessibility to oxygen. Mutagenesis studies have shown that even a partial blocking of the water channel decreases the production of ROS and reduces phototoxicity. For example, interruption of the water chain by introducing bulky mutations in position 199 (e.g., Ile199Phe/Leu/Lys in KillerOrange[258]) leads to increased photostability and an almost 2-fold increase in Y_f. In eGFP, the connection between bleaching and the chromophore's accessibility to oxygen has also been confirmed by mutations.[127]

Several studies have attributed the low photostability of some red fluorescent proteins (derived from the tetrameric DsRed) to increased accessibility of the chromophore to oxygen caused by a weakness of their β-barrels.[132] Free energy calculations identified an oxygen-diffusion pathway comprising several oxygen-hosting pockets and accessed from the solvent through a floppy gap between β_7 and β_{10} strands.[132] The diffusion of oxygen and superoxide has been also investigated computationally in KillerRed.[133] The simulations suggested that diffusion of $^3O_2$ and $^1O_2$ is greatly facilitated in KillerRed, in comparison to eGFP, due to the presence of the water-filled channel. In contrast, due to their negative charge, superoxide radical ions putatively produced inside the chromophore pocket were unable to escape the protein in the simulations.

The photostability of fluorescent proteins can be affected by other species present in the surrounding media, whose composition depends on experimental conditions. Malkani and Schmid showed that eCFP in live cells is significantly more photostable than after fixation and mounting in commercial mounting fluids.[260] Interestingly, eYFP demonstrated the opposite behavior, i.e., an increase in photostability approximately 3.5-fold upon mounting.[260] These phenomena remain unexplained.

Recently, new evidence of the influence of the external media components on eYFP's photostability has been reported by Jusuk et al.[261] In an attempt to find the optimal conditions for eYFP-conjugated DNA origami nanorulers super-resolution imaging, the authors tested and compared several buffer compositions.[261] The study was inspired by eYFP's blinking behavior, which suggested a possible use of this protein as a STORM probe.[262,263] Under simultaneous oxygen removal and beta-mercaptoethanol (ME) addition, eYFP single molecules demonstrated a 6-fold increase in photostability.[261] Interestingly, neither of those condition changes (low oxygen or ME presence) alone significantly affected photobleaching. Since the goal of the study was to use eYFP as a fluorophore for STORM

DOI: 10.1021/acs.chemrev.6b00238
Chem. Rev. 2017, 117, 758−795

microscopy, such a photostabilizing effect can be described in terms of a single-molecule behavior, namely, as the increased number of switching cycles prior to permanent bleaching and as the increase in the total number of photons detected per molecule. Moreover, the buffer content that provided enhanced photostability also affected blinking characteristics of eYFP: it increased the average lifetime of the off state. Taken together, the increased photostability and a lower duty cycle provided significant optimization in STORM imaging. This improvement allowed Jusuk et al. to perform high-quality imaging of eYFP-conjugated 12-helix bundle DNA origami nanorulers in vitro as well as the eYFP-tubulin visualization in fixed mammalian cells.[261]

Using modified media in live-cell imaging, the photostability of eGFP, AcGFP1, TagGFP2, and photoactivated forms of PA-GFP and PS-CFP2 can be increased up to an order of magnitude. These modified media were derived from the traditional DMEM (Dulbecco's modified eagle medium) by depleting either riboflavin or all vitamins.[264] Subsequent studies illustrated that among various DMEM components, riboflavin and pyridoxal strongly affect eGFP photobleaching,[265] possibly because the depletion of these vitamins suppresses oxidative redding.[39] While the effect of riboflavin and pyridoxal can be explained by their ability to accept electrons from the electronically excited eGFP chromophore, the action of other compounds affecting photostability in cellulo proceeds via yet unknown indirect mechanisms. For example, the addition of the plant flavonoid rutin to the cell medium decreases photobleaching 3−4-fold;[265] the increased concentrations of $FeSO_4$, cyanocobalamine, lipoic acid, hypoxanthine, and thymidine result in high eGFP photostability (relative to DMEM) during visualization in Ham's F12 medium.[266] Furthermore, the rate of eGFP photobleaching depends on such common cell culture growth parameters as confluency and fetal serum content; specifically 90−100% cell density provided 2-fold photostability enhancement compared to low-density (10−20%) culture.[266] It is possible that differences in cell physiology strongly modulate the amount of intracellular oxidants, which are potentially responsible for the photoreactions leading to bleaching.

GFP's photooxidation during photobleaching is utilized in hybrid high-resolution microscopy techniques.[267,268] GFP recognition after bleaching (GRAB) exploits the property of GFP-like proteins (such as eGFP and eCFP) to generate oxygen radicals during photobleaching for photochemical precipitation of 3,3′-diaminobenzidine (DAB) molecules into electron-dense particles, which, in turn, are used as the labels for transmission electron microscopy or electron tomography.[267,268] Correlation of GFP fluorescence signal detected in live cells with electron microscopy of DAB precipitates in fixed cells gives both high spatial resolution (potentially up to 5 nm) and temporal information about the organization of the labeled molecules.

The mechanistic understanding of photobleaching in fluorescent proteins is quite rudimentary, in stark contrast to synthetic dyes.[34,121] Several recent studies have attempted to establish a molecular-level picture of photobleaching and to relate irreversible photobleaching to structural changes of the chromophore. The crystal structure (PDB id 3GL4) of bleached KillerRed reported by Pletnev et al. shows a disorder in the region of the chromophore.[269] In compliance with standard reporting protocol, the PDB entry 3GL4 lists the coordinates of all atoms including the original undamaged chromophore; however, the plot of electron density of the bleached form (panel B in Figure 3 of ref 269) shows no electron density in the area initially occupied by the phenolic ring, suggesting that bleaching involves the chromophore's decomposition.

Carpentier et al. reported[270] another crystal structure of the photobleached form of KillerRed (PDBid: 2WIS), which shows a distorted electron density between the phenolic and the imidazolinone rings of the chromophore. The authors proposed that the chromophore assumes a structure strongly bent at the methyne bridge, with the phenolic ring pointing into the water channel, leading to the exterior of the protein.

A similar motif, sp^2-sp^3 change of the hybridization of methyne's carbon, has been observed in photobleached IrisFP

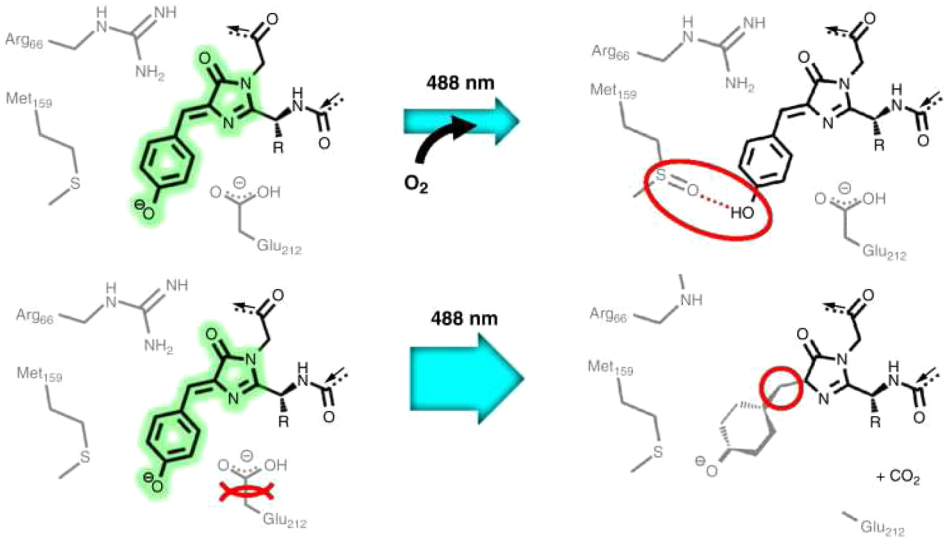

Figure 30. Proposed mechanisms of bleaching in IrisFP. (Top) Bleaching under weak illumination depends on oxygen and results in sulfoxidation of the Met159 and trapping the chromophore in a protonated nonfluorescent form. (Bottom) Bleaching under strong-illumination conditions results in the decarboxylation of Glu212, conformational change of the chromophore pocket, and distorting the chromophore to an sp^3-hybridized state (R denotes histidine). Reproduced with permission from ref 32. Copyright 2014 Elsevier Ltd.

DOI: 10.1021/acs.chemrev.6b00238
Chem. Rev. 2017, 117, 758−795

under high-intensity illumination.[233] This photobleached X-ray structure shows other distortions of the protein including decarboxylation of a glutamate residue. Interestingly, a bleached structure of IrisFP obtained at low-intensity illumination[233] showed no significant changes in the chromophore, suggesting that bleaching under these conditions is due to modifications, such as sulfoxidation of cysteine and methionine, to other parts of the protein. Figure 30 illustrates the proposed mechanisms of bleaching under these two different regimes.

A possible mechanism of photobleaching and generation of superoxide or other phototoxic agents has been proposed in ref 172. The key feature of the proposed mechanism is a photoinduced reaction of the chromophore with molecular oxygen inside the protein barrel, leading to the chromophore's decomposition. QM/MM simulations have shown that a model system comprising the protein-bound anionic chromophore and O_2 can be excited to an electronic state of the charge-transfer $Chro^- \rightarrow O_2$ character (see Figure 17). Once in the CT state, the system undergoes a series of chemical reactions with low activation barriers resulting in cleavage of the bridging bond between the phenolic and the imidazolinone rings and disintegration of the chromophore.

To conclude, various mechanisms of photobleaching might be operational under different conditions; however, ET is likely to be involved in many of them. Better understanding of bleaching mechanisms would provide design principles for improving photostability and increasing the optical output of fluorescent proteins. Rational design principles would allow protein engineering to depart from the most commonly used approach, finding photostability-enhancing mutations by random mutagenesis starting from fluorescent proteins with low photostability.

What can we learn from previously found mutations that have a significant effect on photostability? The V150I plus V224R mutations increased the photostability of eBFP by 2 orders of magnitude.[105,271] Single substitution, S158T (corresponding to position 165 in GFP), considerably improved the photostability of TagRFP.[244] In a chloride-sensitive variant of YFP, ClsM, photobleaching was strongly suppressed by the S205V mutation.[272] The common motif in these examples is the insertion of bulkier residues. Such mutations decrease or eliminate the fast initial phase of bleaching, which is attributed to cis−trans isomerization and/or protonation−deprotonation of the chromophore.[245,273,274] In addition, the photostability enhancement might be due to a better shielding of the chromophore from molecular oxygen by bulky residues. Several crystallographic studies of photobleached fluorescent proteins have demonstrated chromophore destruction[269,270,275] or oxidation of nearby Met and Cys residues.[233] The latter provides a possible explanation for the importance of mutation M163Q (position 167 in GFP) in achieving high photostability in mCherry.[244]

In contrast to these studies, two recent papers[145,276] reported successful design of more photostable fluorescent proteins based on mechanistic insights into photobleaching mechanism. Duan et al. reported that a single-residue mutation, M159A, in photoswitchable IrisFP results in considerably enhanced photostability.[276] This mutation was selected on the basis of their proposed mechanism of photofatigue in IrisFP and other Anthozoan fluorescent proteins such as EosFP, Dendra, or Dronpa derivatives. The key feature of their mechanism is oxygen-dependent reaction resulting in the irreversible sulfoxidation of Met159.

In another recent work, more photostable forms of eGFP and eYFP were obtained by judicious disruption of the main ET route.[145] On the basis of the proposed mechanistic picture of photoinduced ET by a hopping mechanism via Tyr145 (see Figure 15), Tyr145 was replaced by less efficient electron acceptors, Leu and Phe (note that these residues are also less bulky than tyrosine).[145] The mutants have 25−80-fold increased photostability relative to the original fluorescent proteins.

These two works serve as an example of a rational, mechanistic approach to fluorescent protein engineering.[145,276]

9. EXAMPLES OF PHOTOCONVERSIONS

9.1. Decarboxylation

The decarboxylation reaction of the glutamate side chain adjacent to the chromophore leads to photoconversion based on the stabilization of the anionic form of the chromophore relative to the protonated neutral one (Figure 3), which results in the red-shifted absorption.[130] The decarboxylation can also be coupled with other transformations. Figure 31 shows two examples of irreversible photoactivation involving decarboxylation.

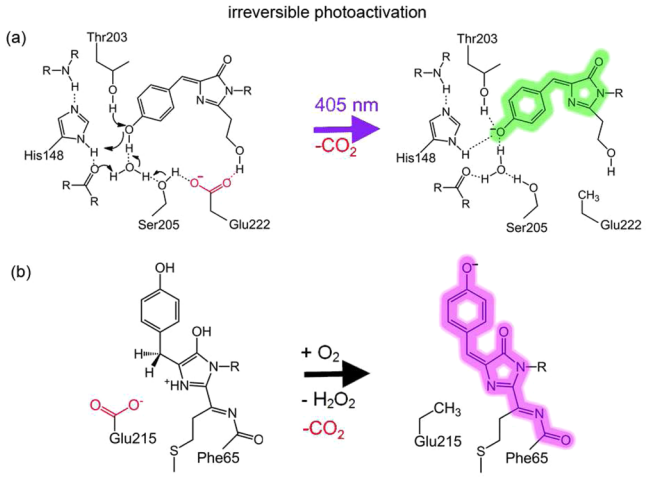

Figure 31. Decarboxylation leads to irreversible photoactivation in (a) PA-GFP and (b) PAmCherry. Reproduced with permission from ref 36. Copyright 2014 The Royal Society of Chemistry.

The proposed mechanism invokes photoinduced ET from nearby Glu to the chromophore.[130,157,173] As discussed in section 4.2.3, the calculations confirmed the accessibility of such CT states.[157] Several scenarios ranging from the direct population of the CT states by photoexcitation to a Marcus-like excited-state process have been proposed.[157,171,173]

The exact details of the decarboxylation mechanism are still unclear. There is strong experimental evidence that this process is initiated through higher excited states, which are accessed either by photoexcitation using high-energy light or by a multiphoton process. For example, the rate of the light-induced decarboxylation of wt-GFP strongly depends on the excitation wavelength and decreases at lower energies (i.e., 254 > 280 > 476 nm) by more than 2 orders of magnitude,[131] and photoconversion at lower energies (404 and 476 nm) does not occur below a certain laser power threshold (no photoconversion occurred upon irradiation of the sample by 404 nm light at 6 mW/cm^2 even after 6 h of irradiation). This

DOI: 10.1021/acs.chemrev.6b00238
Chem. Rev. 2017, 117, 758−795

threshold behavior is strongly suggestive of a two-photon process; however, the reported linear dependence on laser power between 50 and 1 mW/cm^2 contradicted this hypothesis.[131] A later study, which investigated the power dependence of the decarboxylation reaction in the Thr203Val mutant by using a more sensitive technique (accumulative femtosecond spectroscopy),[277] has found that using 400 nm (3.1 eV) excitation the decarboxylation requires two photons, whereas at lower excitation energies (800 nm, 1.55 eV), it becomes a three-photon process. These observations are consistent with the mechanistic picture[157] that decarboxylation proceeds via direct excitation (one or two-photon) to a high-lying electronic state of CT character (Figure 13, bottom right).

Decarboxylation phenomena have been exploited in developing PA-FPs used as optical highlighters and in super-resolution imaging.[22] Patterson and Lippincott-Schwartz developed the PA-GFP variant by substituting Thr203 by histidine in wt-GFP.[71] Irradiation of the Thr203His mutant with intense light (413 nm or 3.00 eV) results in 2 orders of magnitude increased fluorescence (at excitation energy of 2.54 eV or 488 nm); the activated species remain stable for days under aerobic conditions. Electron density maps[278] of the original (dim) and activated (bright) forms confirmed that photoactivation indeed results from the decarboxylation of Glu222.

This photoactivation mechanism is exploited in an interesting dimeric construct, called Phamret,[279] which comprises the PA-GFP and eCFP units. Phamret mimics the behavior of photoconvertible fluorescent proteins but allows one to use a single excitation wavelength (2.71 eV or 458 nm) for both the original and the activated forms. Prior to photoactivation of the PA-GFP subunit, Phamret emits cyan light (2.61 eV or 475 nm). Once photoactivated, excitation of the eCFP unit leads to FRET and green light emission (2.40 eV or 517 nm) from the eGFP moiety.

Photoconversion of DsRed also involves decarboxylation, possibly coupled with cis to trans isomerization.[158] The photoconverted form is red shifted relative to the original DsRed (shift in absorption of 36 nm, from 2.22 to 2.08 eV) and has reduced Y_f (0.01 versus 0.7). The red shift is again consistent with the stabilization of the anionic chromophore. The photoconversion mechanism has been deduced on the basis of absorption, fluorescence, and vibrational spectroscopy as well as mass spectrometry.[158] Recently, decarboxylation of Glu222 has been invoked to explain photoconversion of LSS-mOrange.[191]

The photophysics of the reversibly switchable protein IrisFP features an interplay among different processes including decarboxylation[156,233,246] (see sections 3.3 and 8). The nature of nonfluorescent and fluorescent states and the mechanism of photoswitching have been interrogated by a combination of kinetic X-ray crystallography, in crystallo spectroscopy, mass spectrometry, and modeling.[233] The findings suggested that at least two mechanisms are operational in IrisFP. Under high-intensity illumination (~0.1 kW/cm^2), an oxygen-independent mechanism dominates, which involves decarboxylation of Glu212 (corresponding to Glu222 in GFP) and damage of the chromophore. Thus, in contrast to photoactivation of GFPs[71,130,157,278] where decarboxylation of the glutamate locks the undamaged chromophore in a specific protonation state, the proposed mechanism for IrisFP[233] couples decarboxylation of Glu with chemical modifications of the chromophore and the neighboring residues. The authors concluded that the chromophore is chemically altered because of the deformation of the methyne bridge suggesting an sp^3-hybridized state, in contrast to the initial sp^2 form. The photobleached chromophore is thus likely to be photoreduced, which implies the net transfer of two electrons and two protons, as depicted in Figure 25. Molecular dynamics simulations were carried out to test the feasibility of this reaction. On the basis of the simulations, the authors suggested the formation of a zwitterionic imidazolinone ring in which the oxygen atom is negatively charged and stabilized by two hydrogen bonds to the guanidinium groups of Arg66 and Arg91, whereas the N4 nitrogen atom is protonated and positively charged. It was proposed that the proton ending up on the C_α carbon likely originates from Arg66,[156] whereas the second electron and proton could be provided by a reducing molecule in the surrounding medium. Further experiments are needed to identify possible proton and electron donors and to confirm the proposed mechanism.

To conclude, whereas the basic mechanistic details of photoinduced decarboxylation of the glutamine side chain in fluorescent proteins via transient photoreduction of the chromophore seem to be clear, this process may be coupled with other reactions (cis−trans isomerization, permanent reduction of the chromophore, etc.) in some fluorescent proteins (e.g., DsRed, IrisFP). The exact nature of these processes and the chemical identity of the photoconverted proteins are yet to be confidently determined.

9.2. Green to Cyan Conversion in WasCFP

Another example of photoinduced damage of a nearby amino acid in fluorescent proteins, which leads to changes in its spectral properties, was recently described as green to cyan photoconversion of WasCFP[280] and NowGFP.[110] These proteins carry an unusual anionic tryptophan-based green chromophore, whose negative charge is stabilized by Lys61. Crystallographic studies of NowGFP have demonstrated that upon light illumination decomposition of Lys61 occurs with a predominant loss of the NH_2CH_2CH group of the lysine side chain.[281] In turn, the disappearance of the positively charged Lys61 amino group leads to the appearance of a regular, protonated, cyan chromophore state (CFP-like chromophore).

9.3. Photoswitching in Dreiklang

Yet another mechanism of photoswitching is operational in Dreiklang (Figure 32), a reversible photoswitchable fluorescent protein derived from Citrine.[75] In the on state, the chromophore is the same as in the parent Citrine (or in eYFP); consequently, it has similar spectral properties. The anionic GFP-like chromophore, which is π-stacked with Tyr203, absorbs at 2.43 eV (511 nm) and emits at 2.36 eV (525 nm). Dreiklang also absorbs at 3.01 eV (412 nm), and the excitation of this band converts the chromophore into the dark form. In the off state, the chromophore absorbs at 3.65 eV (340 nm), which facilitates the conversion to the bright state. The mechanism of photoswitching, which was established on the basis of mass spectrometry and crystallographic analysis of the on and off states of the protein,[75] is shown in Figure 32. In contrast to many other photoswitchable proteins, the mechanism in Dreiklang does not involve a cis−trans isomerization reaction. Instead, the chromophore undergoes a reversible hydration/dehydration reaction at the imidazolinone ring. The hydration disrupts the π-conjugation and results in blue-shifted absorption.

DOI: 10.1021/acs.chemrev.6b00238
Chem. Rev. 2017, 117, 758−795

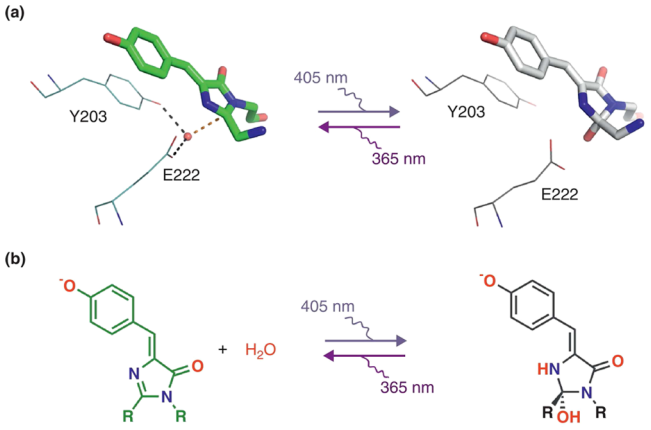

Figure 32. Photoswitching in Dreiklang via photoinduced hydration/dehydration reaction. In the on state, the chromophore is the same as in eYFP. In the off state, the imidazolinone ring of the chromophore is hydrated. Reproduced with permission from ref 70. Copyright 2013 Elsevier Ltd.

Owing to this unique switching mechanism, the wavelengths used for photoswitching and for excitation inducing fluorescence are decoupled in Dreiklang, leading to important advantages for super-resolution microscopy, that is, the switching and fluorescence readouts are not interlocked, alleviating an important limitation of previously characterized RS-FPs in which the wavelength used for generating the fluorescence is identical to one of the wavelengths used for switching. The three-state switching modality of this protein has inspired its name—Dreiklang is the German word for a three-note chord in music.

9.4. Oxidative Redding

Oxidative redding (Figure 33) is a photoconversion that proceeds upon photoexcitation in the presence of oxidative agents.[39] Oxidative redding was observed in a variety of fluorescent proteins that have anionic eGFP-like chromophore. The redding can proceed at relatively small concentrations of oxidants (on a micromolar scale). The red form is unstable and decays within hours.[39] This process may be exploited in various applications.[4,25,40] Photoconvertible orange fluorescent proteins, which undergo orange to red transition in the oxidative media, have also been developed.[30,282] In these fluorescent proteins, the GFP-like anionic chromophore is extended to include a conjugated acylimine tail[30,282] (see Figure 1). Overall, redding appears to be a robust process characteristic of anionic chromophores. No structural information about the red chromophore in eGFP-like proteins is available, although several hypotheses were put forward.[39,40,129]

Bogdanov et al. established[39] that in eGFP redding is a single-photon process involving two or more steps and a net transfer of two electrons from the GFP molecule to an external acceptor(s). The two-electron oxidation was inferred from the measured yields of the reduced species: the yield of two-electron photoreduction of NAD^+ to NADH by eGFP was close to one, whereas the yield of the one-electron-reduced cytochrome *c* was nearly 2, suggesting the production of two reduced cytochromes per one eGFP molecule.[39] A multistep mechanism was proposed on the basis of the relative efficiency of the green form disappearance and the appearance of the red form, that is, the half-maximal effective concentrations of one-electron acceptors were approximately an order of magnitude lower for the green fluorescence decrease than for the red fluorescence increase. This observation can be rationalized by a two-step scheme in which the first step involves light absorption and one-electron chromophore oxidation forming a nonfluorescent intermediate, which could either donate the second electron forming the red chromophore or become permanently nonfluorescent. In terms of Scheme 1, the first step corresponds to photoinduced ET and the second step to slow chemical transformations. Intracellular electron acceptors could also promote oxidative redding, and different mammalian cell lines as well as the particular cells within a single culture show enormously high heterogeneity in their ability to prime this photoconversion.

Subach et al. reported remarkable orange to far-red photoconversion of the monomeric PSmOrange protein, which might be mechanistically similar to the oxidative redding observed in GFP.[30] The original orange form of this mOrange-derived protein emits at 2.19 eV (565 nm), whereas a new far-red form appearing after 488 nm LED irradiation peaks at 1.87 eV (662 nm). In the presence of electron acceptors (potassium ferricyanide as well as intracellular oxidants), the photoswitching efficiency increases dramatically. Using SDS-PAGE and mass spectrometry of protease-cleaved protein before and after conversion, the authors deciphered the structure of the far-red form of the chromophore. They have shown that light-induced two-electron oxidation leads to the polypeptide chain cleavage just before the chromophore-forming tyrosine, accompanied by a substitution of the hydroxyl group of

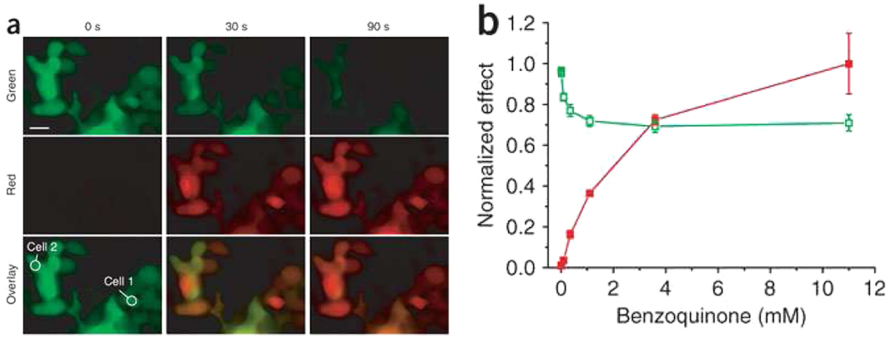

Figure 33. Oxidative redding in GFP. (Left) Fluorescence microscopy of Phoenix Eco cells transiently expressing eGFP-N1 in green (upper row) and red (center row) channels. (Right) Concentration dependence of the yield of oxidant-mediated green to red photoconversion of eGFP in vitro. Green and red curves show benzoquinone concentration dependences on the green fluorescence decrease and the red fluorescence increase in the immobilized eGFP. Reproduced with permission from ref 39. Copyright 2009 Nature America, Inc.

DOI: 10.1021/acs.chemrev.6b00238
Chem. Rev. 2017, 117, 758−795

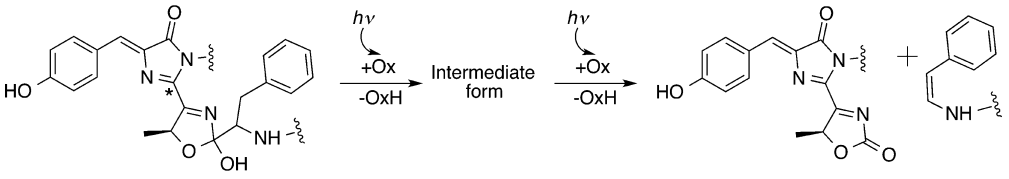

Figure 34. Proposed scheme for the light-induced photooxidation of PSmOrange. Reproduced with permission from ref 30. Copyright 2011 Nature America, Inc.

dihydrooxazole ring by a carbonyl group. Thus, the far-red form of PSmOrange carries a new type of chromophore (Figure 34) with the GFP-like core extended by an *N*-acylimine with a coplanar carbon−oxygen double bond. Since both the original orange and the new far-red chromophore structures were resolved, a hypothetical scheme of the photoconversion process, which includes two-electron two-photon oxidation, was suggested[30] (see Figure 34). In contrast to GFP's oxidative redding, the PSmOrange conversion requires photon absorption at both stages.

Redding was observed also in vivo, particularly in *Zoanthus sp.* button polyp naturally producing GFP-family proteins in ectoderm cells.[39] These observations stimulated discussion about the role of GFPs redox photoreactions in natural function of this protein family. For example, one can hypothesize that the primary function of ancestral GFPs during early evolution of animals was based on light-induced ET in processes such as light sensing or production of reduced equivalents. Also, recent discovery of light-driven enzymatic degradation of plant polysaccharide using excited photosynthetic pigments as electron donors[283] suggests potential functioning of GFPs in some light-assisted digestion reactions.

Molecular-level mechanistic details of oxidative redding are not yet fully established. The formation of the red form occurs on the seconds to minutes time scale[39] and is likely to entail significant chemical transformation, such as extension of the conjugated π-system or breaking of the covalent bonds. Most likely, chemical steps leading to the red chromophore formation are initiated by photoinduced ET from the chromophore to an external oxidant molecule,[39] as given by Scheme 1.

Possible mechanisms, e.g., direct ET versus hopping (Figure 15) of photoinduced ET in eGFP and eYFP, have been recently investigated in a combined experimental and theoretical study.[145] Detailed calculations of the energetics of the one-electron oxidation process and possible ET pathways suggested that excited-state ET proceeds predominantly through a hopping mechanism via the Tyr145 residue. The proposed kinetic model for photoinduced ET is shown in Figure 35. It was assumed that the yield of total bleaching, Y_{totb}, is due to the formation of the red-form precursor and permanent bleaching via competing processes. The model predicts that the yield of the red-form precursor, Y_r, is controlled by the rate of ET to Tyr145, r_1, whereas Y_{totb} results from the combined ET via two competing channels, Tyr145 and ResX.

$$Y_r \approx \frac{r_1}{r_f\left(1+\frac{r_b}{r_2}\right)} \approx \frac{r_1}{r_f} \tag{7}$$

$$Y_{totb} \approx \left(\frac{r_1}{r_f}+\frac{r_4}{r_f}\right)\left(1+\frac{r_b}{r_2}\right) \approx \frac{r_1}{r_f}+\frac{r_4}{r_f} \tag{8}$$

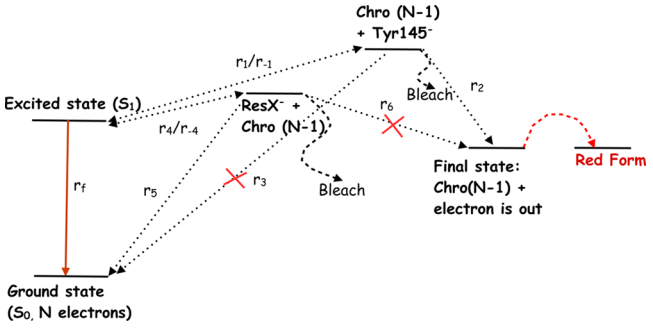

Figure 35. Kinetic model of photoinduced ET via a hopping mechanism (see Figure 15). Excited state decays to the ground state either radiatively or nonradiatively. This channel is characterized by r_f, which is inversely proportional to the excited-state lifetime ($r_f \approx 10^9$ s^{-1}). Alternatively, the excited state can be deactivated via ET from the chromophore to either Tyr145 or another acceptor, ResX (this could be Tyr203 in eYFP). ET to Tyr145 or ResX results in anion−radical (e.g., $Tyr^{-\bullet}$) formation that can lead to permanent bleaching (r_b). ET to Tyr145 can also lead to ET to an outside oxidant (r_2) forming a precursor for the red form. Observed bleaching is the sum of the yields of the red form precursor and of permanently bleached states. Reproduced with permission from ref 145. Copyright 2016 American Chemical Society.

These equations allow one to estimate the bounds on the ET rates and to connect yields with rates. They also show that the bleaching yield increases not only when the rates of ET are faster but also when the fluorescence lifetime increases, i.e., shorter fluorescence lifetimes result in increased photostability.

Structural analysis of the molecular dynamics trajectories has revealed[145] the two coexisting populations in YFP; in one of them the hydrogen bonding between the chromophore and Tyr145 is disrupted, which results in larger distances between these residues. The π-stacking of the chromophore with Tyr203 also reduces the electron-donating ability of the chromophore. These two factors (structural and electronic) suppress the main ET channel by reducing r_1. Moreover, Tyr203 itself can accept the electron, serving as a trap site for ET (ResX). The halide binding restores favorable energetics by upsetting the π-stacking, suppressing the population with the broken Chro··· Tyr145 hydrogen bond, and by modifying local electrostatic field, which results in the increase of r_1 and decrease of r_4. Figure 36 summarizes the most relevant structural parameters controlling r_1 and r_4. The theoretical predictions were validated by point mutations that confirmed that Tyr145 is the key residue controlling ET. Substitution of Tyr145 by less efficient electron acceptors resulted in mutants with extremely high photostabilities.[145]

9.5. Anaerobic Redding

So-called anaerobic redding of GFP is one of the earliest reported examples of photoactivation in fluorescent proteins; it was first described in 1997, independently by two groups.[159,284]

DOI: 10.1021/acs.chemrev.6b00238
Chem. Rev. 2017, 117, 758−795

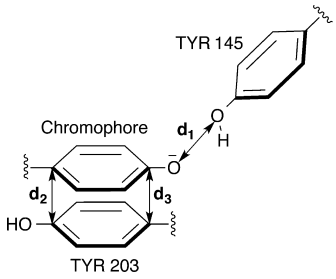

Figure 36. Structural parameters controlling ET between the chromophore and Tyr145 and between the chromophore and Tyr203 (in YFP). Distance between the phenolic oxygens of the chromophore and Tyr145 (d_1) affects the main ET channel (r_1). Extent of π-stacking can be quantified by $D \equiv (d_2 + d_3)/2$ and $\Delta \equiv |d_2 - d_3|$. In eGFP, $d_1 \approx 3.8$ Å. In eYFP and halide-bound eYFP, d_1 = 5.0 and 2.9 Å, respectively. Values of D and Δ are noticeably smaller in the halide-bound eYFP. Reproduced with permission from ref 145. Copyright 2016 American Chemical Society.

The process reported in these publications is quite dissimilar to other photoconversions, which were discovered later and are now widely used.

Elowitz et al. observed that in low-oxygen environments GFP variants can convert into a red-emitting form upon irradiation with blue light. The photoconversion occurs in purified GFP when prepared in a nitrogen environment or when mixed with an oxygen-scavenging system consisting of glucose oxidase, catalase, and β-D-glucose. Sawin and Nurse observed green to red photoconversion of av-GFP, av-GFP S65T, and GFPmut2 in fission yeast cells,[284] whereas Elowitz et al. reported on the analogous process detected in bacteria expressing av-GFP, av-GFP S65T and I167T, GFPuv, GFP mut 1,2,3, as well as in yeasts expressing GFPmut2 and even in purified GFPmut2 protein.[159]

Later, anaerobic redding was found to be common in diverse FPs of different origin with GFP-like chromophore but not for eCFP with tryptophan-based chromophore.[285] This observation indicates primary importance of the chromophore's structure rather than the amino-acid environment for this photoconversion.

The common feature of all these observations was the low oxygen environment required for conversion and fast disappearance of the red form after oxygenation, which suggest an intermolecular nature of redding. One can suppose, for instance, photoinduced reduction of the chromophore.

The characteristic time scale for this photoconversion is slow: 0.7 s. Interestingly, Sawin and Nurse reported the advantage of UV over blue light in wt-GFP redding efficiency.[284] The complex fluorescence emission spectrum of the red form containing two peaks at 590 and 600 nm and a shoulder at 560 nm, as well as the slow light-independent increase of red fluorescence brightness after irradiation, invites speculation about a multistep and/or multiproduct course of photoreaction.

It was proposed[159] that photoactivation is a two-step process: 488 nm (2.54 eV) light stimulates a fast transition to an intermediate (optically dark), which then decays slowly to the red-emitting GFP state (this second step can proceed in the dark). The activated form remains stable in anaerobic environment for about 24 h. The structural basis of this photoconversion is still unknown. Since this photoconversion proceeds in a reductive environment, it is possible that the fast step is the photoreduction of the chromophore.

Applications of anaerobic redding are limited by the dependence of GFP maturation on oxygen. Thus, only biological models where cells are first oxygenated (for GFP maturation) and then deoxygenated (for anaerobic redding) can be used. For example, successful highlighting with GFP anaerobic redding was reported in bacterial and yeast cells for protein tracking or studying mitochondrial organization.[286,287] Also, GFP's anaerobic redding was used as a measure of oxygenation levels in organs of animals.[288]

10. CONCLUSIONS AND OUTLOOK

GFP-like fluorescent proteins occupy a unique niche in modern science. They are the only fluorescent probes of natural origin. Thus, their properties are of interest from both fundamental and applied points of view.

A variety of photochemical reactions occur in fluorescent proteins. An electronically excited chromophore is the main player in these reactions, which include cis−trans isomerization coupled with protonation/deprotonation, ESPT, oxidation or reduction, and protein backbone cleavage. In addition, amino acids adjacent to the chromophore often undergo modification of their side chains (e.g., glutamate decarboxylation). Participation of amino acids around the chromophore in photoinduced proton and electron transfer is also rather common.

Some of these reactions may happen in nature, suggesting possible biological significance. However, most occur in artificial fluorescent protein variants under specific illumination conditions unattainable under natural sunlight. Understanding their mechanisms will enable optimal use of fluorescent proteins in practical applications. Knowledge of the underlying photochemistry will help to minimize undesirable reactions and enhance target processes.

Indeed, recent works show inspiring examples of knowledge-driven optimization of the properties of fluorescent proteins, e.g., the reduction of photobleaching by ET suppression or the increase of photoconversion efficiency by dual-wavelength illumination. It is now clear that light-induced long-lived dark states are quite common in fluorescent proteins. This should be kept in mind for the widely used technique of multicolor imaging with simultaneous or nearly simultaneous (in millisecond time scale) excitation with multiple wavelengths, since direct excitation of these transient spectral forms can result in unexpected outcomes.

Photoinduced proton and electron transport is of fundamental importance in biology. Being a simple single-protein system with clear absorption and fluorescence readouts, fluorescent proteins are a useful vehicle for studying the mechanistic details of these processes in proteins both in vitro and in cellulo. At present, our understanding of photoreactions in fluorescent proteins is not complete and requires further extensive studies. This is especially true for ET in fluorescent proteins, which has been hitherto underappreciated. Advanced time-resolved spectroscopy should be used to identify transient spectral forms. Quantum-mechanical calculations are often the only way to decipher their structures, which cannot be resolved by classical structure-determination methods. We believe that these fundamental studies will ultimately lead to major advances in fluorescent protein applications toward nearly photobleaching-free imaging, efficient photoactivation for protein tracking, and super-resolution microscopy, as well as

DOI: 10.1021/acs.chemrev.6b00238
Chem. Rev. 2017, 117, 758−795

optogenetic control of cell physiology. And who can foretell what other exciting applications of fluorescent proteins in biotechnology will become a reality in the future?

AUTHOR INFORMATION

Corresponding Authors

*E-mail: kluk@ibch.ru.
*E-mail: krylov@usc.edu.

Notes

The authors declare no competing financial interest.

Biographies

Atanu Acharya is a graduate student at the University of Southern California, Los Angeles. He received his B.Sc. degree in Chemistry (with honors) from the Department of Chemistry, Jadavpur University, Kolkata, India. After completing his M.Sc. degree in Chemistry at the Indian Institute of Technology Madras (IITM), Chennai, India, in 2011, he joined Professor Krylov's group at USC. He received the best dissertation award for his Master's thesis from the Department of Chemistry, IITM. His research at USC has been recognized with the Michael J. Dulligan Memorial Award for outstanding graduate research in physical chemistry by the Department of Chemistry, USC. He will be defending his Ph.D. thesis "Photoinduced redox reactions in biologically relevant systems" in the Fall 2016.

Alexey M. Bogdanov graduated from the Biology Department of the Moscow State University in 2006 and received his Ph.D. degree in Molecular Biology from the Shemyakin and Ovchinnikov Institute of Bioorganic Chemistry (IBCH), Moscow, Russia, in 2010. He is currently a research scientist at the Laboratory of Biophotonics (IBCH) and a senior research scientist at the Fluorescent Bioimaging Laboratory (Nizhny Novgorod State Medical Academy). His research interests include light-induced processes in fluorescent proteins and the development of molecular sensors based on fluorescent proteins.

Bella L. Grigorenko received her Ph.D. degree in Solid State Physics from the Physics Department of the M. V. Lomonosov Moscow State University. Her Doctoral degree (2004) is from the Department of Chemistry at the Moscow State University, where she is currently a senior scientist in the Laboratory of Chemical Cybernetics. Her main interests are the development and application of molecular modeling methods to study biomolecular systems.

Ksenia B. Bravaya received her M.Sc. (2005) and Ph.D. (2008) degrees in Chemistry from the M. V. Lomonosov Moscow State University, Russia. She then joined the group of Professor A.I. Krylov at the University of Southern California, where she conducted postdoctoral research on method development for electronically excited and open-shell states in complex systems and applications to photoinduced processes in biologically relevant systems. Her postdoctoral work has been recognized with the ACS Physical Chemistry and WISE (USC) Postdoctoral Recognition awards. She is currently an assistant professor at Boston University, Massachusetts. Her major research focus is on theoretical studies of photoinduced processes in biomolecules and complex environments including electronically bound and metastable species.

Alexander V. Nemukhin is currently Professor of Physical Chemistry in the Chemistry Department of the M. V. Lomonosov Moscow State University and the Director of the Laboratory for Computer Modeling of Biomolecules and Nanomaterials at the N. M. Emanuel Institute of Biochemical Physics of the Russian Academy of Sciences. He received his Ph.D. degree in 1975 and his Doctoral degree in 1989. His theses were devoted to quantum-chemical studies of molecular properties and included collaboration with Professor Jan Almlof (University of Oslo, Norway, and Minnesota State University) and Professor Frank Weinhold (University of Wisconsin—Madison). A substantial part of his early work was focused on modeling properties of matrix-isolated species at low temperatures. Since 2000 his main research interest has been the development and application of molecular-modeling methods to study biomolecular systems.

Konstantin A. Lukyanov graduated from the Moscow State University in 1991 and received his Ph.D. degree in Molecular Biology from the Shemyakin-Ovchinnikov Institute of Bioorganic Chemistry in 1998. He is currently the Head of the Laboratory of Biophotonics at the Shemyakin-Ovchinnikov Institute of Bioorganic Chemistry in Moscow, Russia. His main research interests are the study of complex biochemistry and photochemistry in GFP-like proteins and the development of novel genetically encoded probes for fluorescence microscopy.

Anna I. Krylov received her M.Sc. degree (with honors) in Chemistry from the Moscow State University (Russia) in 1990 and her Ph.D. degree (cum laude) in Physical Chemistry from the Hebrew University of Jerusalem (Israel) in 1996. After postdoctoral training in Professor M. Head-Gordon's group at UC Berkeley, she started her research in electronic structure theory and methodology at the Department of Chemistry of the University of Southern California in Los Angeles, where she is currently Professor of Chemistry and Gabilan Distinguished Professor in Science and Engineering. Her vision is to develop and devise accurate computational tools for treatment of complicated open-shell electronic structures ranging from bound and unbound excited states to complicated polyradical species in the gas phase and in complex environments such as solutions, molecular solids, and proteins. Her contributions to electronic structure method development (in particular, the spin-flip method) have been recognized by several awards including the WATOC's Dirac Medal (2007), the Bessel Prize from the Humboldt Foundation (2011), and the Theoretical Chemistry Award from the Physical Chemistry Division of the American Chemical Society (2012). She is a member of the International Academy of Quantum Molecular Science and a Fellow of the American Physical Society, the American Chemical Society, and the American Association for the Advancement of Science.

ACKNOWLEDGMENTS

This work was supported by the U.S. National Science Foundation (CHE-1566428, A.I.K.) and the Russian Science Foundation (14-25-00129, K.A.L. and A.M.B.). A.V.N. was partially supported by the Russian Foundation for Basic Research (Project 16-03-00078). B.L.G. and A.V.N. acknowledge the use of the supercomputer resources at the Lomonosov Moscow State University. A.I.K. is grateful to Mr. Jay Tanzman for careful proofreading of the manuscript.

ABBREVIATIONS

CT	charge transfer
DMEM	Dulbecco's modified eagle medium
DAB	3,3′-diaminobenzidine
EA	electron attachment
ET	electron transfer
ESPT	excited-state proton transfer
GRAB	GFP recognition after bleaching
PC-FP	photoconvertible fluorescent protein
RS-FP	reversibly switchable fluorescent protein
PA-FP	photoactivatable fluorescent protein
PS-FP	photoswitchable fluorescent protein

DOI: 10.1021/acs.chemrev.6b00238
Chem. Rev. 2017, 117, 758−795

FLIM	fluorescence lifetime imaging microscopy
FP	fluorescent protein
FPALM	fluorescence photoactivation localization microscopy
FqRET	fluorescence quenching resonance energy transfer
FRET	fluorescence resonance energy transfer
MO	molecular orbital
HOMO	highest occupied molecular orbital
LSS	large Stokes shift
LSS-FP	large Stokes shift fluorescent protein
LUMO	lowest unoccupied molecular orbital
ISC	intersystem crossing
PALM	photoactivated localization microscopy
RESOLFT	reversible saturable optical fluorescence transitions
ROS	reactive oxygen species
SOFI	super-resolution optical fluctuation imaging
STED	stimulated emission depletion
STORM	stochastic optical reconstruction microscopy
TA	transient absorption
QM/MM	quantum mechanics/molecular mechanics

NAMES OF FLUORESCENT PROTEINS

A5	enhanced blue fluorescent protein
AcGFP, AcGFP1	*Aequorea coerulescens* green fluorescent protein
asFP595	GFP-like protein, isolated from the sea anemone *Anemonia sulcata*
av-GFP	*Aequorea victoria* green fluorescent protein
GFPmut2	mutant of wt-GFP with three mutations: S65A, V68L, and S72A
Azurite	enhanced blue fluorescent protein
BFP	blue fluorescent protein
CFP	cyan fluorescent protein
Citrine	enhanced variant of YFP
CyOFP1	bright, engineered, orange-red FP that is excitable by cyan light
Dendra	green to red photoswitchable FP derived from octocoral *Dendronephthya sp.*
Dendra2	improved version of Dendra with single mutation: A224V
Dreiklang	reversibly photoswitchable variant of GFP
Dronpa	reversibly photoswithcable fluorescent protein
DsRed	*Discosoma sp.* red fluorescent protein
eBFP	enhanced blue fluorescent protein
eCFP	enhanced cyan fluorescent protein
eqFP578	wild-type red fluorescent protein derived from sea anemone *Entacmaea quadricolor*; λ_{em} = 578 nm
eqFP611	red fluorescent protein derived from the sea anemone *E. quadricolor*; λ_{em} = 611 nm
eGFP	enhanced green fluorescent protein
EosFP	photoconvertible fluorescent protein
eYFP	enhanced yellow fluorescent protein
GFP	green fluorescent protein
GFPuv	variant of GFP optimized for maximal fluorescence under UV light
HcRed1	far-red (λ_{em} = 618 nm) FP derived from a nonfluorescent chromoprotein found in the sea anemone *Heteractis crispa*
laRFP	red-emitting (λ_{em} = 592 nm) FP derived from the lancelet *Branchiostoma lanceolatum*
IrisFP	P173S mutant of the tetrameric variant of EosFP, capable of reversible photoswitching and irreversible photoconversion
Kaede	PC-FP derived from a stony coral, *Trachyphyllia geoffroyi*; Kaede means "maple" in Japanese.
Katushka	far-red variant of eqFP578; λ_{em} = 635 nm
Keima	FP derived from coral; it is acid stable and emits different colored signals at acidic and neutral pH
KFP	kindling fluorescent protein
kikGR	Kikume Green-Red FP; it is a PC-FP
KillerOrange	orange-emitting protein photosensitizer with Trp-based chromophore
KillerRed	first genetically encoded photosensitizer RFP
LSS-mKate1, LSS-mKate2	large Stokes shift monomeric RFPs; they are also mutants of mKate
LSS-mOrange	large Stokes shift monomeric orange FP
mCherry	a monomeric red fluorescent protein
mEos2	improved mEosFP with mutations: N11K, E70K, H74N, and H121Y
mEosFP	monomeric mutant (V123T-T158H) of EosFP
mIrisFP	monomeric IrisFP
mKate	variant of eqFP578
modBFP	modulatable BFP
mOrange, mOrange1	monomeric orange FPs
mOrange2	monomeric orange FP with increased photostability
mPlum	far-red monomeric RFP with large Stokes shift
mStrawberry	bright monomeric RFP
mTFP0.7	variant of monomeric teal FP
mTurquoise2	improved variant of mTurquoise FP
mKO	monomeric version of Kusabira Orange FP
NowGFP	GFP with a TRP-based anionic chromophore
Padron	RS-FP with positive switching; derivative of Dronpa
Padron0.9	RS-FP with positive switching; Padron-Y116C, K198I
PAmCherry	photoactivatable mCherry
Phamret	dimeric construct with PA-GFP and eCFP unit
PS-CFP	photoswitchable cyan fluorescent protein
PS-CFP2	improved mutant of PS-CFP
psamFP488	CFP isolated from the genus *Psammocora* of reef-building corals
PSmOrange	photoswitchable monomeric orange FP
RFP	red fluorescent protein
rseGFP	reversibly switchable enhanced green fluorescent protein
rseGFP2	improved variant of rseGFP with faster switching
rsFastLime	mutant of Dronpa; Dronpa-V157G
rsKame	mutant of Dronpa; Dronpa-V157I
Sirius	blue fluorescent protein with shortest emission wavelength
Spinach	RNA aptamer that binds and activates fluorescence of synthetic GFP chromophore
SuperNova	monomeric variant of KillerRed
TagBFP	monomeric blue fluorescent protein derived from TagRFP
TagGFP2	improved variant of TagGFP
TagRFP-S	original TagRFP
TagRFP-T	improved variant of TagRFP with increased photostability; TagRFP-S158T

DOI: 10.1021/acs.chemrev.6b00238
Chem. Rev. 2017, 117, 758−795

TagRFP675	near-infrared derivative of mKate; λ_{em} = 675 nm
wt-GFP	wild-type green fluorescent protein from *Aequorea victoria*
WasCFP	W (tryptophan) in anionic state cyan fluorescent protein
YFP	yellow fluorescent protein
Ypet	yellow fluorescent protein optimized for FRET with CPet
zFP538	YFP derived from the button polyp *Zoanthus sp.*

REFERENCES

(1) Tsien, R. Y. The green fluorescent protein. *Annu. Rev. Biochem.* **1998**, *67*, 509−544.
(2) Day, R. N.; Davidson, M. W. The fluorescent protein pallete: Tools for cellular imaging. *Chem. Soc. Rev.* **2009**, *38*, 2887−2921.
(3) Zimmer, M. GFP: from jellyfish to the Nobel prize and beyond. *Chem. Soc. Rev.* **2009**, *38*, 2823−2832.
(4) Chudakov, D. M.; Matz, M. V.; Lukyanov, S.; Lukyanov, K. A. Fluorescent proteins and their applications in imaging living cells and tissues. *Physiol. Rev.* **2010**, *90*, 1103−1163.
(5) Mishin, A. S.; Belousov, V. V.; Solntsev, K. M.; Lukyanov, K. A. Novel uses of fluorescent proteins. *Curr. Opin. Chem. Biol.* **2015**, *27*, 1−9.
(6) Johnson, F. H.; Shimomura, O.; Saiga, Y.; Gershman, L. C.; Reynolds, G. T.; Waters, J. R. Quantum efficiency of Cypridina luminescence, with a note on that of Aequorea. *J. Cell. Comp. Physiol.* **1962**, *60*, 85−103.
(7) Prasher, D. C.; Eckenrode, V. K.; Ward, W. W.; Prendergast, F. G.; Cormier, M. J. Primary structure of the Aequorea victoria green fluorescent protein. *Gene* **1992**, *111*, 229−233.
(8) Chalfie, M.; Tu, Y.; Euskirchen, G.; Ward, W. W.; Prasher, D. C. Green fluorescent protein as a marker for gene expression. *Science* **1994**, *263*, 802−805.
(9) Alieva, N. O.; Konzen, K. A.; Field, S. F.; Meleshkevitch, E. A.; Hunt, M. E.; Beltran-Ramirez, V.; Miller, D. J.; Wiedenmann, J.; Salih, A.; Matz, M. V. Diversity and evolution of coral fluorescent proteins. *PLoS One* **2008**, *3*, e2680.
(10) Haddock, S. H.; Moline, M. A.; Case, J. F. Bioluminescence in the sea. *Annu. Rev. Mar. Sci.* **2010**, *2*, 443−493.
(11) Salih, A.; Larkum, A.; Cox, G.; Kuhl, M.; Hoegh-Guldberg, O. Fluorescent pigments in corals are photoprotective. *Nature* **2000**, *408*, 850−853.
(12) Haddock, S. H.; Dunn, C. W. Fluorescent proteins function as a prey attractant: experimental evidence from the hydromedusa Olindias formosus and other marine organisms. *Biol. Open* **2015**, *4*, 1094−1104.
(13) Strader, M. E.; Aglyamova, G. V.; Matz, M. V. Red fluorescence in coral larvae is associated with a diapause-like state. *Mol. Ecol.* **2016**, *25*, 559−569.
(14) Zimmer, M. Green fluorescent protein (GFP): Applications, structure, and related photophysical behavior. *Chem. Rev.* **2002**, *102*, 759−781.
(15) Meech, S. R. Excited state reactions in fluorescent proteins. *Chem. Soc. Rev.* **2009**, *38*, 2922−2934.
(16) Sample, V.; Newman, R. H.; Zhang, J. The structure and function of fluorescent proteins. *Chem. Soc. Rev.* **2009**, *38*, 2852−2864.
(17) van Thor, J. J. Photoreactions and dynamics of the green fluorecent protein. *Chem. Soc. Rev.* **2009**, *38*, 2935−2950.
(18) Wachter, R. M. The family of GFP-like proteins: Structure, function, photophysics, and biosensor applications. introduction and perspective. *Photochem. Photobiol.* **2006**, *82*, 339−344.
(19) Nemukhin, A. V.; Grigorenko, B. L.; Savitsky, A. P. Computer modeling of the structure and spectra of fluorescent proteins. *Acta Nat.* **2009**, *2*, 41−52.
(20) Seward, H. E.; Bagshaw, C. R. The photochemistry of fluorescent proteins: implications for their biological applications. *Chem. Soc. Rev.* **2009**, *38*, 2842−2851.
(21) Bravaya, K.; Grigorenko, B. L.; Nemukhin, A. V.; Krylov, A. I. Quantum chemistry behind bioimaging: Insights from ab initio studies of fluorescent proteins and their chromophores. *Acc. Chem. Res.* **2012**, *45*, 265−275.
(22) Lukyanov, K. A.; Chudakov, D. M.; Lukyanov, S.; Verkhusha, V. V. Photoactivatable fluorescent proteins. *Nat. Rev. Mol. Cell Biol.* **2005**, *6*, 885−891.
(23) Lukyanov, K. A.; Serebrovskaya, E. O.; Lukyanov, S.; Chudakov, D. M. Fluorescent proteins as light-inducible photochemical partners. *Photochem. Photobiol. Sci.* **2010**, *9*, 1301−1306.
(24) Subach, F. V.; Verkhusha, V. V. Chromophore transformations in red fluorescent proteins. *Chem. Rev.* **2012**, *112*, 4308−4327.
(25) Shcherbakova, D. M.; Verkhusha, V. V. Chromophore chemistry of fluorescent proteins controlled by light. *Curr. Opin. Chem. Biol.* **2014**, *20*, 60−68.
(26) Ganesan, S.; Ameer-beg, S. M.; Ng, T. T. C.; Vojnovic, B.; Wouters, F. S. A dark yellow fluorescent protein (YFP)-based Resonance Energy-Accepting Chromoprotein (REACh) for förster resonance energy transfer with GFP. *Proc. Natl. Acad. Sci. U. S. A.* **2006**, *103*, 4089−4094.
(27) Pettikiriarachchi, A.; Gong, L.; Perugini, M. A.; Devenish, R. J.; Prescott, M. Ultramarine, a chromoprotein acceptor for Förster resonance energy transfer. *PLoS One* **2012**, *7*, e41028.
(28) Li, Y.; Forbrich, A.; Wu, J.; Shao, P.; Campbell, R. E.; Zemp, R. Engineering dark chromoprotein reporters for photoacoustic microscopy and FRET imaging. *Sci. Rep.* **2016**, *6*, 22129.
(29) Wang, L.; Jackson, W. C.; Steinbach, P. A.; Tsien, R. Y. Evolution of new nonantibody proteins via iterative somatic hypermutation. *Proc. Natl. Acad. Sci. U. S. A.* **2004**, *101*, 16745−16749.
(30) Subach, O. M.; Patterson, G. H.; Ting, L.-M.; Wang, Y.; Condeelis, J. S.; Verkhusha, V. V. A photoswitchable orange-to-far-red fluorescent protein, PSmOrange. *Nat. Methods* **2011**, *8*, 771−777.
(31) Dedecker, P.; De Schryver, F. C.; Hofkens, J. Fluorescent proteins: Shine on, you crazy diamond. *J. Am. Chem. Soc.* **2013**, *135*, 2387−2402.
(32) Adam, V.; Berardozzi, R.; Byrdin, M.; Bourgeois, D. Phototransformable fluorescent proteins: Future challenges. *Curr. Opin. Chem. Biol.* **2014**, *20*, 92−102.
(33) Hofmann, M.; Eggeling, C.; Jakobs, S.; Hell, S. W. Breaking the diffraction barrier in fluorescence microscopy at low light intensities by using reversibly photoswitchable proteins. *Proc. Natl. Acad. Sci. U. S. A.* **2005**, *102*, 17565−17569.
(34) Ha, T.; Tinnefeld, P. Photophysics of fluorescent probes for single-molecule biophysics and super-resolution and imaging. *Annu. Rev. Phys. Chem.* **2012**, *63*, 595−617.
(35) Burnette, D. T.; Sengupta, P.; Dai, Y.; Lippincott-Schwartz, J.; Kachar, B. Bleaching/blinking assisted localization microscopy for superresolution imaging using standard fluorescent molecules. *Proc. Natl. Acad. Sci. U. S. A.* **2011**, *108*, 21081−21086.
(36) Nienhaus, K.; Nienhaus, G. U. Fluorescent proteins for live-cell imaging with super-resolution. *Chem. Soc. Rev.* **2014**, *43*, 1088−1106.
(37) Sengupta, P.; van Engelenburg, S. B.; Lippincott-Schwartz, J. Superresolution imaging of biological systems using photoactivated localization microscopy. *Chem. Rev.* **2014**, *114*, 3189−3202.
(38) Bulina, M. E.; Lukyanov, K. A.; Britanova, O. V.; Onichtchouk, D.; Lukyanov, S.; Chudakov, D. M. Chromophore-assisted light inactivation (CALI) using the phototoxic fluorescent protein KillerRed. *Nat. Protoc.* **2006**, *1*, 947−953.
(39) Bogdanov, A. M.; Mishin, A. S.; Yampolsky, I. V.; Belousov, V. V.; Chudakov, D. M.; Subach, F. V.; Verkhusha, V. V.; Lukyanov, S.; Lukyanov, K. A. Green fluorescent proteins are light-induced electron donors. *Nat. Chem. Biol.* **2009**, *5*, 459−461.
(40) Lukyanov, K. A.; Belousov, V. V. Genetically encoded fluorescent redox sensors. *Biochim. Biophys. Acta, Gen. Subj.* **2014**, *1840*, 745−756.
(41) In *Handbook of Single-Molecule Biophysics*; Hinterdorfer, P., van Oijen, A., Eds.; Springer: Dordrecht, Heidelberg, London, New York, 2009.
(42) Lakowicz, J. *Principles of Fluorescence Spectroscopy*, 3rd ed.; Springer: New York, 2009.

DOI: 10.1021/acs.chemrev.6b00238
Chem. Rev. 2017, 117, 758−795

(43) Tiwari, D. K.; Nagai, T. Smart fluorescent proteins: Innovation for barrier-free superresolution imaging in living cells. *Develop. Growth Differ.* **2013**, *55*, 491−507.
(44) Ishikawa-Ankerhold, H. C.; Ankerhold, R.; Drummen, G. P. C. Advanced fluorescent microscopy techniques — FRAP, FLIP, FLAP, FRET and FLIM. *Molecules* **2012**, *17*, 4047−4132.
(45) Takeda, S.; Kamiya, N.; Arai, R.; Nagamune, T. Design of an artificial light-harvesting unit by protein engineering: Cytochrome b_{562} -green fluorescent protein chimera. *Biochem. Biophys. Res. Commun.* **2001**, *289*, 299−304.
(46) Chuang, W.-T.; Chen, B.-S.; Chen, K.-Y.; Hsieh, C.-C.; Chou, P.-T. Fluorescent protein red Kaede chromophore; one-step, high-yield synthesis and potential application for solar cells. *Chem. Commun.* **2009**, 6982−6984.
(47) Chiragwandi, Z. G.; Gillespie, K.; Zhao, Q. X.; Willander, M. Ultraviolet driven negative current and rectifier effect in self-assembled green fluorescent protein device. *Appl. Phys. Lett.* **2006**, *89*, 162909.
(48) Chirgwandi, Z. G.; Panas, I.; Johansson, L. G.; Nordén, B.; Willander, M.; Winkler, D.; Årgen, H. Properties of biophotovoltaic nanodevice. *J. Phys. Chem. C* **2008**, *112*, 18717−18721.
(49) Adam, V.; Mizuno, H.; Grichine, A.; Hotta, J. I.; Yamagata, Y.; Moeyaert, B.; Nienhaus, G. U.; Miyawaki, A.; Bourgeois, D.; Hofkens, J. Data storage based on photochromic and photoconvertible fluorescent proteins. *J. Biotechnol.* **2010**, *149*, 289−298.
(50) Grotjohann, T.; Testa, I.; Leutenegger, M.; Bock, H.; Urban, N. T.; Lavoie-Cardinal, F.; Willig, K. I.; Eggeling, C.; Jakobs, S.; Hell, S. W. Diffraction-unlimited all-optical imaging and writing with a photochromic GFP. *Nature* **2011**, *478*, 204−208.
(51) Shcherbakova, D. M.; Sengupta, P.; Lippincott-Schwartz, J.; Verkhusha, V. V. Photocontrollable fluorescent proteins for super-resolution imaging. *Annu. Rev. Biophys.* **2014**, *43*, 303.
(52) Fernández-Suárez, M.; Ting, A. Y. Fluorescent probes for super-resolution imaging in living cells. *Nat. Rev. Mol. Cell Biol.* **2008**, *9*, 929−943.
(53) Griesbeck, O.; Baird, G. S.; Campbell, R. E.; Zacharias, D. A.; Tsien, R. Y. Reducing the environmental sensitivity of yellow fluorescent protein — mechanism and applications. *J. Biol. Chem.* **2001**, *276*, 29188−29194.
(54) Peterman, E. J. G.; Brasselet, S.; Moerner, W. E. The fluorescence dynamics of single molecules of green fluorescent protein. *J. Phys. Chem. A* **1999**, *103*, 10553−10560.
(55) Heikal, A. A.; Hess, S. T.; Baird, G. S.; Tsien, R. Y.; Webb, W. W. Molecular spectroscopy and dynamics of intrinsically fluorescent proteins: Coral red (dsRed) and yellow (Citrine). *Proc. Natl. Acad. Sci. U. S. A.* **2000**, *97*, 11996−12001.
(56) Garcia-Parajo, M. F.; Segers-Nolten, G. M. J.; Veerman, J. A.; Greve, J.; van Hulst, N. F. Real-time light-driven dynamics of the fluorescence emission in single green fluorescent protein molecules. *Proc. Natl. Acad. Sci. U. S. A.* **2000**, *97*, 7237−7242.
(57) Piatkevich, K. D.; Hulit, J.; Subach, O. M.; Wu, B.; Abdulla, A.; Segall, J. E.; Verkhusha, V. V. Monomeric red fluorescent proteins with a large Stokes shift. *Proc. Natl. Acad. Sci. U. S. A.* **2010**, *107*, 5369−5374.
(58) Abbyad, P.; Childs, W.; Shi, X.; Boxer, S. G. Dynamic Stokes shift in green fluorescent protein variants. *Proc. Natl. Acad. Sci. U. S. A.* **2007**, *104*, 20189−20194.
(59) Topol, I.; Collins, J.; Savitsky, A.; Nemukhin, A. Computational strategy for tuning spectral properties of red fluorescent proteins. *Biophys. Chem.* **2011**, *158*, 91−95.
(60) Chu, J.; Oh, Y.; Sens, A.; Ataie, N.; Dana, H.; Macklin, J. J.; Laviv, T.; Welf, E. S.; Dean, K. M.; Zhang, F.; Kim, B. B.; Tang, C. T.; Hu, M.; Baird, M. A.; Davidson, M. W.; Kay, M. A.; Fiolka, R.; Yasuda, R.; Kim, D. S.; Ng, H.-L.; Lin, M. Z. A bright cyan-excitable orange fluorescent protein facilitates dual-emission microscopy and enhances bioluminescence imaging in vivo. *Nat. Biotechnol.* **2016**, *34*, 760−767.
(61) Chudakov, D. M.; Verkhusha, V. V.; Staroverov, D. B.; Souslova, E. A.; Lukyanov, S.; Lukyanov, K. A. Photoswitchable cyan fluorescent protein for protein tracking. *Nat. Biotechnol.* **2004**, *22*, 1435−1439.
(62) Gurskaya, N. G.; Verkhusha, V. V.; Shcheglov, A. S.; Staroverov, D. B.; Chepurnykh, T. V.; Fradkov, A. F.; Lukyanov, S.; Lukyanov, K. A. Engineering of a monomeric green-to-red photoactivatable fluorescent protein induced by blue light. *Nat. Biotechnol.* **2006**, *24*, 461−465.
(63) Wiedenmann, J.; Ivanchenko, S.; Oswald, F.; Schmitt, F.; Röcker, C.; Salih, A.; Spindler, K.-D.; Nienhaus, G. U. Eosfp, a fluorescent marker protein with UV-inducible green-to-red fluorescence conversion. *Proc. Natl. Acad. Sci. U. S. A.* **2004**, *101*, 15905−15910.
(64) Ando, R.; Hama, H.; Yamamoto-Hino, M.; Mizuno, H.; Miyawaki, A. An optical marker based on the UV-induced green-to-red photoconversion of a fluorescent protein. *Proc. Natl. Acad. Sci. U. S. A.* **2002**, *99*, 12651−12656.
(65) Tsutsui, H.; Karasawa, S.; Shimizu, H.; Nukina, N.; Miyawaki, A. Semi-rational engineering of a coral fluorescent protein into an efficient highlighter. *EMBO Rep.* **2005**, *6*, 233−238.
(66) Fuchs, J.; Böhme, S.; Oswald, F.; Hedde, P. N.; Krause, M.; Wiedenmann, J.; Nienhaus, G. U. A photoactivatable marker protein for pulse-chase imaging with superresolution. *Nat. Methods* **2010**, *7*, 627−630.
(67) Andresen, M.; Stiel, A. C.; Fölling, J.; Wenzel, D.; Schönle, A.; Egner, A.; Eggeling, C.; Hell, S. W.; Jakobs, S. Photoswitchable fluorescent proteins enable monochromatic multilabel imaging and dual color fluorescence nanoscopy. *Nat. Biotechnol.* **2008**, *26*, 1035−1040.
(68) Irie, M. Diarylethenes for memories and switches. *Chem. Rev.* **2000**, *100*, 1685−1716.
(69) Kremers, G.-J.; Hazelwood, K. L.; Murphy, C. S.; Davidson, M. W.; Piston, D. W. Photoconversion in orange and red fluorescent proteins. *Nat. Methods* **2009**, *6*, 355−358.
(70) Zhou, X. X.; Lin, M. Z. Photoswitchable fluorescent proteins: ten years of colorful chemistry and exciting applications. *Curr. Opin. Chem. Biol.* **2013**, *17*, 682−690.
(71) Patterson, G. H.; Lippincott-Schwartz, J. A photoactivatable GFP for selective photolabeling of proteins and cells. *Science* **2002**, *297*, 1873−1877.
(72) Ando, R.; Hama, H.; Yamamoto-Hino, M.; Mizuno, H.; Miyawaki, A. An optical marker based on the UV-induced green-to-red photoconversion of a fluorescent protein. *Proc. Natl. Acad. Sci. U. S. A.* **2002**, *99*, 12651−12656.
(73) Ando, R.; Mizuno, H.; Miyawaki, A. Regulated fast nucleocytoplasmic shuttling observed by reversible protein high-lighting. *Science* **2004**, *306*, 1370−1373.
(74) Chudakov, D. M.; Feofanov, A. V.; Mudrik, N. N.; Lukyanov, S.; Lukyanov, K. A. Chromophore environment provides clue to "kindling fluorescent protein" riddle. *J. Biol. Chem.* **2003**, *278*, 7215−7219.
(75) Brakemann, T.; Stiel, A. C.; Weber, G.; Andresen, M.; Testa, I.; Grotjohann, T.; Leutenegger, M.; Plessmann, U.; Urlaub, H.; Eggeling, C.; Wahl, M. C.; Hell, S. W.; Jakobs, S. A reversibly photoswitchable GFP-like protein with fluorescence excitation decoupled from switching. *Nat. Biotechnol.* **2011**, *29*, 942−947.
(76) Lippincott-Schwartz, J.; Patterson, G. H. Photoactivatable fluorescent proteins for diffraction-limited and super-resolution imaging. *Trends Cell Biol.* **2009**, *19*, 555−565.
(77) Bourgeois, D.; Adam, V. Reversible photoswitching in fluorescent proteins: a mechanistic view. *IUBMB Life* **2012**, *64*, 482−491.
(78) Marchant, J. S.; Stutzmann, G. E.; Leissring, M. A.; LaFerla, F. M.; Parker, I. Multiphoton-evoked color change of DsRed as an optical highlighter for cellular and subcellular labeling. *Nat. Biotechnol.* **2001**, *19*, 645−649.
(79) Berezin, M. Y.; Achilefu, S. Fluorescence lifetime measurements and biological imaging. *Chem. Rev.* **2010**, *110*, 2641−2684.
(80) Sarkisyan, K. S.; Bolotin, D. A.; Meer, M. V.; Usmanova, D. R.; Mishin, A. S.; Sharonov, G. V.; Ivankov, D. N.; Bozhanova, N. G.; Baranov, M. S.; Soylemez, O.; Bogatyreva, N. S.; Vlasov, P. K.; Egorov, E. S.; Logacheva, M. D.; Kondrashov, A. S.; Chudakov, D. M.; Putintseva, E. V.; Mamedov, I. Z.; Tawfik, D. S.; Lukyanov, K. A.;

DOI: 10.1021/acs.chemrev.6b00238
Chem. Rev. 2017, 117, 758−795

Kondrashov, F. A. Local fitness landscape of the green fluorescent protein. *Nature* **2016**, *533*, 397−401.
(81) Patterson, G.; Day, R. N.; Piston, D. Fluorescent protein spectra. *J. Cell Sci.* **2001**, *114*, 837−838.
(82) Nguyen, A. W.; Daugherty, P. S. Evolutionary optimization of fluorescent proteins for intracellular FRET. *Nat. Biotechnol.* **2005**, *23*, 355.
(83) McKinney, S. A.; Murphy, C. S.; Hazelwood, K. L.; Davidson, M. W.; Looger, L. L. A bright and photostable photoconvertible fluorescent protein. *Nat. Methods* **2009**, *6*, 131−133.
(84) Goedhart, J.; von Stetten, D.; Noirclerc-Savoye, M.; Lelimousin, M.; Joosen, L.; Hink, M. A.; van Weeren, L.; Gadella, T. W., Jr; Royant, A. Structure-guided evolution of cyan fluorescent proteins towards a quantum yield of 93%. *Nat. Commun.* **2012**, *3*, 751.
(85) Shu, X.; Shaner, N. C.; Yarbrough, C. A.; Tsien, R. Y.; Remington, S. J. Novel chromophores and buried charges control color in mFruits. *Biochemistry* **2006**, *45*, 9639−9647.
(86) Shcherbakova, D. M.; Hink, M. A.; Joosen, L.; Gadella, T. J., Jr.; Verkhusha, V. V. An orange fluorescent protein with a large Stokes shift for single-excitation multicolor FCCS and FRET imaging. *J. Am. Chem. Soc.* **2012**, *134*, 7913−7923.
(87) Baranov, M. S.; Lukyanov, K. A.; Borissova, A. O.; Shamir, J.; Kosenkov, D.; Slipchenko, L. V.; Tolbert, L. M.; Yampolsky, I. V.; Solntsev, K. M. Conformationally locked chromophores as models of excited-state proton transfer in fluorescent proteins. *J. Am. Chem. Soc.* **2012**, *134*, 6025−6032.
(88) Niwa, H.; Inouye, S.; Hirano, T.; Matsuno, T.; Kojima, S.; Kubota, M.; Ohashi, M.; Tsuji, F. I. Chemical nature of the light emitter of the Aequorea green fluorescent protein. *Proc. Natl. Acad. Sci. U. S. A.* **1996**, *93*, 13617−13622.
(89) Toniolo, A.; Olsen, S.; Manohar, L.; Martinez, T. J. Conical intersection dynamics in solution: The chromophore of green fluorescent protein. *Faraday Discuss.* **2004**, *127*, 149.
(90) Baldridge, A.; Samanta, S. R.; Jayaraj, N.; Ramamurthy, V.; Tolbert, L. M. Steric and electronic effects in capsule-confined green fluorescent protein chromophores. *J. Am. Chem. Soc.* **2011**, *133*, 712−715.
(91) Dolgopolova, E. A.; Rice, A. M.; Smith, M. D.; Shustova, N. B. Photophysics, dynamics, and energy transfer in rigid mimics of GFP-based systems. *Inorg. Chem.* **2016**, *55*, 7257.
(92) Baldridge, A.; Feng, S.; Chang, Y.-T.; Tolbert, L. M. Recapture of GFP chromophore fluorescence in a protein host. *ACS Comb. Sci.* **2011**, *13*, 214−217.
(93) Scheyhing, C. H.; Meersman, F.; Ehrmann, M. A.; Heremans, K.; Vogel, R. F. Temperature-pressure stability of green fluorescent protein: A fourier transform infrared spectroscopy study. *Biopolymers* **2002**, *65*, 244−253.
(94) Ehrmann, M. A.; Scheyhing, C. H.; Vogel, R. F. In vitro stability and expression of green fluorescent protein under high pressure conditions. *Lett. Appl. Microbiol.* **2001**, *32*, 230−234.
(95) Leiderman, P.; Huppert, D.; Remington, S. J.; Tolbert, L. M.; Solntsev, K. M. The effect of pressure on the excited-state proton transfer in the wild-type green fluorescent protein. *Chem. Phys. Lett.* **2008**, *455*, 303−306.
(96) Verkhusha, V. V.; Pozhitkov, A. E.; Smirnov, S. A.; Borst, J. W.; van Hoek, A.; Klyachko, N. L.; Levashov, A. V.; Visser, A. J. W. G. Effect of high pressure and reversed micelles on the fluorescent proteins. *Biochim. Biophys. Acta, Gen. Subj.* **2003**, *1622*, 192−155.
(97) Malavasi, N. V.; Foguel, D.; Bonafe, C. F. S.; Braga, C.; Chura-Chambi, R. M.; Vieira, J. M.; Morganti, L. Protein refolding at high pressure: Optimization using eGFP as a model. *Process Biochem.* **2011**, *46*, 512−518.
(98) Mauring, K.; Krasnenko, V.; Miller, S. Photophysics of the blue fluorescent protein. *J. Lumin.* **2007**, *122-123*, 291−293.
(99) Mauring, K.; Deich, J.; Rosell, F. I.; McAnaney, T. B.; Moerner, W. E.; Boxer, S. G. Enhancement of the fluorescence of the blue fluorescent proteins by high pressure or low temperature. *J. Phys. Chem. B* **2005**, *109*, 12976−12981.
(100) Herberhold, H.; Marchal, S.; Lange, R.; Scheyhing, C. H.; Vogel, R. F.; Winter, R. Characterization of the pressure-induced intermediate and unfolded state of red-shifted green fluorescent protein — A static and kinetic FTIR, UV/VIS and fluorescence spectroscopy study. *J. Mol. Biol.* **2003**, *330*, 1153−1164.
(101) Barstow, B.; Ando, N.; Kim, C. U.; Gruner, S. M. Alteration of citrine structure by hydrostatic pressure explains the accompanying spectral shift. *Proc. Natl. Acad. Sci. U. S. A.* **2008**, *105*, 13362−13366.
(102) Barstow, B.; Ando, N.; Kim, C. U.; Gruner, S. M. Coupling of pressure-induced structural shifts to spectral changes in a yellow fluorescent protein. *Biophys. J.* **2009**, *97*, 1719−1727.
(103) Pozzi, E. A.; Schwall, L. R.; Jimenez, R.; Weber, J. M. Pressure induced changes in the fluorescence behavior of red fluorescent proteins. *J. Phys. Chem. B* **2012**, *116*, 10311−10316.
(104) Laurent, A. D.; Mironov, V. A.; Chapagain, P. P.; Nemukhin, A. V.; Krylov, A. I. Exploring structural and optical properties of fluorescent proteins by squeezing: Modeling high-pressure effects on the mStrawberry and mCherry red fluorescent proteins. *J. Phys. Chem. B* **2012**, *116*, 12426−12440.
(105) Mena, M. A.; Treynor, T. P.; Mayo, S. L.; Daugherty, P. S. Blue fluorescent proteins with enhanced brightness and photostability from a structurally targeted library. *Nat. Biotechnol.* **2006**, *24*, 1569−1571.
(106) Pandelieva, A. T.; Baran, M. J.; Calderini, G. F.; McCann, J. L.; Tremblay, V.; Sarvan, S.; Davey, J. A.; Couture, J.-F.; Chica, R. A. Brighter red fluorescent proteins by rational design of triple-decker motif. *ACS Chem. Biol.* **2016**, *11*, 508−517.
(107) Warner, K. D.; Chen, M. C.; Song, W.; Strack, R. L.; Thorn, A.; Jaffrey, S. R.; Ferré-D'Amaré, A. R. Structural basis for activity of highly efficient RNA mimics of green fluorescent protein. *Nat. Struct. Mol. Biol.* **2014**, *21*, 658−663.
(108) Kremers, G.-J.; van Munster, E. B.; Goedhart, J.; Gadella, T. W. J., Jr Quantitative lifetime unmixing of multiexponentially decaying fluorophores using single-frequency fluorescence lifetime imaging microscopy. *Biophys. J.* **2008**, *95*, 378−389.
(109) Goedhart, J.; van Weeren, L.; Hink, M. A.; Vischer, N. O. E.; Jalink, K.; Gadella, T. W. J., Jr. Bright cyan fluorescent protein variants identified by fluorescence lifetime screening. *Nat. Methods* **2010**, *7*, 137−139.
(110) Sarkisyan, K. S.; Goryashchenko, A. S.; Lidsky, P. V.; Gorbachev, D. A.; Bozhanova, N. G.; Gorokhovatsky, A. Y.; Pereverzeva, A. R.; Ryumina, A. P.; Zherdeva, V. V.; Savitsky, A. P.; Solntsev, K. M.; Bommarius, A. S.; Sharonov, G. V.; Lindquist, J. R.; Drobizhev, M.; Hughes, T. E.; Rebane, A.; Lukyanov, K. A.; Mishin, A. S. Green fluorescent protein with anionic tryptophan-based chromophore and long fluorescence lifetime. *Biophys. J.* **2015**, *109*, 380−389.
(111) Becker, W. Fluorescence lifetime imaging - techniques and applications. *J. Microsc.* **2012**, *247*, 119−136.
(112) Piatkevich, K. D.; Malashkevich, V. N.; Almo, S. C.; Verkhusha, V. V. Engineering ESPT pathways based on structural analysis of LSSmKate red fluorescent proteins with large Stokes shift. *J. Am. Chem. Soc.* **2010**, *132*, 10762−10770.
(113) Faraji, S.; Krylov, A. I. On the nature of an extended Stokes shift in the mPlum fluorescent protein. *J. Phys. Chem. B* **2015**, *119*, 13052−13062.
(114) Piatkevich, K. D.; Malashkevich, V. N.; Morozova, K. S.; Nemkovich, N. A.; Almo, S. C.; Verkhusha, V. V. Extended Stokes shift in fluorescent proteins: Chromophore-protein interactions in a near-infrared TagRFP675 variant. *Sci. Rep.* **2013**, *3*, 1847−1851.
(115) Shu, X.; Wang, L.; Colip, L.; Kallio, K.; Remington, S. J. Unique interactions between the chromophore and glutamate 16 lead to far-red emission in a red fluorescent protein. *Protein Sci.* **2009**, *18*, 460−466.
(116) Konold, P.; Regmi, C. K.; Chapagain, P. P.; Gerstman, B. S.; Jimenez, R. Hydrogen bond flexibility correlates with Stokes shifts in mPlum variants. *J. Phys. Chem. B* **2014**, *118*, 2940−2948.
(117) Konold, P. E.; Jimenez, R. Excited state electronic landscape of mPlum revealed by two-dimensional double quantum coherence spectroscopy. *J. Phys. Chem. B* **2015**, *119*, 3414−3442.

DOI: 10.1021/acs.chemrev.6b00238
Chem. Rev. 2017, 117, 758−795

(118) Yoon, E.; Konold, P. E.; Lee, J.; Joo, T.; Jimenez, R. Far-red emission of mPlum fluorescent protein results from excited-state interconversion between chromophore hydrogen-bonding states. *J. Phys. Chem. Lett.* **2016**, *7*, 2170−2174.
(119) Konold, P. E.; Yoon, E.; Lee, J.; Allen, S.; Chapagain, P. P.; Gerstman, B. S.; Regmi, C. K.; Piatkevich, K. D.; Verkhusha, V. V.; Joo, T.; Jimenez, R. Fluorescence from multiple chromophore hydrogen-bonding states in the far-red protein TagRFP675. *J. Phys. Chem. Lett.* **2016**, *7*, 3046−3051.
(120) Berardozzi, R.; Adam, V.; Martins, A.; Bourgeois, D. Arginine 66 controls dark-state formation in green-to-red photoconvertible fluorescent proteins. *J. Am. Chem. Soc.* **2016**, *138*, 558−565.
(121) Stennett, E. M. S.; Ciuba, M. A.; Levitus, M. Photophysical processes in single molecule organic fluorescent probes. *Chem. Soc. Rev.* **2014**, *43*, 1057−1075.
(122) Moerner, W. E. Single-molecule optical spectroscopy of autofluorescent proteins. *J. Chem. Phys.* **2002**, *117*, 10925.
(123) Andresen, M.; Stiel, A. C.; Trowitzsch, S.; Weber, G.; Eggeling, C.; Wahl, M. C.; Hell, S. W.; Jakobs, S. Structural basis for reversible photoswitching in Dronpa. *Proc. Natl. Acad. Sci. U. S. A.* **2007**, *104*, 13005−13009.
(124) Sinnecker, D.; Voigt, P.; Hellwig, N.; Schaefer, M. Reversible photobleaching of enhanced green fluorescent proteins. *Biochemistry* **2005**, *44*, 7085−7094.
(125) Vegh, R. B.; Solntsev, K. M.; Kuimova, M. K.; Cho, S.; Liang, Y.; Loo, B. L. W.; Tolbert, L. M.; Bommarius, A. S. Reactive oxygen species in photochemistry of the red fluorescent protein "Killer Red. *Chem. Commun.* **2011**, *47*, 4887−4889.
(126) Jimenez-Banzo, A.; Nonell, S.; Hofkens, J.; Flors, C. Singlet oxygen photosensitization by EGFP and its chromophore HBDI. *Biophys. J.* **2008**, *94*, 168.
(127) Jiménez-Banzo, A.; Ragás, X.; Abbruzzetti, S.; Viappiani, C.; Campanini, B.; Flors, C.; Nonell, S. Singlet oxygen photosensitisation by GFP mutants: oxygen accessibility to the chromophore. *Photochem. Photobiol. Sci.* **2010**, *9*, 1336−1341.
(128) Vegh, R. B.; Bravaya, K. B.; Bloch, D. A.; Bommarius, A. S.; Tolbert, L. M.; Verkhovsky, M.; Krylov, A. I.; Solntsev, K. M. Chromophore photoreduction in red fluorescent proteins is responsible for bleaching and phototoxicity. *J. Phys. Chem. B* **2014**, *118*, 4527−4534.
(129) Epifanovsky, E.; Polyakov, I.; Grigorenko, B. L.; Nemukhin, A. V.; Krylov, A. I. The effect of oxidation on the electronic structure of the green fluorescent protein chromophore. *J. Chem. Phys.* **2010**, *132*, 115104.
(130) van Thor, J. J.; Gensch, T.; Hellingwerf, K. J.; Johnson, L. N. Phototransformation of green fluoresecent protein with UV and visible light leads to decarboxilation of glutamate 222. *Nat. Struct. Biol.* **2002**, *9*, 37−41.
(131) Bell, A. F.; Stoner-Ma, D.; Wachter, R. M.; Tonge, P. J. Light-driven decarboxylation of wild-type green fluorescent protein. *J. Am. Chem. Soc.* **2003**, *125*, 6919−6926.
(132) Chapagain, P. P.; Regmi, C. K.; Castillo, W. Fluorescent protein barrel fluctuations and oxygen diffusion pathways in mCherry. *J. Chem. Phys.* **2011**, *135*, 235101.
(133) Roy, A.; Carpentier, P.; Bourgeois, D.; Field, M. Diffusion pathways of oxygen species in the phototoxic fluorescent protein KillerRed. *Photochem. Photobiol. Sci.* **2010**, *9*, 1342−1350.
(134) Park, J. W.; Rhee, Y. M. Emission shaping in fluorescent proteins: role of electrostatics and π-stacking. *Phys. Chem. Chem. Phys.* **2016**, *18*, 3944−3955.
(135) Armengol, P.; Gelabert, R.; Moreno, M.; Lluch, J. M. Chromophore interactions leading to different absorption spectra in mNeptune1 and mCardinal red fluorescent proteins. *Phys. Chem. Chem. Phys.* **2016**, *18*, 16964−16976.
(136) Ong, W. J.-H.; Alvarez, S.; Leroux, I. E.; Shahid, R. S.; Samma, A. A.; Peshkepija, P.; Morgan, A. L.; Mulcahy, S.; Zimmer, M. Function and structure of GFP-like proteins in the protein data bank. *Mol. BioSyst.* **2011**, *7*, 984−922.
(137) Royant, A.; Noirclerc-Savoye, M. Stabilizing role of glutamic acid 222 in the structure of enhanced green fluorescent protein. *J. Struct. Biol.* **2011**, *174*, 385−390.
(138) Henderson, J. N.; Remington, S. J. The kindling fluorescent protein: A transient photoswitchable marker. *Physiology* **2006**, *21*, 162−170.
(139) Pletneva, N. V.; Pletnev, V. Z.; Shemiakina, I. I.; Chudakov, D. M.; Artemyev, I.; Wlodawer, A.; Dauter, Z.; Pletnev, S. Crystallographic study of red fluorescent protein eqFP578 and its far-red variant katushka reveals opposite pH-induced isomerization of chromophore. *Protein Sci.* **2011**, *20*, 1265−1274.
(140) Petersen, J.; Wilmann, P. G.; Beddoe, T.; Oakley, A. J.; Devenish, R. J.; Prescott, M.; Rossjohn, J. The 2.0-Å crystal structure of eqFP611, a far red fluorescent protein from the sea anemone Entacmaea quadricolor. *J. Biol. Chem.* **2003**, *278*, 44626−44631.
(141) Åqvist, J.; Warshel, A. Simulation of enzyme reactions using valence bond force fields and other hybrid quantum/classical approaches. *Chem. Rev.* **1993**, *93*, 2523−2544.
(142) Sham, Y. Y.; Chu, Z. T.; Warshel, A. Consistent calculations of pK_a's of ionizable residues in proteins: semi-microscopic and macroscopic approaches. *J. Phys. Chem. B* **1997**, *101*, 4458−4472.
(143) Brakemann, T.; Weber, G.; Andresen, M.; Groenhof, G.; Stiel, A. C.; Trowitzsch, S.; Eggeling, C.; Grubmüller, H.; Hell, S. W.; Wahl, M. C.; Jakobs, S. Molecular basis of the light-driven switching of the photochromic fluorescent protein Padron. *J. Biol. Chem.* **2010**, *285*, 14603−14609.
(144) Bravaya, K. B.; Subach, O. M.; Korovina, N.; Verkhusha, V. V.; Krylov, A. I. Insight into the common mechanism of the chromophore formation in the red fluorescent proteins: The elusive blue intermediate revealed. *J. Am. Chem. Soc.* **2012**, *134*, 2807−2814.
(145) Bogdanov, A. M.; Acharya, A.; Titelmayer, A. V.; Mamontova, A. V.; Bravaya, K. B.; Kolomeisky, A. B.; Lukyanov, K. A.; Krylov, A. I. Turning on and off photoinduced electron transfer in fluorescent proteins by π-stacking, halide binding, and Tyr145 mutations. *J. Am. Chem. Soc.* **2016**, *138*, 4807−4817.
(146) Mironov, V. A.; Khrenova, M. G.; Grigorenko, B. L.; Savitsky, A. P.; Nemukhin, A. V. Thermal isomerization of the chromoprotein asFP595 and its kindling mutant A143G: QM/MM molecular dynamics simulations. *J. Phys. Chem. B* **2013**, *117*, 13507−13514.
(147) Voityuk, A. A.; Michel-Beyerle, M.-E.; Rösch, N. Protonation effects on the chromophore of green fluorescent protein. Quantum chemical study of the absorption spectrum. *Chem. Phys. Lett.* **1997**, *272*, 162−167.
(148) Weber, W.; Helms, V.; McCammon, J. A.; Langhoff, P. W. Shedding light on the dark and weakly fluorescent states of green fluorescent proteins. *Proc. Natl. Acad. Sci. U. S. A.* **1999**, *96*, 6177−6182.
(149) Bell, A. F.; He, X.; Wachter, R. M.; Tonge, P. J. Probing the ground state structure of the green fluorescent protein chromophore using Raman spectroscopy. *Biochemistry* **2000**, *39*, 4423−4431.
(150) Schüttrigkeit, T. A.; von Feilitzsch, T.; Kompa, C. K.; Lukyanov, K. A.; Savitsky, A. P.; Voityuk, A. A.; Michel-Beyerle, M.-E. Femtosecond study of light-induced fluorescence increase of the dark chromoprotein asFP595. *Chem. Phys.* **2006**, *323*, 149−160.
(151) Subach, O. M.; Malashkevich, V. N.; Zencheck, W. D.; Morozova, K. S.; Piatkevich, K. D.; Almo, S. C.; Verkhusha, V. V. Structural characterization of acylimine-containing blue and red chromophore in mTagBFP and TagRFP fluorescent proteins. *Chem. Biol.* **2010**, *17*, 333−341.
(152) Subach, F. V.; Malashkevich, V. N.; Zencheck, W. D.; Xiao, H.; Filonov, G. S.; Almo, S. C.; Verkhusha, V. V. Photoactivation mechanism of PAmCherry based on crystal structures of the protein in the dark and fluorescent states. *Proc. Natl. Acad. Sci. U. S. A.* **2009**, *106*, 21097−21102.
(153) Verkhusha, V. V.; Chudakov, D. M.; Gurskaya, N. G.; Lukyanov, S.; Lukyanov, K. A. Common pathway for the red chromophore formation in fluorescent proteins and chromoproteins. *Chem. Biol.* **2004**, *11*, 845−854.

DOI: 10.1021/acs.chemrev.6b00238
Chem. Rev. 2017, 117, 758−795

(154) Pletnev, S.; Subach, F. V.; Dauter, Z.; Wlodawer, A.; Verkhusha, V. V. Understanding blue-to-red conversion in monomeric fluorescent timers and hydrolytic degradation of their chromophores. *J. Am. Chem. Soc.* **2010**, *132*, 2243−2253.
(155) Subach, O. M.; Gundorov, I. S.; Yoshimura, M.; Subach, F. V.; Zhang, J.; Grüenwald, D.; Souslova, E. A.; Chudakov, D. M.; Verkhusha, V. V. Conversion of red fluorescent protein into a bright blue probe. *Chem. Biol.* **2008**, *15*, 1116−1124.
(156) Roy, A.; Field, M. J.; Adam, V.; Bourgeois, D. The nature of transient dark states in a photoactivatable fluorescent protein. *J. Am. Chem. Soc.* **2011**, *133*, 18586−18589.
(157) Grigorenko, B. L.; Nemukhin, A. V.; Morozov, D. I.; Polyakov, I. V.; Bravaya, K. B.; Krylov, A. I. Toward molecular-level characterization of photo-induced decarboxylation of the green fluorescent protein: Accessibility of the charge-transfer states. *J. Chem. Theory Comput.* **2012**, *8*, 1912−1920.
(158) Habuchi, S.; Cotlet, M.; Gensch, T.; Bednarz, T.; Haber-Pohlmeier, S.; Rozenski, J.; Dirix, G.; Michiels, J.; Vanderleyden, J.; Heberle, J.; De Schryver, F. C.; Hofkens, J. Evidence for the isomerization and decarboxylation in the photoconversion of the red fluorescent protein DsRed. *J. Am. Chem. Soc.* **2005**, *127*, 8977−8984.
(159) Elowitz, M. B.; Surette, M. G.; Wolf, P.-E.; Stock, J.; Leibler, S. Photoactivation turns green fluorescent protein red. *Curr. Biol.* **1997**, *7*, 809−812.
(160) Gray, H. B.; Winkler, J. R. Electron tunneling through proteins. *Q. Rev. Biophys.* **1999**, *36*, 341−372.
(161) Gray, H. B.; Winkler, J. R. Long-range electron transfer. *Proc. Natl. Acad. Sci. U. S. A.* **2005**, *102*, 3534−3539.
(162) Warren, J. J.; Ener, M. E.; Vlček, A., Jr.; Winkler, J. R.; Gray, H. B. Electron hopping through proteins. *Coord. Chem. Rev.* **2012**, *256*, 2478−2487.
(163) Solntsev, K. M.; Ghosh, D.; Amador, A.; Josowicz, M.; Krylov, A. I. What drives the redox properties of model green fluorescence protein chromophores? *J. Phys. Chem. Lett.* **2011**, *2*, 2593−2597.
(164) Bravaya, K. B.; Khrenova, M. G.; Grigorenko, B. L.; Nemukhin, A. V.; Krylov, A. I. Effect of protein environment on electronically excited and ionized states of the green fluorescent protein chromophore. *J. Phys. Chem. B* **2011**, *115*, 8296−8303.
(165) Ghosh, D.; Acharya, A.; Tiwari, S. C.; Krylov, A. I. Towards understanding the redox properties of model chromophores from the green fluorescent protein family: An interplay between conjugation, resonance stabilization, and solvent effects. *J. Phys. Chem. B* **2012**, *116*, 12398−12405.
(166) Olsson, M. H. M.; Hong, G.; Warshel, A. Frozen density functional free energy simulations of redox proteins: Computational studies of the reduction potential of plastocyanin and rusticyanin. *J. Am. Chem. Soc.* **2003**, *125*, 5025−5039.
(167) Isse, A. A.; Gennaro, A. Absolute potential of the standard hydrogen electrode and the problem of interconversion of potentials in different solvents. *J. Phys. Chem. B* **2010**, *114*, 7894−7899.
(168) Lazzari-Dean, J.; Krylov, A. I.; Bravaya, K. B. The effects of resonance delocalization and the extent of π-system on ionization energies of model fluorescent proteins chromophores. *Int. J. Quantum Chem.* **2015**, *115*, 1258−1264.
(169) Wittekindt, C.; Schwarz, M.; Friedrich, T.; Koslowski, T. Aromatic amino acids as stepping stones in charge transfer in respiratory complex I: An unusual mechanism deduced from atomistic theory and bioinformatics. *J. Am. Chem. Soc.* **2009**, *131*, 8134−8140.
(170) Gray, H. B.; Winkler, J. R. Hole hopping through tyrosine/tryptophan chains protects proteins from oxidative damage. *Proc. Natl. Acad. Sci. U. S. A.* **2015**, *112*, 10920−10925.
(171) Ding, L.; Chung, L. W.; Morokuma, K. Reaction mechanism of photoinduced decarboxylation of the photoactivatable green fluorescent protein: an ONIOM(QM:MM) study. *J. Phys. Chem. B* **2013**, *117*, 1075−1084.
(172) Grigorenko, B. L.; Nemukhin, A. V.; Polyakov, I. V.; Khrenova, M. G.; Krylov, A. I. A light-induced reaction with oxygen leads to chromophore decomposition and irreversible photobleaching in GFP-type proteins. *J. Phys. Chem. B* **2015**, *119*, 5444−5452.
(173) van Thor, J. J.; Sage, J. T. Charge transfer in green fluorescent protein. *Photochem. Photobiol. Sci.* **2006**, *5*, 597−602.
(174) Simkovitch, R.; Huppert, A.; Huppert, D.; Remington, S. J.; Miller, Y. Proton transfer in wild-type GFP and S205V mutant is reduced by conformational changes of residues in the proton wire. *J. Phys. Chem. B* **2013**, *117*, 11921−11931.
(175) Wineman-Fisher, V.; Simkovitch, R.; Shomer, S.; Gepshtein, R.; Huppert, D.; Saif, M.; Kallio, K.; Remington, S. J.; Miller, Y. Insight into the structure and the mechanism of the slow proton transfer in the GFP double mutant T203V/S205A. *Phys. Chem. Chem. Phys.* **2014**, *16*, 11211−11223.
(176) Chattoraj, M.; King, B. A.; Bublitz, G. U.; Boxer, S. G. Ultra-fast excited state dynamics in green fluorescent protein: Multiple states and proton transfer. *Proc. Natl. Acad. Sci. U. S. A.* **1996**, *93*, 8362−8367.
(177) Brejc, K.; Sixma, T. K.; Kitts, P. A.; Kain, S. R.; Tsien, R. Y.; Ormö, M.; Remington, S. J. Structural basis for dual excitation and photoisomerization of the Aequorea victoria green fluorescent protein. *Proc. Natl. Acad. Sci. U. S. A.* **1997**, *94*, 2306−2311.
(178) Remington, S. J. Green fluorescent protein: A perspective. *Protein Sci.* **2011**, *20*, 1509−1519.
(179) Grigorenko, B. L.; Nemukhin, A. V.; Polyakov, I. V.; Morozov, D. I.; Krylov, A. I. First-principle characterization of the energy landscape and optical spectra of the green fluorescent protein along A-I-B proton transfer route. *J. Am. Chem. Soc.* **2013**, *135*, 11541−11549.
(180) Tolbert, L. M.; Solntsev, K. M. Excited-state proton transfer: From constrained systems to "super" photoacids to superfast proton transfer. *Acc. Chem. Res.* **2002**, *35*, 19−27.
(181) Scharnagl, C.; Raupp-Kossmann, R. A. Solution pKa values of the green fluorescent protein chromophore from hybrid quantum-classical calculations. *J. Phys. Chem. B* **2004**, *108*, 477−489.
(182) Armengol, P.; Gelabert, R.; Moreno, M.; Lluch, J. M. Unveiling how an archetypal fluorescent protein operates: Theoretical perspective on the ultrafast excited state dynamics of GFP variant S65T/H148D. *J. Phys. Chem. B* **2015**, *119*, 2274−2291.
(183) Fang, C.; Frontiera, R. R.; Tran, R.; Mathies, R. A. Mapping GFP structure evolution during proton transfer with femtosecond Raman spectroscopy. *Nature* **2009**, *462*, 200−204.
(184) Vendrell, O.; Gelabert, R.; Moreno, M.; Lluch, J. M. Photoinduced proton transfer from the green fluorescent protein chromophore to a water molecule: analysis of the transfer coordinate. *Chem. Phys. Lett.* **2004**, *396*, 202−207.
(185) Vendrell, O.; Gelabert, R.; Moreno, M.; Lluch, J. M. Potential energy landscape of the photoinduced multiple proton-transfer process in the green fluorescent protein: Classical molecular dynamics and multiconfigurational electronic structure calculations. *J. Am. Chem. Soc.* **2006**, *128*, 3564−3574.
(186) Vendrell, O.; Gelabert, R.; Moreno, M.; Lluch, J. M. Operation of the proton wire in green fluorescent protein. A quantum dynamics simulation. *J. Phys. Chem. B* **2008**, *112*, 5500−5511.
(187) Kennis, J. T. M.; van Stokkum, I. H. M.; Peterson, D. S.; Pandit, A.; Wachter, R. M. Ultrafast proton shuttling in psammocora cyan fluorescent protein. *J. Phys. Chem. B* **2013**, *117*, 11134−11143.
(188) Di Donato, M.; van Wilderen, L. J. G. W.; Van Stokkum, I. H. M.; Stuart, T. C.; Kennis, J. T. M.; Hellingwerf, K. J.; van Grondelle, R.; Groot, M. L. Proton transfer events in GFP. *Phys. Chem. Chem. Phys.* **2011**, *13*, 16295−16305.
(189) Piatkevich, K. D.; English, B. P.; Malashkevich, V. N.; Xiao, H.; Almo, S. C.; Singer, R. H.; Verkhusha, V. V. Photoswitchable red fluorescent protein with a large Stokes shift. *Chem. Biol.* **2014**, *21*, 1402−1414.
(190) Randino, C.; Moreno, M.; Gelabert, R.; Lluch, J. M. Peek at the potential energy surfaces of the LSSmKate1 and LSSmKate2 proteins. *J. Phys. Chem. B* **2012**, *116*, 14302−14310.
(191) Fron, E.; De Keersmaecker, H.; Rocha, S.; Baeten, Y.; Lu, G.; Uji-i, H.; Van der Auweraer, M.; Hofkens, J.; Mizuno, H. Mechanism behind the apparent large stokes shift in LSSmOrange investigated by time-resolved spectroscopy. *J. Phys. Chem. B* **2015**, *119*, 14880−14891.

DOI: 10.1021/acs.chemrev.6b00238
Chem. Rev. 2017, 117, 758−795

(192) Mathes, T.; Zhu, J. Y.; van Stokkum, I. H. M.; Groot, M. L.; Hegemann, P.; Kennis, J. T. M. Hydrogen bond switching among flavin and amino acids determines the nature of proton-coupled electron transfer in BLUF photoreceptors. *J. Phys. Chem. Lett.* **2012**, *3*, 203−208.
(193) Goyal, P.; Schwerdtfeger, C. A.; Soudackov, A. V.; Hammes-Schiffer, S. Nonadiabatic dynamics of photoinduced proton-coupled electron transfer in a solvated phenol-amine complex. *J. Phys. Chem. B* **2015**, *119*, 2758−2768.
(194) Michl, J.; Bonačić-Koutecký, V. *Electronic Aspects of Organic Photochemistry*; Wiley: New York, 1990.
(195) Ernst, O. P.; Lodowski, D. T.; Elstner, M.; Hegemann, P.; Brown, L. S.; Kandori, H. Microbial and animal rhodopsins: Structures, functions, and molecular mechanisms. *Chem. Rev.* **2014**, *114*, 126−163.
(196) Deisseroth, K. Optogenetics: 10 years of microbial opsins in neuroscience. *Nat. Neurosci.* **2015**, *18*, 1213−1225.
(197) McIsaac, R. S.; Bedbrook, C. N.; Arnold, F. H. Recent advances in engineering microbial rhodopsins for optogenetics. *Curr. Opin. Struct. Biol.* **2015**, *33*, 8−15.
(198) Habuchi, S.; Ando, R.; Dedecker, P.; Verheijen, W.; Mizuno, H.; Miyawaki, A.; Hofkens, J. Reversible single-molecule photoswitching in the GFP-like fluorescent protein Dronpa. *Proc. Natl. Acad. Sci. U. S. A.* **2005**, *102*, 9511−9516.
(199) Habuchi, S.; Dedecker, P.; Hotta, J.-I.; Flors, C.; Ando, R.; Mizuno, H.; Miyawaki, A.; Hofkens, J. Photo-induced protonation/deprotonation in the GFP-like fluorescent protein Dronpa: Mechanism responsible for the reversible photoswitching. *Photochem. Photobiol. Sci.* **2006**, *5*, 567−576.
(200) Mizuno, H.; Mal, T. K.; Wälchli, M.; Kikuchi, A.; Fukano, T.; Ando, R.; Jeyakanthan, J.; Taka, J.; Shiro, Y.; Ikura, M.; Miyawaki, A. Light-dependent regulation of structural flexibility in a photochromic fluorescent protein. *Proc. Natl. Acad. Sci. U. S. A.* **2008**, *105*, 9227−9232.
(201) Mizuno, H.; Mal, T. K.; Wälchli, M.; Fukano, T.; Ikura, M.; Miyawaki, A. Molecular basis of photochromism of a fluorescent protein revealed by direct ^{13}C detection under laser illumination. *J. Biomol. NMR* **2010**, *48*, 237−246.
(202) Zhou, X. X.; Chung, H. K.; Lam, A. J.; Lin, M. Z. Optical control of protein activity by fluorescent protein domains. *Science* **2012**, *338*, 810−814.
(203) Warren, M. M.; Kaucikas, M.; Fitzpatrick, A.; Champion, P.; Sage, J. T.; van Thor, J. J. Ground-state proton transfer in the photoswitching reactions of the fluorescent protein Dronpa. *Nat. Commun.* **2013**, *4*, 1461.
(204) Higashino, A.; Mizuno, M.; Mizutani, Y. Chromophore structure of photochromic fluorescent protein Dronpa: Acid-base equilibrium of two cis configurations. *J. Phys. Chem. B* **2016**, *120*, 3353−3359.
(205) Fron, E.; Van der Auweraer, M.; Hofkens, J.; Dedecker, P. Excited state dynamics of photoswitchable fluorescent protein Padron. *J. Phys. Chem. B* **2013**, *117*, 16422−16427.
(206) Faro, A. R.; Carpentier, P.; Jonasson, G.; Pompidor, G.; Arcizet, D.; Demachy, I.; Bourgeois, D. Low-temperature chromophore isomerization reveals the photoswitching mechanism of the fluorescent protein Padron. *J. Am. Chem. Soc.* **2011**, *133*, 16362−16365.
(207) Yadav, D.; Lacombat, F.; Dozova, N.; Rappaport, F.; Plaza, P.; Espagne, A. Real-time monitoring of chromophore isomerization and deprotonation during the photoactivation of the fluorescent protein Dronpa. *J. Phys. Chem. B* **2015**, *119*, 2404−2414.
(208) Walter, A.; Andresen, M.; Jakobs, S.; Schroeder, J.; Schwarzer, D. Primary light-induced reaction steps of reversibly photoswitchable fluorescent protein Padron0.9 investigated by femtosecond spectroscopy. *J. Phys. Chem. B* **2015**, *119*, 5136−5144.
(209) Maddalo, S. L.; Zimmer, M. The role of the protein matrix in green fluorescent protein fluorescence. *Photochem. Photobiol.* **2006**, *82*, 367−372.
(210) Morozov, D.; Groenhof, G. Hydrogen bond fluctuations control photo-switching in a reversibly photo-switchable fluorescent protein. *Angew. Chem., Int. Ed.* **2016**, *55*, 576−578.
(211) Warshel, A. Bicycle-pedal model for the first step in the vision process. *Nature* **1976**, *260*, 679.
(212) Martin, M. E.; Negri, F.; Olivucci, M. Origin, nature, and fate of the fluorescent state of the green fluorescent protein chromophore at the CASPT2//CASSCF resolution. *J. Am. Chem. Soc.* **2004**, *126*, 5452−5464.
(213) Altoe, P.; Bernardi, F.; Garavelli, M.; Orlandi, G.; Negri, F. Solvent effects on the vibrational activity and photodynamics of the green fluorescent protein chromophore: A quantum-chemical study. *J. Am. Chem. Soc.* **2005**, *127*, 3952−3963.
(214) Olsen, S.; Smith, S. C. Bond selection in the photoisomerization reaction of anionic green fluorescent protein and kindling fluorescent protein chromophore models. *J. Am. Chem. Soc.* **2008**, *130*, 8677−8689.
(215) Polyakov, I. V.; Grigorenko, B. L.; Epifanovsky, E. M.; Krylov, A. I.; Nemukhin, A. V. Potential energy landscape of the electronic states of the GFP chromophore in different protonation forms: Electronic transition energies and conical intersections. *J. Chem. Theory Comput.* **2010**, *6*, 2377−2387.
(216) Grigorenko, B. L.; Nemukhin, A. V.; Polyakov, I. V.; Krylov, A. I. Triple-decker motif for red-shifted fluorescent protein mutants. *J. Phys. Chem. Lett.* **2013**, *4*, 1743−1747.
(217) Megley, C. M.; Dickson, L. A.; Maddalo, S. L.; Chandler, G. J.; Zimmer, M. Photophysics and dihedral freedom of the chromophore in yellow, blue, and green fluorescent protein. *J. Phys. Chem. B* **2009**, *113*, 302−308.
(218) Faro, A. R.; Adam, V.; Carpentier, P.; Darnault, C.; Bourgeois, D.; de Rosny, E. Low-temperature switching by photoinduced protonation in photochromic fluorescent proteins. *Photochem. Photobiol. Sci.* **2010**, *9*, 254−262.
(219) Smyrnova, D.; Moeyaert, B.; Michielssens, S.; Hofkens, J.; Dedecker, P.; Ceulemans, A. Molecular dynamic indicators of the photoswitching properties of green fluorescent proteins. *J. Phys. Chem. B* **2015**, *119*, 12007−12016.
(220) Kao, Y.-T.; Zhu, X.; Min, W. Protein-flexibility mediated coupling between photoswitching kinetics and surrounding viscosity of a photochromic fluorescent protein. *Proc. Natl. Acad. Sci. U. S. A.* **2012**, *109*, 3220−3225.
(221) Quillin, M. L.; Anstrom, D. M.; Shu, X.; O'Leary, S.; Kallio, K.; Chudakov, D. M.; Remington, S. J. Kindling fluorescent protein from anemonia sulcata: Dark-state structure at 1.38 Å. *Biochemistry* **2005**, *44*, 5774−5787.
(222) Lukyanov, K. A.; Fradkov, A. F.; Gurskaya, N. G.; Matz, M. V.; Labas, Y. A.; Savitsky, A. P.; Markelov, M. L.; Zaraisky, A. G.; Zhao, X.; Fang, Y.; Tan, W.; Lukyanov, S. A. Natural animal coloration can be determined by a nonfluorescent green fluorescent protein homolog. *J. Biol. Chem.* **2000**, *275*, 25879−25882.
(223) Andresen, M.; Wahl, M. C.; Stiel, A. C.; Gräter, F.; Schäfer, L. V.; Trowitzsch, S.; Weber, G.; Eggeling, C.; Grubmüller, H.; Hell, S. W.; Jakobs, S. Structure and mechanism of the reversible photoswitch of a fluorescent protein. *Proc. Natl. Acad. Sci. U. S. A.* **2005**, *102*, 13070−13074.
(224) Mironov, V. A.; Bravaya, K. B.; Nemukhin, A. V. Role of zwitterions in kindling fluorescent protein photochemistry. *J. Phys. Chem. B* **2015**, *119*, 2467−2474.
(225) Schäfer, L. V.; Groenhof, G.; Klingen, A. R.; Ullmann, G. M.; Boggio-Pasqua, M.; Robb, M. A.; Grubmüller, H. Photoswitching of the fluorescent protein asFP595: Mechanism, proton pathways, and absorption spectra. *Angew. Chem., Int. Ed.* **2007**, *46*, 530−536.
(226) Schäfer, L. V.; Groenhof, G.; Boggio-Pasqua, M.; Robb, M. A.; Grubmüller, H. Chromophore protonation state controls photoswitching of the fluoroprotein asFP595. *PLoS Comput. Biol.* **2008**, *4*, e1000034.
(227) Grigorenko, B.; Savitsky, A.; Topol, I.; Burt, S.; Nemukhin, A. Ground-state structures and vertical excitations for the kindling

DOI: 10.1021/acs.chemrev.6b00238
Chem. Rev. 2017, 117, 758−795

fluorescent protein asFP595. *J. Phys. Chem. B* **2006**, *110*, 18635−18640.
(228) Grigorenko, B.; Savitsky, A.; Topol, I.; Burt, S.; Nemukhin, A. Trans and cis chromophore structures in the kindling fluorescent protein asFP595. *Chem. Phys. Lett.* **2006**, *424*, 184−188.
(229) Bravaya, K. B.; Bochenkova, A. V.; Granovsky, A. A.; Savitsky, A. P.; Nemukhin, A. V. Modeling photoabsorption of the asFP595 chromophore. *J. Phys. Chem. A* **2008**, *112*, 8804−8810.
(230) Nemukhin, A. V.; Topol, I. A.; Grigorenko, B. L.; Savitsky, A. P.; Collins, J. R. Conformation dependence of pKa's of the chromophores from the purple asFP595 and yellow zFP538 fluorescent proteins. *J. Mol. Struct.: THEOCHEM* **2008**, *863*, 39−43.
(231) Topol, I.; Collins, J.; Nemukhin, A. Modeling structures and spectra of fluorescent proteins in the coordinate-locking cluster approach: Application to the photoswitchable protein asFP595. *Comput. Mol. Biosci.* **2012**, *2*, 83−91.
(232) Rusanov, A. L.; Mironov, V. A.; Goryashenko, A. S.; Grigorenko, B. L.; Nemukhin, A. V.; Savitsky, A. P. Conformational partitioning in pH-induced fluorescence of the kindling fluorescent protein (KFP). *J. Phys. Chem. B* **2011**, *115*, 9195−9201.
(233) Duan, C.; Adam, V.; Byrdin, M.; Ridard, J.; Kieffer-Jaquinod, S.; Morlot, C.; Arcizet, D.; Demachy, I.; Bourgeois, D. Structural evidence for a two-regime photobleaching mechanism in a reversibly switchable fluorescent protein. *J. Am. Chem. Soc.* **2013**, *135*, 15841−15850.
(234) Grigorenko, B. L.; Polyakov, I. V.; Savitsky, A. P.; Nemukhin, A. V. Unusual emitting states of the kindling fluorescent protein: Appearance of the cationic chromophore in the GFP family. *J. Phys. Chem. B* **2013**, *117*, 7228−7234.
(235) Betzig, E.; Patterson, G. H.; Sougrat, R.; Lindwasser, O. W.; Olenych, S.; Bonifacino, J. S.; Davidson, M. W.; Lippincott-Schwartz, J.; Hess, H. F. Imaging intracellular fluorescent proteins at nanometer resolution. *Science* **2006**, *313*, 1642−1645.
(236) Hess, S. T.; Girirajan, T. P.; Mason, M. D. Ultra-high resolution imaging by fluorescence photoactivation localization microscopy. *Biophys. J.* **2006**, *91*, 4258−4272.
(237) Rust, M. J.; Bates, M.; Zhuang, X. Sub-diffraction-limit imaging by stochastic optical reconstruction microscopy (STORM). *Nat. Methods* **2006**, *3*, 793−795.
(238) Grotjohann, T.; Testa, I.; Reuss, M.; Brakemann, T.; Eggeling, C.; Hell, S. W.; Jakobs, S. rsEGFP2 enables fast RESOLFT nanoscopy of living cells. *eLife* **2012**, *1*, e00248.
(239) Haupts, U.; Maiti, S.; Schwille, P.; Webb, W. W. Dynamics of fluorescence fluctuations in green fluorescent protein observed by fluorescence correlation spectroscopy. *Proc. Natl. Acad. Sci. U. S. A.* **1998**, *95*, 13573−13578.
(240) Liu, Y.; Kim, H.-R.; Heikal, A. A. Structural basis of fluorescence fluctuation dynamics of green fluorescent proteins in acidic environments. *J. Phys. Chem. B* **2006**, *110*, 24138−24146.
(241) Schenk, A.; Ivanchenko, S.; Röcker, C.; Wiedenmann, J.; Nienhaus, G. U. Photodynamics of red fluorescent proteins studied by fluorescence correlation spectroscopy. *Biophys. J.* **2004**, *86*, 384−394.
(242) David, C. C.; Dedecker, P.; De Cremer, G.; Verstraeten, N.; Kint, C.; Michiels, J.; Hofkens, J. Spectroscopic characterization of venus at the single molecule level. *Photochem. Photobiol. Sci.* **2012**, *11*, 358−363.
(243) Annibale, P.; Scarselli, M.; Kodiyan, A.; Radenovic, A. Photoactivatable fluorescent protein mEos2 displays repeated photoactivation after a long-lived dark state in the red photoconverted form. *J. Phys. Chem. Lett.* **2010**, *1*, 1506.
(244) Shaner, N. C.; Lin, M. Z.; McKeown, M. R.; Steinbach, P. A.; Hazelwood, K. L.; Davidson, M. W.; Tsien, R. Y. Improving the photostability of bright monomeric orange and red fluorescent proteins. *Nat. Methods* **2008**, *5*, 545−551.
(245) McAnaney, T. B.; Zeng, W.; Doe, C. F. E.; Bhanji, N.; Wakelin, S.; Pearson, D. S.; Abbyad, P.; Shi, X.; Boxer, S. G.; Bagshaw, C. R. Protonation, photobleaching, and photoactivation of yellow fluorescent protein (YFP 10C): A unifying mechanism. *Biochemistry* **2005**, *44*, 5510−5524.
(246) Adam, V.; Carpentier, P.; Violot, S.; Lelimousin, M.; Darnault, C.; Nienhaus, G. U.; Bourgeois, D. Structural basis of X-ray induced transient photobleaching in a photactivable green fluorescent protein. *J. Am. Chem. Soc.* **2009**, *131*, 18063−18065.
(247) Wong, F. H. C.; Banks, D. S.; Abu-Arish, A.; Fradin, C. A molecular thermometer based on fluorescent protein blinking. *J. Am. Chem. Soc.* **2007**, *129*, 10302.
(248) Dertinger, T.; Colyer, R.; Iyer, G.; Weiss, S.; Enderlein, J. Fast, background-free, 3D super-resolution optical fluctuation imaging (SOFI). *Proc. Natl. Acad. Sci. U. S. A.* **2009**, *106*, 22287−22292.
(249) Dertinger, T.; Colyer, R.; Vogel, R.; Enderlein, J.; Weiss, S. Achieving increased resolution and more pixels with Superresolution Optical Fluctuation Imaging (SOFI). *Opt. Express* **2010**, *18*, 18875−18885.
(250) Geissbuehler, S.; Dellagiacoma, C.; Lasser, T. Comparison between SOFI and STORM. *Biomed. Opt. Express* **2011**, *2*, 408−420.
(251) Gabor, K. A.; Kim, D.; Kim, C. H.; Hess, S. T. Nanoscale imaging of caveolin-1 membrane domains in vivo. *PLoS One* **2015**, *10*, e0117225.
(252) Jablonski, A. E.; Hsiang, J.-C.; Bagchi, P.; Hull, N.; Richards, C. I.; Fahrni, C. J.; Dickson, R. M. Signal discrimination between fluorescent proteins in live cells by long-wavelength optical modulation. *J. Phys. Chem. Lett.* **2012**, *3*, 3585−3591.
(253) Jablonski, A. E.; Vegh, R. B.; Hsiang, J.-C.; Bommarius, B.; Chen, Y.-C.; Solntsev, K. M.; Bommarius, A. S.; Tolbert, L. M.; Dickson, R. M. Optically modulatable blue fluorescent protein. *J. Am. Chem. Soc.* **2013**, *135*, 16410−16417.
(254) Dempsey, W. P.; Georgieva, L.; Helbling, P. M.; Sonay, A. Y.; Truong, T. V.; Haffner, M.; Pantazis, P. In vivo single-cell labeling by confined primed conversion. *Nat. Methods* **2015**, *12*, 645−648.
(255) Bulina, M. E.; Chudakov, D. M.; Britanova, O. V.; Yanushevich, Y. G.; Staroverov, D. B.; Chepurnykh, T. V.; Merzlyak, E. M.; Shkrob, M. A.; Lukyanov, S.; Lukyanov, K. A. A genetically encoded photosensitizer. *Nat. Biotechnol.* **2006**, *24*, 95−99.
(256) Takemoto, K.; Matsuda, T.; Sakai, N.; Fu, D.; Noda, M.; Uchiyama, S.; Kotera, I.; Arai, Y.; Horiuchi, M.; Fukui, K.; Ayabe, T.; Inagaki, F.; Nagai, H.; Suzuki, T. SuperNova, a monomeric photosensitizing fluorescent protein for chromophore-assisted light inactivation. *Sci. Rep.* **2013**, *3*, 2629.
(257) Sarkisyan, K. S.; Zlobovskaya, O. A.; Gorbachev, D. A.; Bozhanova, N. G.; Sharonov, G. V.; Staroverov, D. B.; Egorov, E. S.; Ryabova, A. V.; Solntsev, K. M.; Mishin, A. S.; Lukyanov, K. A. KillerOrange, a genetically encoded photosensitizer activated by blue and green light. *PLoS One* **2015**, *10*, e0145287.
(258) Pletneva, N. V.; Pletnev, V. Z.; Sarkisyan, K. S.; Gorbachev, D. A.; Egorov, E. S.; Mishin, A. S.; Lukyanov, K. A.; Dauter, Z.; Pletnev, S. Crystal structure of phototoxic orange fluorescent proteins with a tryptophan- based chromophore. *PLoS One* **2015**, *10*, e0145740.
(259) Ragás, X.; Cooper, L. P.; White, J. H.; Nonell, S.; Flors, C. Quantification of photosensitized singlet oxygen production by a fluorescent protein. *ChemPhysChem* **2011**, *12*, 161−165.
(260) Malkani, N.; Schmid, J. A. Some secrets of fluorescent proteins: Distinct bleaching in various mounting fluids and photoactivation of cyan fluorescent proteins at YFP-excitation. *PLoS One* **2011**, *6*, e18586.
(261) Jusuk, I.; Raab, M.; Vietz, C.; Dammeyer, T.; Tinnefeld, P. Tinnefeld, Philip Super-resolution imaging conditions for enhanced yellow fluorescent protein (eYFP) demonstrated on DNA origami nanorulers. *Sci. Rep.* **2015**, *5*, 14075.
(262) Biteen, J. S.; Thompson, M. A.; Tselentis, N. K.; Bowman, G. R.; Shapiro, L.; Moerner, W. E. Super-resolution imaging in live Caulobacter crescentus cells using photoswitchable EYFP. *Nat. Methods* **2008**, *5*, 947−949.
(263) Lew, M. D.; Lee, S. F.; Ptacin, J. L.; Lee, M. K.; Twieg, R. J.; Shapiro, L.; Moerner, W. E. Three-dimensional superresolution colocalization of intracellular protein superstructures and the cell surface in live Caulobacter crescentus. *Proc. Natl. Acad. Sci. U. S. A.* **2011**, *108*, E1102−1110.

DOI: 10.1021/acs.chemrev.6b00238
Chem. Rev. 2017, 117, 758−795

(264) Bogdanov, A. M.; Bogdanova, E. A.; Chudakov, D. M.; Gorodnicheva, T. V.; Lukyanov, S.; Lukyanov, K. A. Cell culture medium affects GFP photostability: a solution. *Nat. Methods* **2009**, *6*, 859−860.
(265) Bogdanov, A. M.; Kudryavtseva, E. I.; Lukyanov, K. A. Antifading media for live cell GFP imaging. *PLoS One* **2012**, *7*, e53004.
(266) Mamontova, A. V.; Bogdanov, A. M.; Lukyanov, K. A. Influence of cell growth conditions and medium composition on EGFP photostability in live cells. *BioTechniques* **2015**, *58*, 258−261.
(267) Monosov, E. Z.; Wenzel, T. J.; Lüers, G. H.; Heyman, J. A.; Subramani, S. Labeling of peroxisomes with green fluorescent protein in living P-pastoris cells. *J. Histochem. Cytochem.* **1996**, *44*, 581−589.
(268) Grabenbauer, M.; Geerts, W. J. C.; Fernadez-Rodriguez, J.; Hoenger, A.; Koster, A. J.; Nilsson, T. Correlative microscopy and electron tomography of GFP through photooxidation. *Nat. Methods* **2005**, *2*, 857−862.
(269) Pletnev, S.; Gurskaya, N. G.; Pletneva, N. V.; Lukyanov, K. A.; Chudakov, D. M.; Martynov, V. I.; Popov, V. O.; Kovalchuk, M. V.; Wlodawer, A.; Dauter, Z.; Pletnev, V. Structural basis for phototoxicity of the genetically encoded photosensitizer KillerRed. *J. Biol. Chem.* **2009**, *284*, 32028−32039.
(270) Carpentier, P.; Violot, S.; Blanchoin, L.; Bourgeois, D. Structural basis for the phototoxicity of the fluorescent protein KillerRed. *FEBS Lett.* **2009**, *583*, 2839−2842.
(271) Ai, H.-W.; Shaner, N. C.; Cheng, Z.; Tsien, R. Y.; Campbell, R. E. Exploration of new chromophore structures leads to the identification of improved blue fluorescent proteins. *Biochemistry* **2007**, *46*, 5904−5910.
(272) Zhong, S.; Navaratnam, D.; Santos-Sacchi, J. A genetically-encoded YFP sensor with enhanced chloride sensitivity, photostability and reduced ph interference demonstrates augmented transmembrane chloride movement by gerbil prestin (SLC26a5). *PLoS One* **2014**, *9*, e99095.
(273) Dean, K. M.; Lubbeck, J. L.; Binder, J. K.; Schwall, L. R.; Jimenez, R.; Palmer, A. E. Analysis of red-fluorescent proteins provides insight into dark-state conversion and photodegradation. *Biophys. J.* **2011**, *101*, 961−969.
(274) Drobizhev, M.; Hughes, T. E.; Stepanenko, Y.; Wnuk, P.; O'Donnell, K.; Scott, J. N.; Callis, P. R.; Mikhaylov, A.; Dokken, L.; Rebane, A. Primary role of the chromophore bond length alternation in reversible photoconversion of red fluorescence proteins. *Sci. Rep.* **2012**, *2*, 688.
(275) de Rosny, E.; Carpentier, P. GFP-like phototransformation mechanisms in the cytotoxic fluorescent protein KillerRed unraveled by structural and spectroscopic investigations. *J. Am. Chem. Soc.* **2012**, *134*, 18015−18021.
(276) Duan, C.; Byrdin, M.; El Kathib, M.; Henry, X.; Adam, V.; Bourgeois, D. Rational design of enhanced photoresistance in a photoswitchable fluorescent protein. *Methods Appl. Fluoresc.* **2015**, *3*, 014004.
(277) Langhojer, F.; Dimler, F.; Jung, G.; Brixner, T. Ultrafast photoconversion of the green fluorescent protein studied by accumulative femtosecond spectroscopy. *Biophys. J.* **2009**, *96*, 2763−2770.
(278) Henderson, J. N.; Gepshtein, R.; Heenan, J. R.; Kallio, K.; Huppert, D.; Remington, S. J. Structure and mechanism of the photoactivatable green fluorescent protein. *J. Am. Chem. Soc.* **2009**, *131*, 4176−4177.
(279) Matsuda, T.; Miyawaki, A.; Nagai, T. Direct measurement of protein dynamics inside cells using a rationally designed photoconvertible protein. *Nat. Methods* **2008**, *5*, 339−345.
(280) Sarkisyan, K. S.; Yampolsky, I. V.; Solntsev, K. M.; Lukyanov, S. A.; Lukyanov, K. A.; Mishin, A. S. Tryptophan-based chromophore in fluorescent proteins can be anionic. *Sci. Rep.* **2012**, *2*, 608.
(281) Pletnev, V. Z.; Pletneva, N. V.; Sarkisyan, K. S.; Mishin, A. S.; Lukyanov, K. A.; Goryacheva, E. A.; Ziganshin, R. H.; Dauter, Z.; Pletnev, S. Structure of the green fluorescent protein NowGFP with an anionic tryptophan-based chromophore. *Acta Crystallogr., Sect. D: Biol. Crystallogr.* **2015**, *71*, 1699−1707.
(282) Pletnev, S.; Shcherbakova, D. M.; Subach, O. M.; Pletneva, N. V.; Malashkevich, V. N.; Almo, S. C.; Dauter, Z.; Verkhusha, V. V. Orange fluorescent proteins: Structural studies of LSSmOrange, PSmOrange and PSmOrange2. *PLoS One* **2014**, *9*, e99136.
(283) Cannella, D.; Möllers, K. B.; Frigaard, N.-U.; Jensen, P. E.; Bjerrum, M. J.; Johansen, K. S.; Felby, C. Light-driven oxidation of polysaccharides by photosynthetic pigments and a metalloenzyme. *Nat. Commun.* **2016**, *7*, 11134.
(284) Sawin, K. E.; Nurse, P. Photoactivation of green fluorescent protein. *Curr. Biol.* **1997**, *7*, R606−R607.
(285) Kiseleva, Y. V.; Mishin, A. S.; Bogdanov, A. M.; Labas, Y. A.; Lukyanov, K. A. The ability of green gluorescent proteins for photoconversion under oxygen-free conditions is determined by the chromophore structure rather than its amino acid environment. *Russ. J. Bioorg. Chem.* **2008**, *34*, 638−641.
(286) Elowitz, M. B.; Surette, M. G.; Wolf, P.-E.; Stock, J. B.; Leibler, S. Protein mobility in the cytoplasm of Escherichia coli. *J. Bacteriol.* **1999**, *181*, 197−203.
(287) Jakobs, S.; Schauss, A. C.; Hell, S. W. Photoconversion of matrix targeted GFP enables analysis of continuity and intermixing of the mitochondrial lumen. *FEBS Lett.* **2003**, *554*, 194−200.
(288) Takahashi, E.; Takano, T.; Nomura, Y.; Okano, S.; Nakajima, O.; Sato, M. In vivo oxygen imaging using green fluorescent protein. *Am. J. Physiol. Cell Physiol.* **2006**, *291*, C781−C787.

DOI: 10.1021/acs.chemrev.6b00238
Chem. Rev. 2017, 117, 758−795